



Virginia Commonwealth University
VCU Scholars Compass

Theses and Dissertations

Graduate School

2009

Novel Analogs of m-Chlorophenylguanidine as 5-HT₃ Receptor Ligands

Katie Alix
Virginia Commonwealth University

Follow this and additional works at: <https://scholarscompass.vcu.edu/etd>

 Part of the [Chemicals and Drugs Commons](#)

© The Author

Downloaded from

<https://scholarscompass.vcu.edu/etd/1734>

This Thesis is brought to you for free and open access by the Graduate School at VCU Scholars Compass. It has been accepted for inclusion in Theses and Dissertations by an authorized administrator of VCU Scholars Compass. For more information, please contact libcompass@vcu.edu.

© Katie Elizabeth Alix 2008

All Rights Reserved

NOVEL ANALOGS OF *m*-CHLOROPHENYLGUANIDINE AS 5-HT₃ RECEPTOR
LIGANDS

A thesis submitted in partial fulfillment of the requirements for the degree of Master of
Science at Virginia Commonwealth University.

by

KATIE ELIZABETH ALIX
Bachelor of Science in Biochemistry, Virginia Tech 2006
Bachelor of Arts in Chemistry, Virginia Tech 2006

Director: MAŁGORZATA DUKAT
Associate Professor, Department of Medicinal Chemistry

Virginia Commonwealth University
Richmond, Virginia
May 2009

Acknowledgement

First, I would like to thank Dr. Dukat for her patience and guidance over the last three years. She has helped mold me into a better scientist with a deeper understanding and appreciation of medicinal chemistry as an entire discipline. I would like to thank Dr. Richard Glennon for his help with my thesis and numerous useful insights. I would also like to thank Dr. Richard Young, Jessica Worsham, and Genevieve Sirles for teaching me how to handle mice and the various animal assays. I would also like to thank Dr. Jin-Sung Kim, Dr. Eliseu De Oliveria, Dr. Nadezhda German, and Dr. Mikhail Bonderov for their guidance with synthetic problems and a special thanks to Dr. Mikhail Bonderov for his help using the HPLC system. I would like to thank Justin Elenewski and Dr. Phil Moiser for their help with molecular modeling. I would like to thank my committee members Dr. Richard Glennon, Dr. Richard Young, and Dr. Aron Lichtman. And a special thank you to Shawquia Young for the synthesis of analog **48** and Samantha Casterlow for the synthesis of analogs **43** and **44** used throughout these studies. These studies were supported by the Jeffress Memorial Trust RG-J-778.

I would also like to thank my loving husband for his support and confidence in me throughout this endeavor. I would like to thank the rest of my family as well for their moments of inspiration and motivation and for always being there.

Table of Contents

List of Tables	vii
List of Figures	viii
List of Schemes	xii
List of Abbreviations	xiii
Abstract	xv
I. Introduction	1
II. Background	4
A. History of Serotonin	4
B. Classification of 5-HT Receptors	5
1. G-Protein Coupled-Receptors	6
2. Ligand-Gated Ion-Channel Receptors	7
C. 5-HT ₃ receptors	9
1. Classification	9
2. Structure and Distribution	11
3. Pharmacology and Biological Functions	12
4. Agonists	17
5. Antagonists	24
6. Quantitative Structure-Activity Relationships	26
7. Behavioral Assays for Antidepressants	29
8. Locomotor Activity Assay	31
III. Specific Aims and Rationale	33

IV. Results and Discussion	43
A. Halogen Series	43
1. Synthesis of <i>N</i> -(3-Fluorophenyl)guanidine Nitrate (42).....	43
2. Binding Studies.....	44
3. Hansch Analysis.....	46
4. Log P Analysis.....	52
5. Molecular Modeling.....	56
6. Designed Ligand	67
B. Conformationally-Constrained Analogs	68
1. Synthesis of 2-Amino-7-chloro-3,4-dihydroquinazoline (46)	68
2. Synthesis of 2-Amino-6-chloro-3,4-dihydroquinazoline (47)	69
3. Binding Studies.....	70
4. Log P Analysis.....	71
5. Behavioral Studies	73
a. Tail Suspension Test	73
b. Locomotor Activity Assay	79
6. Molecular Modeling.....	84
7. Synthesis of 2-Amino-8-chloro-1,3-benzodiazepine (49)	88
V. Conclusions.....	94
VI. Experimental.....	100
A. Synthesis	100
<i>N</i> -(3-Fluorophenyl)guanidine, Nitrate (42)	100
2-Amino-7-chloro-3,4-dihydroquinazoline, Hydrochloride (46)	101
2-Amino-6-chloro-3,4-dihydroquinazoline, Hydrochloride (47)	102
<i>N</i> -(3-Chloro-4-hydroxyphenyl)guanidine, Hydrochloride (51).....	103

2-Chloro-4-nitrophenol (53)	103
3-Chloro-4-hydroxyaniline, Hydrochloride (54)	104
2-Amino-7-chloro-quinazolin-4-(3 <i>H</i>)-one (56)	104
2-Amino-6-chloro-quinazolin-4-(3 <i>H</i>)-one (58)	105
2-Amino-4-chlorobenzylalcohol (60 , R = H)	105
2-Amino-4-chlorobenzylbromide (61 , R = H)	106
2-(2-Amino-4-chlorophenyl)acetic Acid (65)	106
4-Chloro-2-nitrobenzaldehyde (69)	107
4-Chloro-2-nitro-1-(2-nitrovinyl)benzene (70)	108
(4-Chloro-2-nitrophenyl)(1 <i>H</i> -imidazol-1-yl)methanone (72)	108
4-Chloro-2-nitrobenzylbromide (75)	109
2,3-Bis(4-chloro-2-nitrophenyl)propanenitrile (77)	109
B. Log P Analysis	111
1. Standards	111
2. Halogen Series	113
3. Quinazoline Series	113
C. Behavioral Studies	114
1. Animals	114
2. Drugs	115
3. Tail Suspension Test	115
4. Locomotor Activity Assay	117
5. Statistical Analysis	117
D. Molecular Modeling	118
Bibliography	119
Appendix A	137

Vita.....139

List of Tables

Table 1:	Criteria for receptor characterization.....	6
Table 2:	Binding affinities of several arylbiguanides and arylguanidines.	22
Table 3:	Definition of various Hansch analysis parameters.	27
Table 4:	5-HT ₃ receptor ligands assessed in antidepressant assays.....	32
Table 5:	Electronic, lipophilic, and steric effects of 3-substituted arylguanidines.....	35
Table 6:	Measurements of biplanarity of MD-354 and its constrained analogs.....	38
Table 7:	Binding affinity of halogen series at the mouse 5-HT _{3A} receptors.....	44
Table 8:	Hansch analysis of the 5-HT ₃ receptor binding of 3-substituted arylguanidines.....	47
Table 9:	Linear regression analysis results ($n = 11$).....	48
Table 10:	Multiple linear regression analysis results ($n = 11$).....	51
Table 11:	Capacity factors ($\log k'_w$) determined by linear regression and calculated/determined log P values for the selected arylguanidines and an arylbiguanide.....	55
Table 12:	Binding affinity of quinazoline series at 5-HT ₃ receptors.....	70
Table 13:	Capacity factors ($\log k'_w$) determined by linear regression and calculated/determined log P values for the quinazolines.....	72
Table 14:	Binding profile of selected cyclic guanidines at 5-HT ₃ , 5-HT _{5a} , and 5-HT ₇ receptors.....	77

List of Figures

Figure 1:	The structure of serotonin (5-HT).	4
Figure 2:	Schematic representation of a single protomer of a LGIC receptor.	8
Figure 3:	Bottom view of the homopentameric h5-HT _{3A} ECD (left). Side view of the ligand binding domain; loops A, B, and C are on one protomer (“principle subunit”; red) and loops D, E, and F are on the adjacent protomer (“complementary subunit”; blue) (right).	8
Figure 4:	The structure of <i>m</i> -chlorophenylguanidine (mCPG; MD-354).	13
Figure 5:	Clinically available 5-HT ₃ receptor antagonists: ondansetron (3), granisetron (4), tropisetron (5), dolasetron (6), palonosetron (7), and alosetron (8).	15
Figure 6:	The structure of methylated analogs of 5-HT.	18
Figure 7:	The structure of a few arylpiperazine analogs.	18
Figure 8:	The structure of phenylbiguanide analogs.	21
Figure 9:	Dukat’s pharmacophore for the binding of arylguanidines and arylbiguanides at 5-HT ₃ receptors.	23
Figure 10:	The structure of a few benzoate ester and benzamide 5-HT ₃ receptor antagonists.	25
Figure 11:	Superimposition of the Van der Waals surface of 3-CF ₃ (cyan), 3-I (purple), 3-Br (orange), 3-Cl (pink), 3-F (green), and 3-H (black) PGs (left). Superimposition of the Van der Waals surface of 3-CF ₃ (cyan) and 3-Cl (pink) PGs (right).	35
Figure 12:	Representation of a rotatable bond in MD-354 (2).	36
Figure 13:	Structure of conformationally-constrained analogs of MD-354.	37

- Figure 14: Linear regression plots of pK_i versus π (left) and volume (right). The analysis including the unsubstituted compound are shown in red, excluding the unsubstituted compound are shown in blue.45
- Figure 15: Linear regression plot of pK_i versus σ_m ($r = 0.730$; eq 2; Table 9).48
- Figure 16: Linear regression plots of pK_i versus polarizability ($r = 0.704$; eq 12; Table 9) (top) and pK_i versus volume ($r = 0.656$; eq 7; Table 9) (bottom).49
- Figure 17: Linear regression plot of pK_i versus CMR ($r = 0.670$; eq 9; Table 9).....50
- Figure 18: Plot of $\log k'$ of benzophenone versus concentration of aqueous CH_3CN53
- Figure 19: Plot of literature $\log P$ values from shake-flask data versus $\log k'_w$ values. ...54
- Figure 20: Plot of $\log k'$ of various arylguanidines and mCPBG versus concentration of aqueous CH_3CN55
- Figure 21: Ramachadarn plot of a single subunit of the h5-HT3A receptor model developed using Sybyl's Biopolymer package (Method A).58
- Figure 22: Proposed binding mode of serotonin (5-HT; **1**) in the h5-HT3A receptor model developed using Sybyl's Biopolymer package (Method A). 5-HT (**1**) is in magenta and the side chains of residues within 5 Å of the ligand are shown.59
- Figure 23: Proposed binding mode of MD-354 (**2**) to the h5-HT3A receptor model developed using Sybyl's Biopolymer package (Method A). MD-354 (**2**) is in cyan and the side chains of residues within 5 Å of the ligand are shown.....60
- Figure 24: Overlap of 5-HT (**1**) and MD-354 (**2**) from the proposed binding modes to the h5-HT3A receptor developed using Sybyl's Biopolymer package (left) (Method A). The designed ligand *N*-(3-chloro-4-hydroxyphenyl)guanidine (right).61
- Figure 25: Proposed binding mode of 5-HT (**1**) in the h5-HT3A receptor agonist model developed using Modeller (Method B). 5-HT (**1**) is in magenta and the side chains of residues within 5 Å of the ligand are shown.62
- Figure 26: Ramachadran plot of the h5-HT3A receptor agonist model developed using Modeller (Method B).63

- Figure 27: Proposed binding mode of MD-354 (**2**) to the h5-HT3A receptor agonist model developed using Modeller (Method B). MD-354 (**2**) is in cyan and the side chains of residues within 5 Å of the ligand are shown.....65
- Figure 28: Proposed binding mode of MD-354 (cyan), 3-FPG (red), 3-BrPG (blue), 3-IPG (yellow) to the h5-HT3A receptor agonist model developed using Modeller (Method B).66
- Figure 29: Linear regression analysis from the $\log k'$ values of **46**, **47**, **48** at various concentrations of acetonitrile for the quinazoline analogs.72
- Figure 30: Effect (\pm SEM) of standards (ip) on duration of immobility in the mouse tail suspension test ($n = 8-11$ mice/treatment). The significance of the effect was evaluated with a one-way ANOVA test ($F_{4,41} = 3.256, p < 0.05$), Newman-Keuls post-hoc test ($p < 0.05$).74
- Figure 31: Effect (\pm SEM) of **46** (top left), **47** (top right), **48** (bottom left), and **2** (bottom right) (ip) on duration of immobility in the mouse tail suspension test ($n = 8-10$ mice/treatment). The significance of the effects were evaluated using one-way ANOVA tests. For **46** ($F_{6,63} = 5.036, p < 0.01$), Dunnett's post-hoc test (** $p < 0.01$, * $p < 0.05$). For **47** ($F_{6,58} = 3.232, p < 0.01$), Dunnett's post-hoc test (** $p < 0.01$, * $p < 0.05$).75
- Figure 32: Effect (\pm SEM) of **47** (1.0 and 3.0 mg/kg) and **46** (0.3 mg/kg) on total number of movement episodes, total movement time, total movement distance, total number of jumps, and average velocity ($n = 12-13$ mice/treatment).80
- Figure 33: Effect (\pm SEM) of **47** (1.0 and 3.0 mg/kg) and **46** (0.3 mg/kg) on total number of retraced local movements, total number of retraced local movement episodes, and total time spent on retraced local movements ($n = 12-13$ mice/treatment).82
- Figure 34: Effect (\pm SEM) of **47** (1.0 and 3.0 mg/kg) and **46** (0.3 mg/kg) on total distance traveled in the margin, total time spent in the margin, total distance traveled in the center, total time spent in the center, the number of center entries, and the number of vertical entries ($n = 12-13$ mice/treatment).83

- Figure 35: Proposed binding mode of granisetron (**4**) to the h5-HT3A receptor antagonist model developed using Modeller (Method B). Granisetron is shown in magenta and residues within 5 Å are shown.85
- Figure 36: Ramachadran plot of the h5-HT3A receptor antagonist model developed using Modeller (Method B).86
- Figure 37: Proposed binding mode of the quinazoline analogs **46-48** to the h5-HT3A receptor antagonist model developed using Modeller (Method B). The 5-Cl analog (**48**) is shown in cyan, the 7-Cl analog (**46**) is shown in yellow, and the 6-Cl analog (**47**) is shown in purple. Residues within 5 Å are also shown.87
- Figure 38: Overlap of the proposed binding modes of MD-354 (**2**; cyan) and the highest binding affinity analog, 6-Cl quinazoline (**47**; purple).88

List of Schemes

Scheme 1.....	43
Scheme 2.....	68
Scheme 3.....	69
Scheme 4.....	89
Scheme 5.....	90
Scheme 6.....	91
Scheme 7.....	92
Scheme 8.....	93

List of Abbreviations

2-NP	1-(2-Naphthyl)piperazine
5-HT	5-Hydroxytryptamine/Serotonin
5-HTQ	N,N,N-Trimethyl-5-hydroxytryptamine
AC	Adenylate cyclase
AChBP	Acetylcholine binding protein
AcOH	Acetic acid
ANOVA	Analysis of variance
BBB	Blood-brain barrier
BCC	Bond correction charges
CMR	Complete molar refraction
CNS	Central nervous system
DMF	<i>N,N</i> -Dimethylformamide
DMF-DMA	<i>N,N</i> -Dimethylformamide dimethylacetyl
EC ₅₀	Activation concentration (half-maximal effect)
ECD	Extracellular domain
EL	Extracellular loop
epmr	Equipotent molar ratio
EtOAc	Ethyl acetate
EtOH	Ethanol
FDA	Food and Drug Administration
FST	Forced swim test
GABA	γ -Aminobutyric acid
GI	Gastrointestinal tract
GOLD	Genetic optimization of ligand docking
GPCR	G-protein coupled receptor
HPLC	High performance liquid chromatography
IACUC	Institutional Animal Care and Use Committee
IBS	Irritable bowel syndrome
IC ₅₀	Inhibition concentration (half-maximal effect)
i.d.	Inside diameter
IL	Intracellular loop
ip	Intraperitoneal
<i>i</i> -PrOH	Isopropanol
IUPHAR	International Union of Pharmacology
iv	Intravenous
K _i	Dissociation constant

KO	Knock-out
l.	Length
LGIC	Ligand-gated ion channel
LSD	(+)Lysergic acid diethylamide
M (M1-M4)	Transmembrane-spanning helix
mCPBG	<i>meta</i> -Chlorophenylbiguanide
mCPG	<i>meta</i> -Chlorophenylguanidine (MD-354)
MCVH	Medical College of Virginia Hospital
MD-354	<i>meta</i> -Chlorophenylguanidine
MOPAC	Molecular orbital package
MR	Molar refraction
MV	Molar volume
nACh	nicotinic acetylcholine
NAMD	Nanoscale molecular dynamics
NIH	National Institutes of Health
NMQ	<i>N</i> -Methylquipazine
NTS	Nucleus tractus solitaries
NVE	Number of valence electrons
PBG	Phenylbiguanide
Pc	Parachor
PDB	Protein data bank
PG	Phenylguanidine
PLC	Phospholipase C
po	Per os (orally)
QSAR	Quantitative structure-activity relationships
SAFIR	Structure-affinity relationships
SAR	Structure-activity relationships
sc	Subcutaneous
SCWRL	Side-chain assignment with rotamer library
SEM	Standard error of the mean
SERT	Serotonin reuptake transporter
SNRI	Serotonin-norepinephrine reuptake inhibitor
SSRI	Selective serotonin reuptake inhibitor
TBAB	Tetrabutylammonium bromide
TCA	Tricyclic antidepressant
THF	Tetrahydrofuran
TLC	Thin layer chromatography
TM	Transmembrane
TMS	Tetramethylsilane
TST	Tail suspension test
WT	Wild-type

Abstract

NOVEL ANALOGS OF *m*-CHLOROPHENYLGUANIDINE AS 5-HT₃ RECEPTOR LIGANDS

By Katie Elizabeth Alix

A thesis submitted in partial fulfillment of the requirements for the degree of Master of Science at Virginia Commonwealth University.

Virginia Commonwealth University, 2009

Major Director: Małgorzata Dukat, Associate Professor
Department of Medicinal Chemistry

Serotonin receptors play a variety of functional roles in the body. Some indications and treatment claims for one of the classes of serotonin receptors, the 5-HT₃ receptor family, include: anxiety, depression, chemotherapy- and radiation-induced emesis, constipation, irritable bowel syndrome, pain, drug addiction, and satiety control.

A 5-HT₃ receptor partial agonist, MD-354, served as a lead compound in the development of new 5-HT₃ receptor ligands. Using halogenated analogs the study investigated their effect on binding to the 5-HT₃ receptor. Conformationally-constrained analogs (quinazolines) were shown to be a novel class of 5-HT₃ receptor antagonists. The

log P values were determined for several analogs, and indicated that these ligands should be able to penetrate the blood-brain barrier. A homology model of the 5-HT₃ receptor was built and the docking modes were assessed for these two series. Quinazolines were investigated for antidepressant properties using the mouse tail suspension test, and were shown to possess antidepressant-like activity.

I. Introduction

Serotonin (5-HT) research in the central nervous system (CNS) has come a long way since serotonin was first proposed to be a neurotransmitter.¹ After the identification of the first two serotonin receptors in 1957,² the list has expanded several times to include seven major families and their subtypes. Most serotonin receptors are G-protein coupled-receptors (GPCRs); however, one family of serotonin receptors consists of ligand-gated ion-channel (LGIC) receptors—the 5-HT₃ receptor family.

Ligand-gated ion-channels are fast acting. Once a ligand activates the receptor, an agonist, binds to the receptor; the receptor is depolarized and ions quickly travel through the pore, changing the synaptic polarity. 5-HT₃ receptors are generally co-localized on nerve endings with other neurotransmitter receptors. The change in synaptic polarity from activation of 5-HT₃ receptors can stimulate the release of nearby neurotransmitters (i.e., dopamine, norepinephrine, glutamate, acetylcholine, γ -aminobutyric acid, and serotonin).^{3,4} Since 5-HT₃ receptors can stimulate the release of so many neurotransmitters it seems to have the potential to be involved in several different functions.

Most notably, 5-HT₃ receptors are known for their antagonists, most of which are clinically available as anti-emetics. These drugs are effective in the treatment of chemotherapy- and radiation-induced emesis.⁵ From the investigations into treating

emesis, other 5-HT₃ receptor antagonists have been identified to be useful in the treatment of irritable bowel syndrome (IBS).⁵ The 5-HT₃ receptors have also been implicated in depression, pain modulation, the reward pathway, schizophrenia, and anxiety.^{5,6} No known therapeutic function has been identified for 5-HT₃ receptor agonists.

m-Chlorophenylguanidine (mCPG; MD-354) is a partial agonist at the 5-HT₃ receptor, it behaves as an agonist in some assays and as antagonist in other assays; but binds with high affinity to the 5-HT₃ receptor ($K_i = 35$ nM).^{7,8} Because of the partial agonist characteristic, it would be valuable to develop novel analogs to explore which aspects are necessary for binding to the 5-HT₃ receptor as well as ways to improve binding affinity.

The 5-HT₃ receptors are located in the CNS as well as in the periphery. In order to study the effects of the 5-HT₃ receptors in the CNS, agents must be able to get into the brain and cross the blood-brain barrier (BBB). MD-354 has a log P value of -0.64 suggesting it may not be able to easily penetrate the BBB;⁹ thus, developing analogs that can cross the BBB would be necessary for studying 5-HT₃ receptors in the CNS.

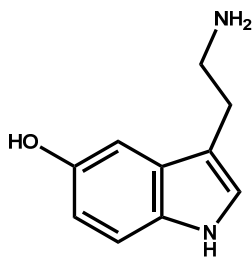
In drug development, molecular modeling has proven to be a powerful tool. Since the structure of the 5-HT₃ receptor has yet to be determined by X-ray crystallography, homology models of the receptor can be built from other ligand-gated ion-channels of the Cys-loop family whose structure has been determined to identify possible binding modes of known agents and aid in the design of new agents.

From data compiled since 1960, depression affects up to 38% of cancer patients.^{10,11} The idea of being able to treat the emesis from chemotherapy as well as the depression with one drug is an inviting possibility. Both 5-HT₃ receptor antagonists and agonists have been shown to behave as antidepressants in the forced swim and tail suspension tests in rodents.¹²⁻¹⁷ This suggests that a variety of classes of 5-HT₃ receptor agents are capable of having the same interactions with the 5-HT₃ receptor, an analysis of selected agents for antidepressant-like properties may yield a novel class of antidepressants.

II. Background:

A. History of Serotonin

Evidence for the existence of serotonin (5-hydroxytryptamine; 5-HT; **1**) (Figure 1) was detected as early as 1868 as a vasoconstrictor.¹⁸ However, its isolation did not occur for more than another half century. Independently, Erspamer and Vialli¹⁹ isolated enteramine in the late 1930s from enterochromaffin cells in the gut and Rapport et al.²⁰ isolated serotonin as a beef serum vasoconstrictor substance in 1948. In 1949, Rapport determined the structure of serotonin as 5-hydroxytryptamine.²¹ But it was not until 1952 that Erspamer and Asero discovered that enteramine and serotonin were one and the same.²²



1

Figure 1. The structure of serotonin (5-HT).

The central nervous system (CNS) story of serotonin began in 1953 when Twarog and Page discovered serotonin in dog, rat, and rabbit brains;²³ later, in 1954, Twarog

proposed serotonin to be a neurotransmitter.¹ Independently Woolley and Shaw,²⁴ and Gaddum and Hameed²⁵ proposed that the action of 5-HT in the brain and in the gut could be antagonized by the hallucinogen LSD ((+)-lysergic acid diethylamide).

Serotonin has been implicated in a number of different processes in both the periphery and central nervous systems and has been shown to play a role in alcoholism and drug abuse, cognitive disorders, depression, anxiety, schizophrenia, chemotherapy- and radiation-induced emesis, constipation, irritable bowel syndrome, migraines, fibromyalgia, pain, obesity, appetite disorders, and autism.⁶

B. Classification of 5-HT Receptors

The first definitive receptors for 5-HT were identified by Gaddum and Picarelli in 1957.² These receptors were originally called D- and M-receptors because they were antagonized by dibenzyline and morphine, respectively. In 1979 Peroutka and Snyder used ¹⁴C and ³H techniques to determine 5-HT receptor subtypes in vitro.²⁶ A receptor classification scheme was proposed by the Nomenclature Committee of the International Union of Pharmacology (IUPHAR) in 1992.²⁷ Table 1 provides the general criteria for receptor classification as provided by IUPHAR.²⁸ Receptors are classified by operational (drug-binding), structural (sequence of the receptor), and transductional (receptor-effector coupling) characteristics. Upper case lettering is used when the receptor has been identified in whole cells while lower case lettering is used when identifying recombinant receptors.

To date there are seven major families of serotonin receptors (5-HT₁-5-HT₇). All, but the 5-HT₃ (5-HT_{3A}-5-HT_{3E}) receptors, belong to the G-protein coupled-receptor (GPCR) superfamily. The 5-HT₃ receptors belong to the Cys-loop ligand-gated ion-channel (LGIC) receptor superfamily. The 5-HT₁ (5-HT_{1A}, 5-HT_{1B}, 5-HT_{1D}, 5-HT_{1E}, 5-HT_{1F}) receptors inhibit adenylyl cyclase (AC); the 5-HT₂ (5-HT_{2A}, 5-HT_{2B}, 5-HT_{2C}) receptors stimulate phospholipase C (PLC) production. The 5-HT₄, 5-HT₆, 5-HT₇ (5-HT_{7A}, 5-HT_{7B}, 5-HT_{7D}) receptors stimulate adenylyl cyclase while a second messenger system for activation of the 5-HT_{5a} and 5-HT_{5b} receptors has yet to be defined.^{6,28-30}

Table 1. Criteria for receptor characterization.²⁸

Criteria	Definition
Operational	
a. Selective agonists	Agonists showing high selectivity for a particular receptor compared to their potencies at other receptors need to be identified.
b. Selective antagonists	Receptor-blocking drugs are needed that can block the actions of agonists by blocking the receptor.
c. Ligand-binding affinities	Dissociation constants for ligands in binding studies should correlate with data from functional studies.
Structural	
d. Molecular structure	Amino acid sequence of the receptor protein provides evidence for receptor identity; relative homologies can be used for classification and defining families and subfamilies.
Transductional	
e. Intracellular transduction mechanisms	Information that further defines a superfamily and any information that may be indicative of the nature of the intracellular protein structure.

1. G-Protein Coupled-Receptors

GPCRs are characterized by seven transmembrane-spanning helices (TM1-TM7), three intracellular loops (IL1-IL3), and three extracellular loops (EL1-EL3) (as reviewed

by Lagerström and Schiöth).³¹ The amine terminus is extracellular and the carboxyl terminus is intracellular. One of the intracellular loops, usually IL2 or IL3, is coupled to a heterotrimeric G-protein, which upon ligand binding dissociates to a $\beta\gamma$ subunit and an α subunit to activate second messenger systems (e.g., PLC and AC). There are many other GPCRs including the adrenergic receptors and rhodopsin receptors.

2. Ligand-Gated Ion-Channel Receptors

5-HT₃-type receptors are ligand-gated ion-channel receptors and are part of the Cys-loop superfamily.³² Structurally, these receptors are pentamers with each subunit (Figure 2) consisting of a very large extracellular domain (ECD) containing the amine terminus and the ligand-binding domain, four transmembrane-spanning helices (M1-M4), a short intracellular loop connecting M1 to M2, a short extracellular loop connecting M2 to M3, an intracellular loop between M3 and M4, and an extracellular carboxyl terminus.^{33,34} The M2 helix of each subunit makes up the inner lining of the cationic pore. Upon binding of an agonist, the receptor depolarizes and allows the influx of cations through the pore. This change in synaptic polarity may stimulate the release of other nearby neurotransmitters. The long ECD that is associated with the amine terminus consists of six putative loops (A-F); loops A, B, and C make up the principle side of the binding interface and loops D, E, and F make up the complementary side of the binding interface (Figure 3).³⁵ Incidentally, the binding site for agonists and competitive antagonists lies at the interface of two protomers. On the C loop there are two cysteines separated by 13 amino acids; they form a disulfide linkage and thus a Cys-loop. Other

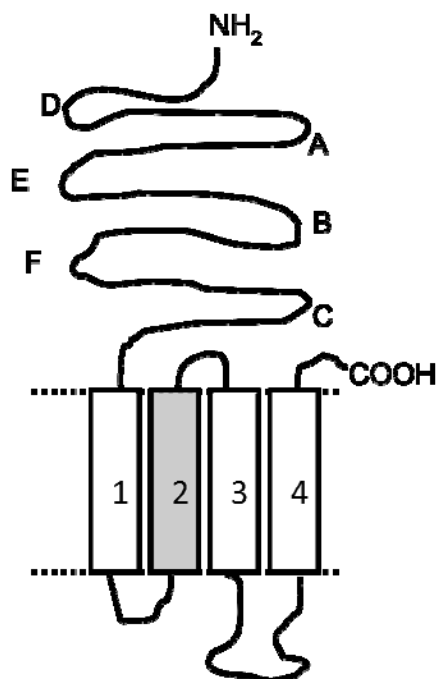


Figure 2. Schematic representation of a single protomer of a LGIC receptor.

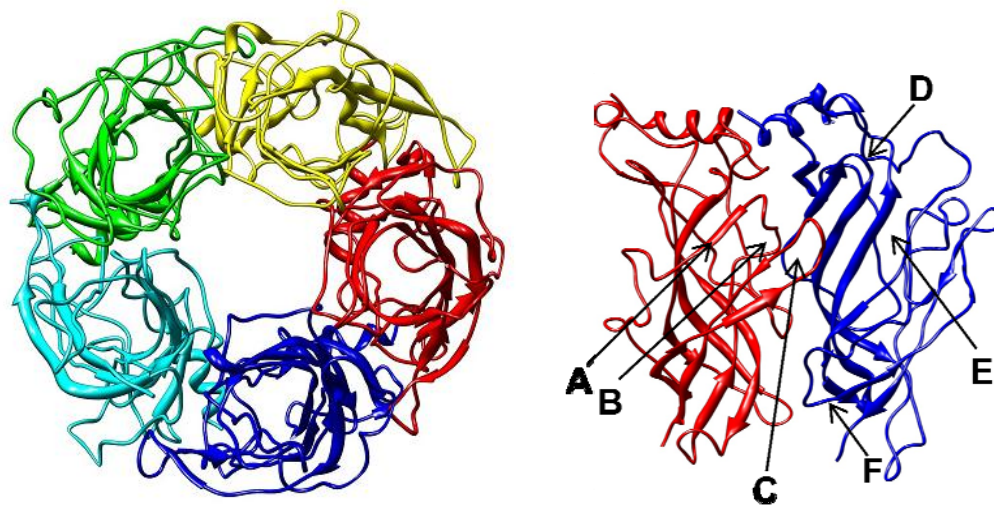


Figure 3. Bottom view of the homopentameric h5-HT3A ECD (left). Side view of the ligand binding domain; loops A, B, and C are on one protomer (“principle subunit”; red) and loops D, E, and F are on the adjacent protomer (“complementary subunit”; blue) (right).

LGIC receptors include nicotinic acetylcholine (nACh), γ -aminobutyric acid type A (GABA_A), and glycine receptors.^{5,6} There is a 22-30% sequence homology between the 5-HT_{3A} receptor subunit sequence and the α -subunits of other members of the LGIC family.³⁶ Ortells and Lunt proposed that 5-HT₃ receptors are a possible common ancestor of all LGIC receptors.³⁷ To date, there are no X-ray crystal structures of 5-HT₃ receptors; however, various acetylcholine binding proteins' structures have been identified by X-ray crystallography.³⁸⁻⁴⁰ The structure of a nicotinic acetylcholine receptor has been derived using electron microscopy.⁴¹ Also, the $\alpha 1$ subunit ECD of a mouse nACh receptor bound to α -bungarotoxin has been crystallized and the structure determined.⁴² Since the 5-HT₃ receptor subunits share features with nACh receptors (i.e., protein sequence homology between 5-HT_{3A} receptor subunit sequences and the α subunit of other LGIC receptors is 22-30%),³⁶ homology models for 5-HT₃ receptors can be developed based on the crystal structures available.³⁸⁻⁴² There have been some reports of chimeric receptors between different members of the LGIC family.^{35,43}

C. 5-HT₃ Receptors

1. Classification

5-HT₃ receptors were identified as the original M receptor but were later renamed 5-HT₃ receptors by Bradley et al.⁴⁴ The 5-HT_{3A} receptor subtype was initially cloned by Maricq et al. in 1991 from NCB-20 murine hybridoma cells.⁴⁵ The first human 5-HT₃ receptors were cloned from the hippocampus, amygdala, and colon.^{46,47} The human *HTR3A* gene is located on chromosome 11 and each receptor subunit consists of 478

amino acids.⁴⁸ Species orthologs of the 5-HT3A receptor have also been identified in the rat,⁴⁷ mouse,⁴⁴ dog,⁴⁹ guinea pig,⁵⁰ and ferret.⁵¹ There are a few splice variants of the 5-HT3A receptor subunits: 5-HT3AS (i.e., short), h5-HT3AT (i.e., short, truncated) and h5-HT3AL (i.e., long).⁵² The 5-HT3AS receptor subunit is found in mouse, rat, and guinea pig, and has six fewer amino acids in the loop between M3 and M4.^{44,47,50} The h5-HT3AT receptor subunit, found in humans, only has 238 amino acids and a single transmembrane helix (M1).⁵² The h5-HT3AL receptor subunit, found in humans, has an additional 32 amino acids in the loop between M2 and M3.⁵² These isoforms do not form functional homomeric receptors but form functional heteromeric receptors with the native h5-HT3A receptor subunits.⁵² Receptors containing h5-HT3AT subunits have decelerated desensitization and therefore, a larger response to Ca^{2+} fluxes.⁵² Those receptors containing h5-HT3AL subunits accelerate desensitization and have reduced Ca^{2+} fluxes.⁵² The 5-HT3B receptor subtype was isolated in 1999 by screening human genomic sequence data by Davies et al.⁵³ It shares 41% amino acid sequence identity with h5-HT3A receptors and is also located on chromosome 11, and each subunit has 441 amino acids.^{53,54} Rat and mouse orthologs of the 5-HT3B receptor have also been identified.⁵⁵ The 5-HT3C, 5-HT3D, 5-HT3E receptor subtypes were cloned by Niesler et al.⁵⁶ and Karnovsky et al.⁵⁷ independently in 2003. The 5-HT3D receptor subtype as predicted by Niesler et al.⁵⁶ lacks a signal peptide and most of the amine terminus ECD including the Cys-loop; not surprisingly, each subunit only has 279 amino acids. The 5-HT3C and 5-HT3E receptor subtypes share 36% and 39% amino acid sequence homology with h5-HT3A receptors,⁵⁷ and have 447 and 471 amino acids, respectively. All three of these

subtypes are located on chromosome 3 and were originally thought to be exclusive to humans. 5-HT3C and 5-HT3E have since been found in chimp and dog.⁵⁸

2. Structure and Distribution

Only the 5-HT3A receptor subtype forms homomeric receptors; the remainder of the subtypes form functional heteromeric receptors with 5-HT3A subunits.^{53,54,59} The composition and stoichiometry of native heteromeric 5-HT₃ receptors has yet to be determined.^{60,61} When h5-HT3A and h5-HT3B receptor subunits were epitope-tagged and expressed heterologously in tsA-201 cells they formed heteromeric receptors containing three 5-HT3B and two 5-HT3A receptor subunits with the order of B-B-A-B-A.⁶² This stoichiometry was determined by atomic force microscopy. However, the heteromeric 5-HT3AB receptors have different biophysical properties than the homomeric 5-HT3A receptors.^{53,54} The pharmacological profile of the heteromeric receptors containing 5-HT3C, 5HT3D, or 5-HT3E subunits in combination with 5-HT3A subunits is similar to homomeric 5-HT3A receptors or heteromeric 5-HT3AB receptors^{59,61} but the biophysical properties have yet to be determined. *HTR3A-C* genes are expressed both centrally and in the periphery, whereas *HTR3D* and *HTR3E* genes are only expressed in the gastrointestinal (GI) tract.⁶¹ In addition, 5-HT3C-E receptors appear to be absent in rodents.⁶¹ Within the CNS there are two main regions in which 5-HT₃ receptors are expressed: the dorsal vagal complex and the forebrain.⁶³⁻⁶⁵ The dorsal vagal complex contains the nucleus tractus solitarius (NTS), area postrema, and dorsal motor nucleus of the vagus nerve. These are important for the vomiting reflex.⁶⁴ Within the forebrain,

human 5-HT₃ receptor recognition sites have been located in the caudate nucleus, putamen, hippocampus, and amygdala.⁶⁶⁻⁶⁸ The caudate nucleus and putamen are involved in learning while the hippocampus and amygdala (part of the limbic system) are involved in memory processing.⁶⁰

3. Pharmacology and Biological Functions

Several different in vivo and in vitro assays are employed for the identification of agonists and antagonists at the 5-HT₃ receptors. The von Bezold-Jarisch reflex is one of the most prominent in vivo assays used.⁶⁹ Upon administration of an agonist there is a cardiopulmonary reflex in which bradycardia is the most prominent response (the other two responses of the reflex are apnea and hypotension). An antagonist would be any agent that blocks the response of the agonist. Another in vivo assay used is the ferret or shrew emesis assay.⁷⁰ Cisplatin is given to the animal to induce vomiting; an antagonist would block this effect, while an agonist would induce vomiting when administered alone. After an application of cantharidin to human skin a blister forms. When 5-HT is applied to the base of the blister it causes pain which can be reversed by 5-HT₃ receptor antagonists.⁷¹ In vitro, the most commonly used assay is contraction of guinea pig ileum.² An agonist produces contraction while an antagonist would block the contraction of the agonist. Other in vitro assays include the rabbit vagus nerve (5-HT₃ receptor agonists produce an increase in the amplitude of C-fiber action potentials), the isolated rabbit heart (release of noradrenaline and acetylcholine by 5-HT₃ receptor agonists), and the uptake of [¹⁴C]guanidinium in NG108-15 cells (5-HT₃ receptor agonists stimulate ion

accumulation).⁷¹ Some agents have been shown to be agonists in one assay while antagonists in another assay. For example, *m*-chlorophenylguanidine (mCPG; MD-354; **2**; Figure 4) behaves as an agonist in the von Bezold-Jarisch assay⁷ and emesis assays in shrews,⁸ but at higher doses behaves as an antagonist in the cisplatin-induced emesis assay.⁸ A novel functional assay was developed based on micromechanical measurement of membrane receptor binding.⁷² The deflection of microcantilevers is dependent on molecular binding and thus radiolabelled ligands are unnecessary.⁷³ These particular microcantilevers are modified with a membrane preparation containing 5-HT₃AS receptors and bend on the application of the 5-HT₃ receptor agonist 5-HT or the 5-HT₃ receptor antagonist MDL-72222.⁷² Agonists and competitive antagonists compete for the binding on these membrane preparations.

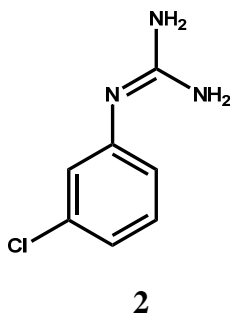


Figure 4. The structure of *m*-chlorophenylguanidine (mCPG; MD-354).

5-HT₃ receptors are concentrated in regions of the brain that are involved in the vomiting reflex, anxiety and depression, pain processing, and the reward system.^{5,6} The receptors are predominantly found in presynaptic regions with the exception of the hippocampus in which they are postsynaptic.⁵ This localization on nerve endings

contributes to 5-HT₃ receptors modulating the release of neurotransmitters.⁵ Activation of 5-HT₃ receptors modulates the release of various neurotransmitters and neuropeptides including: dopamine, norepinephrine, glutamate, acetylcholine, GABA, and even serotonin.^{3,4} Presynaptic activation provides for the influx of Ca²⁺, whereas postsynaptic activation (i.e., in the hippocampus) provides for the influx of K⁺ and Na⁺.²²

There are six 5-HT₃ receptor antagonists (Figure 5) on the global clinical market and five are effective in the treatment of chemotherapy-induced and radiation-induced emesis (i.e., ondansetron **(3)**, granisetron **(4)**, tropisetron **(5)**, dolasetron **(6)**, and palonosetron **(7)**).⁵ These agents are ineffective against motion sickness and apomorphine-induced emesis.^{6,74} They induce a complete blockade of both central and peripheral 5-HT₃ receptors. The sixth available 5-HT₃ receptor antagonist on the market is alosetron **(8)** which is used for the treatment of irritable bowel syndrome (IBS).⁵ Recently, the application for the approval by the FDA of cilansetron was withdrawn, but it is a 5-HT₃ receptor antagonist also used in the treatment of IBS.⁷⁵

5-HT₃ receptors have been implicated in IBS and constipation. In diarrhea-prominent IBS, the 5-HT₃ receptor antagonist, ondansetron **(3)**, has been shown to alleviate symptoms but can also cause excessive constipation.⁷⁶ It is thought that 5-HT₃ receptor partial agonists would be able to alleviate the symptoms without causing side-effects.⁷⁶ Constipation, which is normally treated by laxatives that cause side-effects, can also be treated by 5-HT₃ receptor agonists.⁷⁷

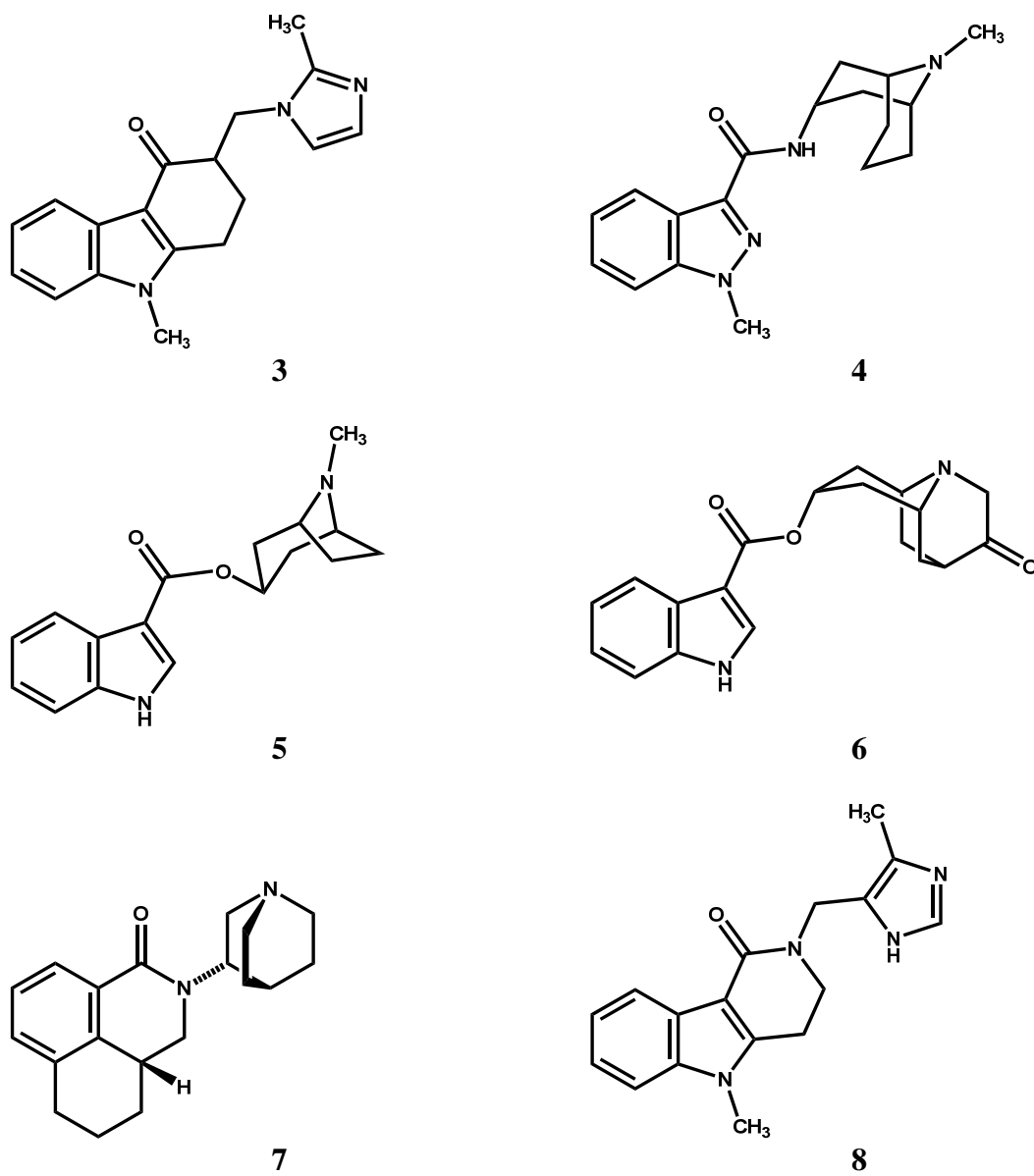


Figure 5. Clinically available 5-HT₃ receptor antagonists: ondansetron (3), granisetron (4), tropisetron (5), dolasetron (6), palonosetron (7), and alosetron (8).

5-HT₃ receptors are located in the dorsal horn as well as in other regions involved in pain modulation.⁷⁸ Stimulation of these receptors produces an antinociceptive effect.⁵ MD-354 (**2**), a 5-HT₃ receptor partial agonist, has been shown to selectively potentiate the antinociceptive action of clonidine in the mouse tail-flick assay without potentiating clonidine's sedative effects.⁷⁹

In the last decade, 5-HT₃ receptors have also been implicated in depression.⁸⁰ Ondansetron (**3**), a 5-HT₃ receptor antagonist, has been shown to be active as an antidepressant in both the tail suspension and forced swim tests (for a detailed description see Section 7) in mice (Swiss 0.01 – 0.1 µg/kg, ip; albino, 0.25 – 2 mg/kg, ip).^{15,17} In earlier studies, however, ondansetron (**3**) (0.01 µg/kg, ip) had been shown to be inactive in the mouse forced swim test by itself but potentiates the sub-active doses of the antidepressants fluoxetine (16 mg/kg), citalopram (16 mg/kg), and fluvoxamine (8 mg/kg).¹⁶ In another study, the 5-HT₃ receptor antagonist bemesetron (**9**) (Figure 10) has been shown to be active by itself (3 mg/kg, sc) and at inactive doses (1 mg/kg, sc) in combination with inactive doses of ketamine (12.5-25 mg/kg, sc) in the mouse tail suspension test (C57BL/6J/Han).¹³ The exact involvement of 5-HT₃ receptors in depression has yet to be identified. However, Bhatnager et al.⁸¹ demonstrated that there are differences between wild-type (WT) and 5-HT₃ receptor knock-out (KO) male and female mice in the forced swim and the defensive withdrawal tests (light-dark test). In the mouse forced swim test, KO females exhibited increased behavioral indices of depression type behavior in comparison to WT females, thus showing that 5-HT₃ receptors do play a

role in depression. In addition, single nucleotide polymorphisms on the *HTR3B* gene have been linked with major depression.⁸²

5-HT₃ receptor antagonists may also be effective in influencing the reward system of drug abuse because of the modulation of dopamine.⁵ Other possible clinical implications for 5-HT₃ receptor antagonists include cognitive functions, schizophrenia, satiety, and anxiety.⁵

4. Agonists

Since serotonin (**1**; 5-HT₃ $K_i \approx 1000$ nM) is a tryptamine, the first ligands studied were other tryptamine analogs. Methylation of the indole nucleus of 5-HT (e.g., 2-methyl-5-hydroxytryptamine; **10**; $K_i \approx 1300$ nM) (Figure 6) was found to result in an agent that was less potent but more selective than 5-HT as a 5-HT₃ receptor agonist.^{83,84} However, **10** is rapidly metabolized and has difficulty crossing the blood-brain barrier (BBB).⁸⁵ Methylation of the terminal amine was also examined.^{86,87} *N*-Monomethyl-5-HT was shown to be active in the depolarization of superior cervical ganglion cells (it has an equipotent molar ratio (empr) of 1.3 relative to 5-HT) while *N,N*-dimethyl— (**11**) and *N,N,N*-trimethyl—5-HT (5-HTQ; **12**) were found to have increased activity (empr of 0.08 and 0.01, respectively).⁸⁷ Similarly, in binding affinity assays, **11** and **12** were found to bind with enhanced affinity ($K_i \approx 280$ nM and 75 nM, respectively) relative to 5-HT.⁸⁶ 5-HTQ (**12**) has a permanent positive charge that was well tolerated by 5-HT₃ receptors ($K_i \approx 75$ nM), but 5-HTQ does not readily cross the BBB.⁸⁶ Longer terminal amine substituents and locking the terminal amine into a ring abolished affinity.⁸⁶

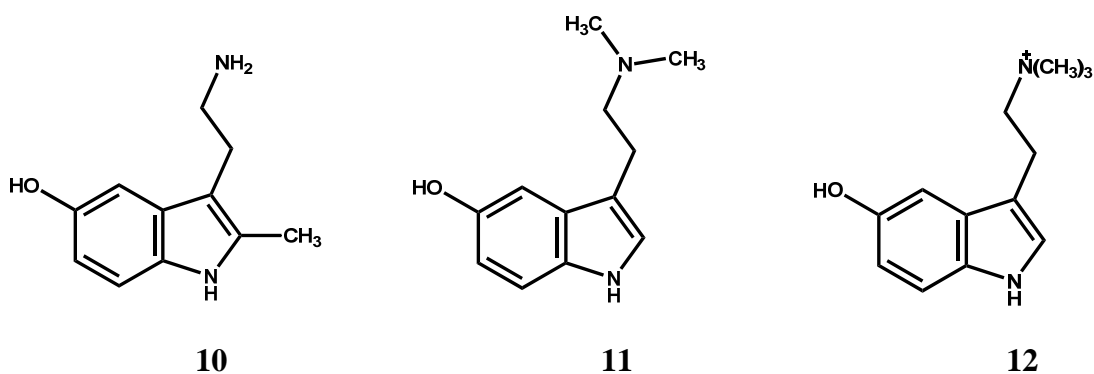


Figure 6. The structure of methylated analogs of 5-HT.

Another of the first agonists investigated were the arylpiperazines (Figure 7).^{7,88} Quipazine (2-(1-piperazinyl)quinoline; **13**; $K_i \approx 3$ nM) was the first of this class to demonstrate 5-HT₃ receptor binding.⁸⁹ Quipazine (**13**) was used as a lead compound to develop two general series: bicyclic and monocyclic arylpiperazines. Phenylpiperazine itself binds with low affinity ($K_i \approx 3000$ nM) at 5-HT₃ receptors.⁷ The 3-position of phenylpiperazine was shown to be important for binding as demonstrated by the impro-

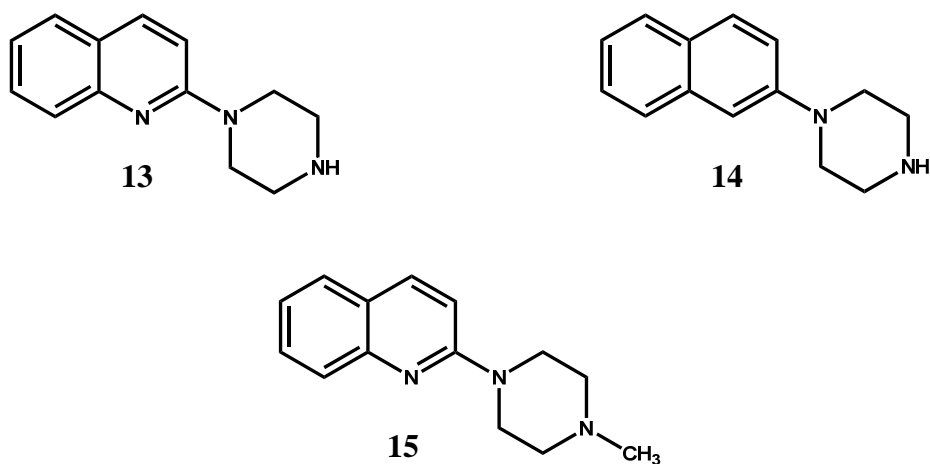


Figure 7. The structure of a few arylpiperazine analogs.

ved affinity of 3-chlorophenylpiperazine ($K_i \approx 62$ nM).⁷ However, the corresponding 3-CF₃ analog displayed decreased affinity ($K_i \approx 1390$ nM).⁷ The affinity of 3-chlorophenylpiperazine could be mimicked by its naphthyl analog 1-(2-naphthyl)piperazine (2-NP; **14**; $K_i \approx 32$ nM).⁸⁸ Methylation of the terminal piperazine nitrogen atom of quipazine further increased binding affinity and selectivity (NMQ; **15**; $K_i \approx 2$ nM).⁸⁸ Tricyclic derivatives have also been studied.⁹⁰⁻⁹² Quite a few arylpiperazines have been shown to bind at 5-HT₃ receptors; some have been shown to be agonists and some have been shown to be antagonists.⁸³ However, none of them have been shown to be highly selective for 5-HT₃ receptors because they also show affinity for other serotonin receptors^{93,94} and the serotonin reuptake transporter (SERT).⁹⁵

The first non-tryptamine, non-arylpiperazine agonist ligand that demonstrated selectivity for 5-HT₃ receptors was phenylbiguanide (PBG; **16**; $K_i \approx 1000$ nM) (Figure 8); despite its low affinity, PBG was shown to be more selective than early arylpiperazines.^{7,87} PBG is a selective low affinity agonist and arylpiperazines are higher affinity non-selective agents. Although there was no evidence suggesting that PBG was binding in the same manner as arylpiperazines, the assumption that they use the same aromatic site served as the starting point for the investigation of novel analogs of PBG. If they bind in a similar manner, then it might be possible to use the structure-affinity relationships (SAFIR) of arylpiperazines to enhance the affinity of the arylbiguanides. Two novel arylbiguanides were looked at initially, 1-(3-chlorophenyl)biguanide (mCPBG; **17**; $K_i \approx 17$ nM) and 1-(2-naphthyl)biguanide (**18**; $K_i \approx 12$ nM).^{7,93} Both have

high affinities. mCPBG not only displayed partial agonist characteristics in functional studies (i.e., rabbit bladder preparation and von Bezold-Jarisch reflex)⁷ but was shown that in a competition for binding to 5-HT₃ receptors mCPBG inhibited [³H]GR67330 with 100 times higher affinity than 5-HT (**1**) or PBG (**16**).⁹⁶ PBG and mCPBG have been two of the most widely used 5-HT₃ receptor agonists even though they may not penetrate the BBB.⁹⁷ Bachy et al.⁹⁷ found that both PBG and mCPBG displayed poor brain penetration in mice because they did not displace the binding of [³H]granisetron in an ex vivo binding experiment. In addition, Rahman et al.⁹ showed that both possess low octanol/water partition coefficients. In contrast, Kilpatrick and Rogers⁹⁸ have shown that mCPBG displaces [³H]GR65630 in rat entorhinal cortex in an ex vivo binding study. Moreover, Steward et al.⁹⁹ have used [³H]mCPBG to label 5-HT₃ receptor recognition sites in rat brain, which would also indicate that mCPBG does cross the BBB. More selective agonists have since been developed (e.g., 2,3,5-tri-Cl-PBG, $K_i = 0.4$ nM)¹⁰⁰; however, mCPBG is still commonly used. A wide variety of substituents on the phenylbiguanide ring have been investigated but will not be discussed here.^{7,83,101}

Using a deconstruction-reconstruction-elaboration approach, the elements needed for binding of mCPBG (**17**) at 5-HT₃ receptors were evaluated.^{7,100} In the deconstruction-reconstruction-elaboration approach all substituents from a ligand that bind well to a particular receptor are removed and then the ligand is reconstructed by re-introducing each of the original substituents individually.¹⁰² This approach allows for each substituent to be evaluated for its effect on binding affinity and/or receptor selectivity.¹⁰² The

resulting ligand is elaborated on to explore new substituents and their role on binding affinity and/or receptor selectivity.¹⁰² During the elaboration process N,N-Dimethylation of the terminal amine of the biguanide moiety was found to abolish affinity.⁷ Replacing the N2 nitrogen atom (Figure 8) of mCPBG with an oxygen atom greatly decreased affinity.⁷ Furthermore, removal of the N4 nitrogen atom abolished affinity.⁷ The N-(2-phenylethyl)guanidine analog binds with high affinity ($K_i \approx 40$ nM), indicating that the

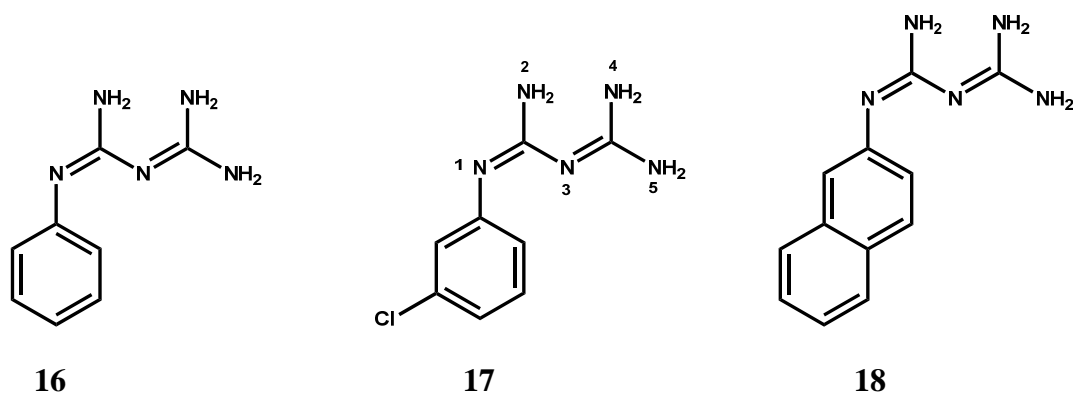
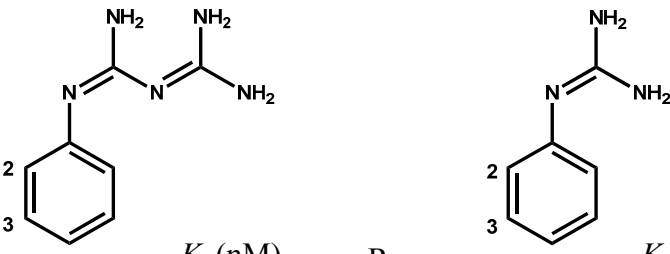


Figure 8. The structure of phenylbiguanide analogs.

biguanide moiety may not be required for binding.⁷ Upon further deconstruction of mCPBG, the biguanide function was shortened to a guanidine yielding a new class of 5-HT₃ receptor agonists—the phenylguanidines (PG). The first member of this class was 3-chlorophenylguanidine (mCPG; MD-354; **2**; $K_i \approx 35$ nM) which has been shown to also be an agonist in the von Bezold-Jarisch assay and the rabbit bladder preparation.⁷ Various aryl substituents have been investigated by our laboratory (Table 2).^{7,100} Parallel changes in the structures of PBGs and PGs led to parallel shifts in affinity suggesting that the two

series bind in a similar manner.¹⁰⁰ For example, removal of the 3-chloro group to give the parent PG (**27**) reduced affinity ($K_i \approx 2340$ nM); likewise removal of the 3-Cl group from mCPBG (**17**) to generate PBG (**16**) decreased affinity ($K_i \approx 1000$ nM). Positional changes of the chloro group (i.e., 2-Cl and 4-Cl) also decreased affinity (**19-20**, **28-29**), but not as

Table 2. Binding affinities of several arylbiguanides and arylguanidines.^{7,8,101}



	K_i (nM)	R		K_i (nM)
16	$\approx 1,000$	H	27	2,340
17	17	3-Cl	2	35
19	62	2-Cl	28	190
20	200	4-Cl	29	320
21	220	3-NO ₂	30	85
22	780	3-CH ₃	31	6,520
23	700	3-CF ₃	32	5,700
24	12	3,4-di-Cl	33	3.1
25	1.8	3,5-di-Cl	34	5
26	2.7	3,4,5-tri-Cl	35	0.7

dramatically as removal of the chloro group. Replacing the 3-chloro group with an electron-donating group (i.e., 3-methyl; **22**, **31**) or a better electron-withdrawing group (i.e., 3-CF₃; **23**, **32**) resulted in a decrease in affinity as shown in Table 2. Replacing the 3-chloro group with the electron-withdrawing group 3-NO₂ (i.e., **21**, **30**) resulted in slightly decreased affinity. Multiple chloro groups (i.e., 3,4-di-Cl, 3,5-di-Cl, 3,4,5-tri-Cl) increased affinity (**24-26**, **33-35**).

Based on the binding profile of several arylguanidines at 5-HT₃ receptors a pharmacophore model was developed. A few pharmacophore models for agonists and partial agonists have been developed but these were for other classes of 5-HT₃ receptor ligands.^{103,104} Dukat developed the current working pharmacophore for arylguanidines and arylbiguanides (Figure 9).⁸³ The three main components of the working pharmacophore for arylguanidines and arylbiguanides are i) an aromatic ring, ii) an adjacent nitrogen atom, N1, to the ring, and iii) a terminal amine; with distances

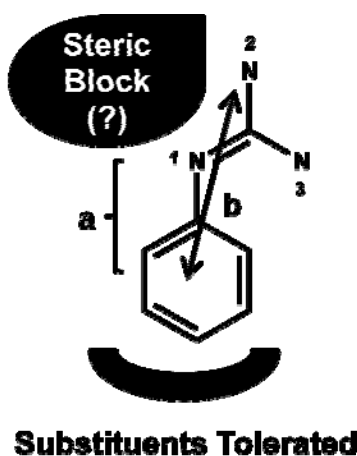


Figure 9. Dukat's pharmacophore for the binding of arylguanidines and arylbiguanides at 5-HT₃ receptors.⁸³

between the aromatic ring centroid and the adjacent nitrogen 2.7 Å (a) and the distance between the centroid and the terminal amine between 4.5 and 4.9 Å (b). Substitution at the *meta* and *para* positions are tolerated and can enhance affinity depending on their lipophilic and electronic character. Steric bulk does not seem to be tolerated near the N1 nitrogen atom.

5. Antagonists

In the late 1970s, Fozard reported metoclopramide and cocaine (which was also reported by Gaddum and Picarelli)² to be weak antagonists of the 5-HT-M receptor.¹⁰⁵ In 1983, bemesetron (MDL-72222; **9**) was first synthesized as an analog of cocaine.¹⁰⁶ Shortly after in 1985, workers at Sandoz identified tropisetron (ICS 205-930; **5**) as a 5-HT₃ receptor antagonist.⁸⁴ Since then, several hundred other compounds have been developed as 5-HT₃ receptor antagonists with a wide range of classifications.¹⁰⁷⁻¹⁰⁹ The two overarching classes are the benzamides or benzoate esters, and 6,5-heteroaromatics.

Benzoate esters (i.e., bemesetron; **9**; Figure 10) and benzamides (i.e., zacopride; **37**; Figure 10) were developed, as mentioned earlier, as analogs of cocaine.¹⁰⁵ Starting with benzoate esters, the endo isomer was found to be more active than the exo isomer.¹⁰⁶ Substitutions at the 3-position were favored over the 4-position, and a 3,5-di substituted analog (e.g., bemesetron; **9**; $pA_2 = 9.3$ rabbit heart) was found to be more active than just the 3-substituted analog (as reviewed by King).¹⁰⁸ However, the 3,5-dichlorobenzamide analog was reported to be more potent than the 3,5-dichlorobenzoate analog.¹¹⁰ Expanding further, it was found that 2-OCH₃, and 4-NH₂ groups increased potency significantly leading to zacopride (**37**; Bezold-Jarish, ID₅₀ 0.7 µg/kg i.v.) and renzapride (**38**) (Figure 9) (as reviewed by King).¹⁰⁸

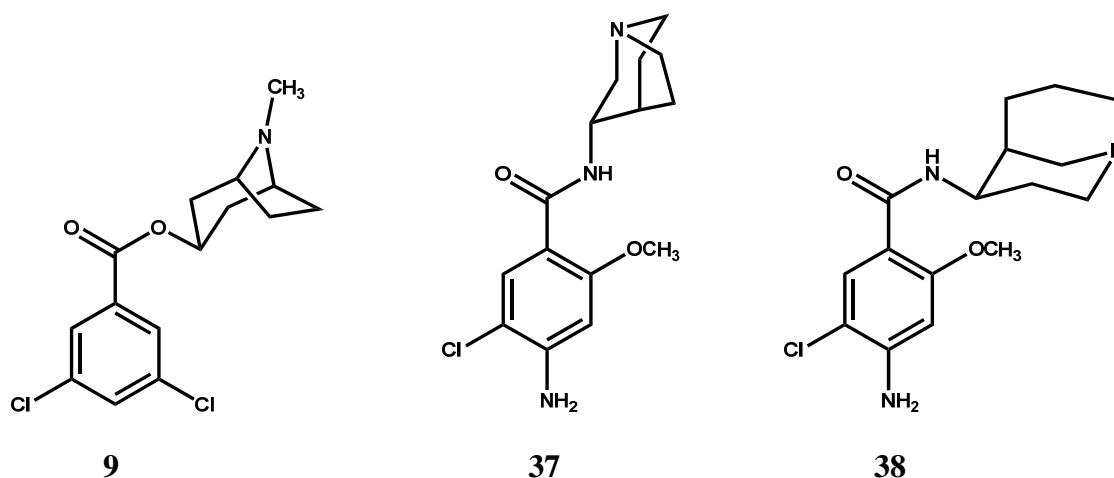


Figure 10. The structure of a few benzoate ester and benzamide 5-HT₃ receptor antagonists.

The largest class, 6,5-heteroaromatics, includes the carbazole ondansetron (**3**; $K_i \approx 7.59\text{-}7.76$ nM), the indole tropisetron (**5**; $K_i \approx 3.80\text{-}5.50$ nM) and the indazole granisetron (**4**; $K_i \approx 2.34\text{-}3.24$ nM).¹¹¹ Richardson et al. identified tropisetron (**5**) as the first highly potent 5-HT₃ receptor antagonist that includes an indole ring and an endo(tropane) side chain.⁸⁴ Variations on the side chain led to the development of dolasetron (**6**).¹⁰⁸ Modifications of the indole ring to indazole produced compounds similar to granisetron (**4**).¹⁰⁸ In the indazole series, the 1-CH₃ analog showed increased potency unlike with the indole series.¹⁰⁸ In the indolylpropanone series, substitutions of the terminal amine with -N(CH₃)₂ ($pA_2 = 6.5$, rat vagus nerve) and -imidazole ($pA_2 = 7.61$, rat vagus nerve) were shown to be active; while -pyrazole and -triazole were inactive.¹¹² Substitutions at the 2- and 4-position of the imidazole of an imidazolyl indolylpropanone were investigated to prevent interactions with Cytochrome P450.¹¹² The methyl group at the 2-position of the imidazole was shown to be the most potent N-linked imidazolyl indolylpropanone

investigated so far in the Bezold-Jarisch assay.¹¹² Conformationally constraining the carbonyl to the indole ring to form an N-linked imidazolylmethyl tetrahydrocarbazolone provided a more potent analog (i.e., ondansetron; **3**; $pA_2 = 8.6$ rat vagus nerve) than the unconstrained analog (i.e., the 2-CH₃ imidazolyl indolylpropanone analog; $pA_2 = 8.0$ rat vagus nerve).¹¹² Ondansetron (**3**) had enhanced oral activity ($ED_{50} = 7 \mu\text{g/kg}$, po) in the rat and a long duration of action (>3 h at $30 \mu\text{g/kg}$, iv) in the Bezold-Jarisch assay in the cat.¹¹² Unusually, both enantiomers of ondansetron had similar activity in vitro ((S)-enantiomer $pA_2 = 8.55$; (R)-enantiomer $pA_2 = 8.95$, rat vagus nerve).¹¹² In determining whether a N-linked imidazole was preferred, several C-linked imidazole analogs were investigated (i.e., GR65630; $pA_2 = 9.9$; alosetron; **8**; $pA_2 = 10.2$, rat vagus nerve).¹¹² This class is of particular interest since it includes all but one of the clinically available and highly selective antagonists for 5-HT₃ receptors (Figure 5). The remaining clinically available agent is a 6,6,6-heteroaromatic compound (i.e., palonosetron; **7**) (Figure 5).

6. Quantitative Structure-Activity Relationships

The concept of quantitative structure-activity relationships (QSAR) was developed by Hansch on the basis that biological activity is a function of chemical structure.^{113,114} By structure, Hansch considered the lipophilic, electronic, and steric effects of a molecule. A Hansch analysis is performed by inspecting the linear regression of the biological activity (e.g., pK_i) and various structural parameters (e.g., σ , π , MR, L, B1, B5) (Table 3). Examples of lipophilic parameters include partition coefficients (log P) and the substituent's hydrophobicity constant (e.g., π).¹¹⁵ Electronic parameters

include Hammett constants (i.e., σ_m and σ_p),¹¹⁵ dissociation constants,¹¹⁵ and dipole moments.¹¹⁶ Steric parameters include Taft's substituent constant (E_s),¹¹⁷ Verloop parameters (e.g., L, B1, B5),^{118,119} and molar refraction (MR).¹¹⁵ Molar refraction and complete molar refraction (CMR) can also be considered a polarizability parameter along with the number of valence electrons (NVE),¹²⁰ the parachor constant (Pc),¹²¹ and the polarizability values.¹²⁰

Table 3. Definition of various Hansch analysis parameters.

Parameter	Definition
π	Hydrophobicity constant ^a
σ_m	Hammett constant, electronic ^a
L	Length between substituent and parent compound ^b
B1	Shortest width of the substituent ^b
B5	Longest width of the substituent ^c
MR	Molar refraction of the substituent; ^a $\left[\frac{(n^2 - 1)}{(n^2 + 2)} \right] * [MW / \rho]$
Vol	Solvent accessible volume ^d
NVE	Number of valence electrons; ^e H = 1; C = 4; N = 5; O = 6, Halogen = 7
CMR	Complete molar refraction ^f
MV	Molar volume; ^g MW / ρ
Pc	Parachor based on surface tension and MV; ^g $\gamma^{1/4} (MW / \rho)$
Polarizability	Polarizability of the compound ^g

^aHansch, et al.¹¹⁵

^bVerloop, et al.¹¹⁸

^cTipker and Verloop¹¹⁹

^dMeasured using Chimera

^eVerma et al.¹²⁰

^fCalculated using ChemDraw

^gCalculated using ChemSketch

Comparative molecular field analysis (CoMFA) is another method of QSAR analysis. A 2001 study by Dukat et al. on the binding of arylguanidines and arylbiguanides was conducted using 33 compounds spanning a 10,000-fold K_i range.¹⁰⁰ The relationship between parallel substituted arylguanidines and arylbiguanides was nearly linear (i.e., $r = 0.932$, $n = 9$), so it was considered acceptable to use a combination of these two classes of agents in the same study.¹⁰⁰ The results showed that binding to 5-HT₃ receptors was sensitive to the electronic character of the 3-position and that the lipophilic character of the 4-position might also contribute to binding. However, these compounds are not co-planar making the two *meta*-positions different; with a sample size this small ($n = 33$) the investigators were unable to determine which *meta*-position is involved in binding.¹⁰⁰ In CoMFA studies the q^2 value is the predictability of a model based on cross-validation,¹²² and a good q^2 value is considered to be greater than 0.6.¹²³ The r^2 value is the fit of the binding affinities; the squared correlation coefficient is usually high when the ligands are well aligned. The q^2 value for this CoMFA study was 0.584 and the r^2 value was 0.851.¹⁰⁰ Based on the results 79.5% steric and 20.5% electronic effects impacted the binding at 5-HT₃ receptors.¹⁰⁰

In 2003, Glennon et al.¹²⁴ performed a QSAR study on the binding of arylguanidines and arylbiguanides at 5-HT₃ receptors. As part of this study the authors found no correlation between affinity and π_3 , but that there is some relationship between affinity and σ_m for the 3-monosubstituted arylguanidines.¹²⁴ As for the 4-monosubstituted arylguanidines it was found to be the opposite of the 3-monosubstituted compounds;

there was a relationship between affinity and the hydrophobicity constant π_4 , but not between affinity and the electronic constant σ_p .¹²⁴ Overall, the electron withdrawing nature of the 3-position substituent and the lipophilic nature of the 4-position substituent contribute to the affinity of arylguanidines.¹²⁴ In addition, the polarizability of the arylguanidines seems to play a role in the affinity of these ligands for 5-HT₃ receptors.¹²⁴

7. Behavioral Assays for Antidepressants

Because a portion of the work to be described herein involves the possible antidepressant actions of 5-HT₃ receptor ligands, it is appropriate to describe a few assays that have been used previously to evaluate possible antidepressant activity and are applicable to the current investigation.

In the late 1970's Porsolt developed a behavioral assay for the screening of antidepressants—the forced swimming test (FST).^{125,126} This test is based on the observation that a mouse placed in water swims (perceivably to escape) then alternates to a period of immobility. Antidepressants decrease the amount of time the mouse spends immobile and increase the amount of time the mouse spends swimming. However, there are a number of issues with the FST that make it less than ideal. Since the water is approximately at room temperature (23-25 °C) and the mouse's body is quite small, hypothermia can occur.¹²⁷ With this test, there is an inherent need for the animals to be able to swim; some genetically altered mice have decreased motor function and cannot swim.¹²⁸ The FST has also been shown to be ineffective in certain strains of mice (i.e., NMRI, C57BL/6J, and DBA2) for almost all known types of antidepressants.¹²⁹ In

addition, the FST has been shown to display inconsistent results regarding selective serotonin reuptake inhibitors (SSRIs).¹³⁰

The mouse tail suspension test (TST) is a behavioral assay developed by Steru et al.¹³¹ based on the observation that a mouse suspended by its tail will exhibit two types of alternating behaviors: a waiting phase characterized by immobility or passive swaying, and a searching phase characterized by running motions, body jerks, and body torsions in which the mouse attempts to catch its tail. This test, similar to the FST, is based on changes in immobility time.¹²⁶ A mouse given an antidepressant will exhibit lower immobility times than a mouse given saline; the mouse will spend more time in the searching phase. With the TST, the mice become immobile more quickly over the course of the test; in the FST, immobility generally occurs in the last half of the test, but in the TST immobility can occur at any point.¹²⁸ However, immobility periods are shorter in duration over the course of the TST.¹²⁸ Occasionally, false positives are encountered if the drug given causes an overall increase in motor activity and which can be interpreted as decreased immobility time (see below for greater detail; “Locomotor activity”). The TST also is more sensitive to lower doses of drugs.¹³¹

In the few studies reported to date, the 5-HT₃ receptor antagonists ondansetron (**3**) and bemesetron (**9**) have been shown to be active in these types of behavioral tests for antidepressants leading investigators to believe that 5-HT₃ receptors may be involved in depression.^{13,15,17} However, in two of the four FST assays, ondansetron was found to be inactive (Table 4). Bemesetron has only been examined in the TST. In one investigation,

the 5-HT₃ receptor agonist, SR 57227A, was studied both in mouse and rat FST and was found to be effective at high doses.¹⁴ Table 4 summarizes the 5-HT₃ receptor ligands that have been tested for antidepressant activity in rodents.

8. Locomotor Activity Assay

The TST and FST are only indicative of antidepressant activity. Decreased immobility time may also occur when the overall movements are increased. This increase in generalized motion can give a false positive result in the TST and FST. Using a locomotor activity assay, the overall motion can be investigated in relation to vehicle (i.e., saline). This test is conducted in square, transparent chambers surrounded by infrared photo detectors. These photo detectors are located near the floor of the chamber (~ 1.75 cm above the floor), as well as, ~ 6.5 cm above the floor of the chamber. Using the breaks in the infrared beams, a computer program identifies precisely where the mouse is located in the chamber and the type of motion. If the compound in question has increased general motion relative to the vehicle, it may indicate that the decreased immobility times of the FST or TST are not because of an antidepressive effect but to an overall increase in movement.

Table 4. 5-HT₃ receptor ligands assessed in antidepressant assays.

Compound	Species	Strain	Assay	Route of Administration ^a	Antidepressant Activity	Doses Examined	Active Dose	Ref
Ondansetron	Mice	Swiss	FST	ip	Yes	0.005-1000 µg/kg	0.01-0.1 µg/kg	¹⁵
	Mice	Swiss	TST	ip	Yes	0.005-1000 µg/kg	0.1-1 µg/kg	¹⁵
	Mice	Swiss	FST	ip	No	0.01 µg/kg	none	¹⁶
	Mice	Albino	FST	ip	Yes	0.25-2 mg/kg	0.25-2 mg/kg	¹⁷
	Mice	Swiss	FST	ip	No	0.01-0.1 µg/kg	none	¹²
Bemesetron	Mice	C57BL/6J/Han	TST	sc	Yes	0.3-3 mg/kg	3 mg/kg	¹³
SR 57227A	Mice	ICR	FST	ip	Yes	1-30 mg/kg	3-30 mg/kg	¹⁴
	Mice	ICR	FST	po	Yes	1-30 mg/kg	10-30 mg/kg	¹⁴
	Rat	Sprague-Dawley	FST	ip	Yes	1-30 mg/kg	10-30 mg/kg	¹⁴
	Rat	Sprague-Dawley	FST	po	Yes	1-30 mg/kg	10-30 mg/kg	¹⁴

^a Intraperitoneal (ip), Subcutaneous (sc), Per os (po).

III. Specific Aims and Rationale

The arylguanidine series of 5-HT₃ receptor ligands has been examined by Dukat and co-workers^{9,100,124} in the past to determine the type of substituents favored for binding. MD-354 (**2**) is a bi-planar molecule where the guanidine function is skewed relative to the aromatic ring; therefore, the *meta*-positions are non-equivalent. Several series of compounds will be synthesized to investigate the role of *meta*-position substituents in binding. One series will investigate the size of the substituent while another will investigate which *meta*-position is important.

Based on prior QSAR studies (see Background), steric and electronic effects at the 3-position, but not lipophilic effects at the 3-position, can influence the fit (i.e., affinity) of the ligand in the 5-HT₃ receptor binding pocket. These previous studies indicated *meta*-position substituents are important for binding. Since the 3-Cl analog (MD-354, **2**; $K_i = 32$ nM), which bears an electron-withdrawing substituent, binds with high affinity, but analogs with electron-donating groups, as seen with the 3-CH₃ (**31**; $K_i = 6520$ nM) and 3-OCH₃ (**39**; $K_i = 1600$ nM) analogs, bind with reduced affinity, it might be concluded that electronic effects play a significant role.¹²⁴ However, the 3-CF₃ analog (**32**; $K_i = 5700$ nM), an analog containing a stronger electron-withdrawing substituent than a chloro group, binds with reduced affinity relative to MD-354 (**2**) which may indicate that the possibility of steric interactions or bulk limitation.¹²⁴ It may be the size

or the shape of the $-CF_3$ group that detracts from binding. The $-Cl$ substituent has a spherical shape whereas a $-CF_3$ substituent does not; its shape may not be tolerated by the receptor. The $-CF_3$ group occupies a slightly larger volume of space than the $-Cl$ group (Table 5) which may also not be tolerated by the receptor. One of the aims of this project is to synthesize other 3-halogenated analogs of MD-354 (**2**) and to examine their electronic and steric effects on binding affinity. Fluoro, bromo, and iodo groups are electron-withdrawing groups and together with the $-Cl$ and $-CF_3$ groups, provide a range of electron-withdrawing substituents of graded size and relatively similar electron-withdrawing capability (Table 5). Examination of the $-F$, $-Br$, and $-I$ analogs (i.e., **42-44**), in comparison with the $-Cl$ (**2**) and $-CF_3$ (**32**) compounds (as well as with the parent unsubstituted molecule **27**), will provide information about the importance of the steric and electronic contribution of 3-position substituents to affinity. With the halogen analogs, substituent size can be varied while keeping shape and electronic character relatively constant (Figure 11). Therefore, compounds **42-44** will be synthesized and examined for comparison with **2**, **27**, and **32**.

A Hansch analysis of 3-substituted analogs might assist in determining which structural features may be important for binding at 5-HT₃ receptors. The relationship between pK_i and various parameters (i.e., π , σ , L, B1, B5, MR, complete molar refraction (CMR), volume, molar volume (MV), NVE, Pc, and polarizability) will be investigated through a Hansch analysis. Correlation coefficients from linear regression analysis would indicate the possible significance of those parameters.

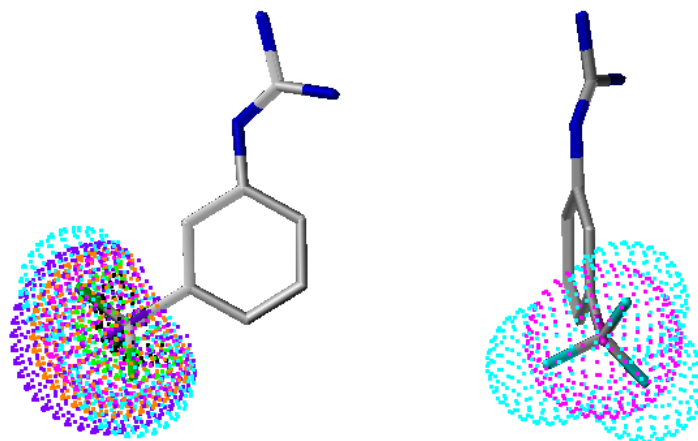


Figure 11. Superimposition of the Van der Waals surface of 3-CF₃ (cyan), 3-I (purple), 3-Br (orange), 3-Cl (pink), 3-F (green), and 3-H (black) PGs (left). Superimposition of the Van der Waals surface of 3-CF₃ (cyan) and 3-Cl (pink) PGs (right.)

Table 5. Electronic, lipophilic, and steric effects of 3-substituted arylguanidines.

	R	π^a	σ^a	Volume ^b	K_i (nM) ^c
27	H	0.00	0.00	121.7	2,340
2	Cl	0.71	0.37	144.8	35
30	NO ₂	-0.28	0.71	143.9	85
31	CH ₃	0.56	-0.07	138.3	6,520
32	CF ₃	0.88	0.43	150.5	5,700
39	OCH ₃	-0.02	0.12	145.6	1,600
40	CN	-0.57	0.56	139.2	123
41	OH	-0.67	0.12	126.8	2020
42	F	0.14	0.34	125.6	
43	Br	0.86	0.35	165.6	
44	I	1.12	0.35	197.7	

^a π and σ values as reported by Hansch et al.¹¹⁵

^b Volume is the solvent accessible volume measured using Chimera.

^c Results from a previous study.^{7,100}

Since MD-354 is bi-planar, it can exist in multiple conformations. In two of the possible rotamers, the substituents can reside at either one of two *meta*-positions (i.e., the 3- or 5-positions) (Figure 12). By constraining the guanidine function, it can be determined which of the two *meta*-positions is more important for binding (Figure 13). Constraining the guanidine to a five-membered ring (e.g., as with **45**) sharply decreased binding affinity ($K_i = 725$ nM) relative to MD-354 (**2**; $K_i = 35$ nM).⁹ Previous literature reported the synthesis of what was thought to be 2-amino-7-chloro-3,4-dihydroquinazoline (**46**);⁹ this was later shown to actually be 2-amino-6-chloro-3,4-dihydroquinazoline (**47**).¹³² In addition, 2-amino-5-chloro-3,4-dihydroquinazoline (**48**) has been synthesized previously.¹³³ Since 2-amino-7-chloro-3,4-dihydroquinazoline (**46**) has not been synthesized previously, it will be targeted for synthesis by this investigation to complete the series.

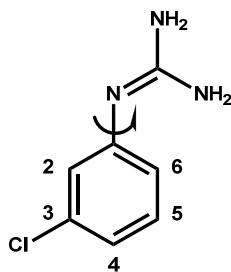
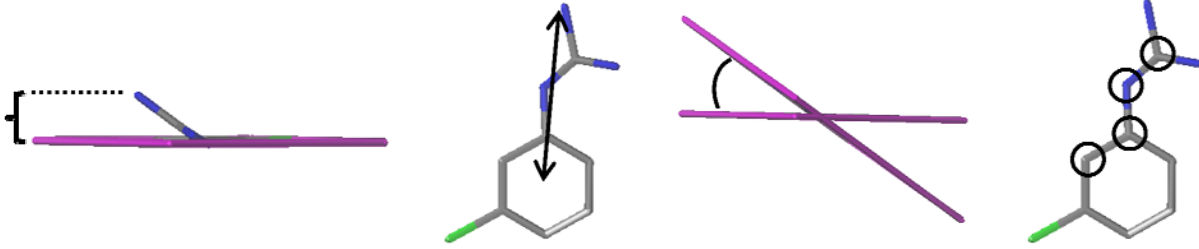


Figure 12. Representation of a rotatable bond in MD-354 (**2**).

Increasing the ring size constraining the guanidine allows for an increase in the angle of the aromatic and guanidine planes, so the seven-membered constrained analog

torsion angle (Table 6). The height above the plane for the nitrogen atoms indicate how much out of the plane of the aromatic ring the guanidine is. Since the guanidine function is in a separate plane from the aromatic ring the angle of these planes can also be calculated. The torsion angle is the twist of the molecule while going from the guanidine portion to the aromatic ring.

Table 6. Measurements of biplanarity of MD-354 and its constrained analogs.



Compound	Amine height above plane	Aromatic centroid to primary amine distance	Plane angle	Torsion angle
2	0.21683 Å	5.122 Å	34.91°	149.9°
45	0.00327 Å	4.537 Å	0.06°	180.0°
46 - 48	0.16662 Å	5.042 Å	8.48°	189.9°
49	0.24949 Å	5.133 Å	7.13°	184.4°

Another goal of this work will be to confirm whether or not 5-HT₃ receptor ligands produce an antidepressant effect in animals. Depression has a life-time prevalence of 17% in the United States.¹³⁴ Current treatments for depression are fully effective for 30% of patients.¹³⁵ The antidepressants currently available (i.e., tricyclic antidepressants (TCAs), selective serotonin reuptake inhibitors (SSRIs), and serotonin-norepinephrine reuptake inhibitors (SNRIs)) have a long onset of action (usually two or more weeks).^{136,137} These drawbacks indicate a need for a new understanding on how to treat

depression. Although studies are scant, two 5-HT₃ receptor antagonists (i.e., ondansetron and bemesetron) and the 5-HT₃ receptor agonist (i.e., SR 57227A) have been shown to behave as potential antidepressants in animal studies (Table 4). If 5-HT₃ receptors play a role in depression then different structural classes of 5-HT₃ receptor agents or different receptor interactions may be able to elicit the same response. To determine if the novel series of quinazoline ligands behaves in the same manner, several analogs will be tested using the mouse tail suspension test for antidepressant activity. The parent compound, MD-354 (**2**), will also be tested. Tricyclic antidepressants (i.e., desipramine and imipramine), an SSRI (i.e., fluoxetine), and a 5-HT₃ receptor antagonist (i.e., ondansetron) will be used as controls. Statistical analysis will be performed to determine the statistical significance of any decreases in immobility time relative to saline using a one-way analysis of variance (ANOVA) test. Overall locomotor activity will be examined at any doses of those drugs that display significantly lower immobility times than saline to determine if the effect is because of hyperactivity or not.

A recurring issue with most 5-HT₃ receptor ligands is their inability to cross the BBB. Compounds with log P values ranging from 1.5 to 2.5 generally can penetrate the BBB.¹³⁸ MD-354 (**2**), PG (**27**), 3,4,5-tri-Cl-PG (**35**) and mCPBG (**17**) have been shown to have log P values of -0.64, -1.32, 1.16, and -0.38, respectively, by the shake-flask method of measuring the concentration of drug in the aqueous layer of an aqueous 1-octanol solution, which would indicate that these compounds should not be able to readily cross the BBB.⁹ Supporting this, Bachy et al.⁹¹ showed that PBG and mCPBG

were unable to displace [^3H]granisetron in an ex vivo study indicating that arylbiguanides probably do not cross the BBB. In contrast, Kilpatrick and Rogers⁹⁸ showed that mCPBG was able to displace [^3H]GR65630 in rat entorhinal cortex ex vivo and Steward et al.⁹⁹ used [^3H]mCPBG to label 5-HT₃ receptor recognition sites in the rat brain. These last two studies indicate that the arylbiguanide mCPBG does cross the BBB. Because the data are controversial, a new method is needed to determine if arylguanidines and arylbiguanides cross the BBB. Using ChemDraw to predict log P values, the predicted log P value for mCPBG is 1.28, which indicates that it is slightly too low for mCPBG to easily cross the BBB, supporting the shake-flask data. Whereas, the predicted log P value for MD-354 is 1.43, which is closer to the threshold for easily crossing the BBB. Both of these predicted values are much higher than the shake-flask data. The determination of log P values using the shake-flask method is time consuming, requires a large amount of sample, and is subject to errors (i.e., sample impurities, inability to detect the sample, dissociation, decomposition, and stable emulsion formation).¹³⁹ In addition, very high and very low partition compounds cannot be measured through the shake flask method.¹³⁹

Another method of determining the log P value is through the relative retention times using high performance liquid chromatography (HPLC) which requires much smaller quantities of sample and provides for better detection. The retention times of several compounds (i.e., imidazole, acetanilide, benzophenone, naphthalene, and diphenylamine) are determined relative to the retention time of uracil for various concentrations of aqueous acetonitrile. Values for the log of the capacity factor (k') are

calculated for each of these compounds at varying concentrations of acetonitrile and water ($\log k' = \log \left[\frac{(t_R - t_0)}{t_0} \right]$).¹⁴⁰⁻¹⁴² For each compound, a plot of $\log k'$ versus the concentration of acetonitrile is used to calculate the $\log k'_w$ (i.e., the log of the capacity factor in 100% water).¹⁴⁰⁻¹⁴² These $\log k'_w$ values can be plotted against experimental $\log P$ values from the literature to construct a standard curve. By identifying the $\log k'_w$ value of unknown compounds the $\log P$ value can be determined using the standard curve obtained from the known compounds. This method will be implemented to determine the $\log P$ values of mCPBG and several arylguanidines.

Different homology models of the h5-HT_{3A} receptor can be built through various modes of construction. Each program uses different methods for developing models. Using the Biopolymer package of Sybyl, residues of a template can be mutated to the sequence of the target receptor. This is followed by optimizing the side-chain orientation with SCRWL. Another method is to use an alignment of the template and the sequence of the target, and allowing the program Modeller to generate multiple models at one time. By using docking programs (e.g., GOLD and AutoDock) and different standards, the models can be validated by mutagenesis data. Since arylguanidines have not been generally studied as a class of 5-HT₃ receptor ligands, their possible binding modes have yet to be determined. In the present study, 5-HT₃ receptor models will be constructed and docking studies performed with both GOLD and AutoDock. Based on the docking poses

of MD-354 and 5-HT, new ligands might be developed which encompass structural features that are beneficial for each.

To summarize, the specific aims of the present work are:

- a) to synthesize various halogen-substituted arylguanidines,
- b) to determine the structural features important for binding through a Hansch analysis,
- c) to synthesize conformationally constrained arylguanidines,
- d) to evaluate the possible antidepressant activity of selected agents through the mouse tail suspension test,
- e) to determine the log P value of various arylguanidines, and
- f) to construct and validate a homology model of the 5-HT₃ receptor.

Overall, the aims of these studies are the rational design and synthesis of novel 5-HT₃ receptor agents that enter the brain, and an initiation of their pharmacological action.

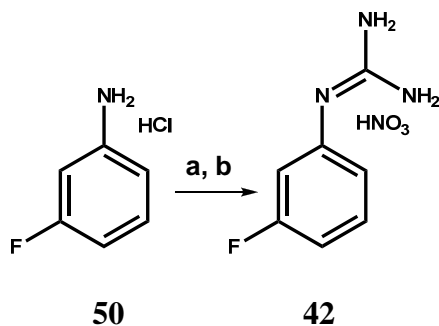
IV. Results and Discussion

A. Halogen Series

1. Synthesis of *N*-(3-Fluorophenyl)guanidine Nitrate (**42**)

N-(3-Fluorophenyl)guanidine nitrate (**42**), was synthesized in the same manner as MD-354 (**2**) (Scheme 1).¹⁴³ *N*-(3-Bromophenyl)guanidine nitrate (**43**) and *N*-(iodophenyl)guanidine nitrate (**44**) analogs were previously synthesized in our laboratory¹³² as nitrate salts and were available for our studies. The hydrochloride salt of the aniline was allowed to react with cyanamide in ethanol and heated at reflux. The hydrochloride salt of the arylguanidine was converted to the nitrate salt (i.e., **42**) with ammonium nitrate. The structure was confirmed by IR spectrometry, ¹H NMR spectrometry, and elemental analysis for C, H, N.

Scheme 1.^a

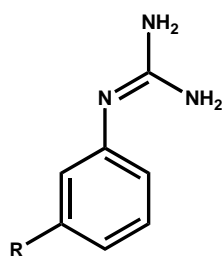


^aReagents and conditions: a. H₂NCN, EtOH, reflux; b. NH₄NO₃, H₂O.

2. Binding Studies

The three new arylguanidine analogs (**42-44**) were evaluated and MD-354 (**2**) was re-evaluated for binding affinity at recombinant mouse 5-HT_{3A} receptors (Table 7) using [³H]LY 278,584. The -Br (i.e., **43**) and -I (i.e., **44**) analogs were found to bind with the highest affinity. MD-354 (**2**) was found to bind with a somewhat lower affinity than previously reported for binding affinity at cloned human 5-HT_{3AB} native receptors.⁷ Based on these results it can be concluded that the size of the electron-withdrawing substituent possibly plays a role in how well these compounds bind to the 5-HT₃ receptor since compounds with smaller *meta*-substituents (i.e., -H (**27**; $K_i = 2340$ nM) and -F (**42**)) bind with decreased affinity and compounds with larger *meta*-substituents (i.e., -Br (**43**) and -I (**44**)) bind with increased affinity compared to the parent compound, MD-354 (**2**).

Table 7. Binding affinity of halogen series at the mouse 5-HT_{3A} receptors.



	R	K_i (nM)	(SEM)
42	F	1420	(105)
2	Cl	166	(16)
43	Br	81	(10)
44	I	40	(5)

This is the reverse of what was expected and suggests that *meta*-substituents larger in size than a chloro group are tolerated by the receptor. Since the $-\text{CF}_3$ analog binds with lower affinity at the 5-HT₃ receptors than any of the mono-halogenated analogs, but takes up less volume than $-\text{Br}$ and $-\text{I}$ it may be concluded that it is the shape and not necessarily the size of the $-\text{CF}_3$ group that interferes with binding. The halogen substituents are spherical but the $-\text{CF}_3$ substituent is not; a more spherical shape might be more tolerated. It might be noted that for the simple halogenated analogs shown in Table 7, affinity increases as the lipophilicity (i.e., π value; see Table 5) increases. Likewise, affinity increases as substituent volume (see Table 5) increases. For example, there is a relationship between $\text{p}K_i$ and π ($r = 0.997$, $n = 4$; Figure 14) as well as with volume ($r = 0.920$, $n = 4$; Figure 14). This trend holds if phenylguanidine **27** is included ($r = 0.998$, $n = 5$; $r = 0.934$, $n = 5$; Figure 14). However, there are too few observations to draw any reliable conclusions.

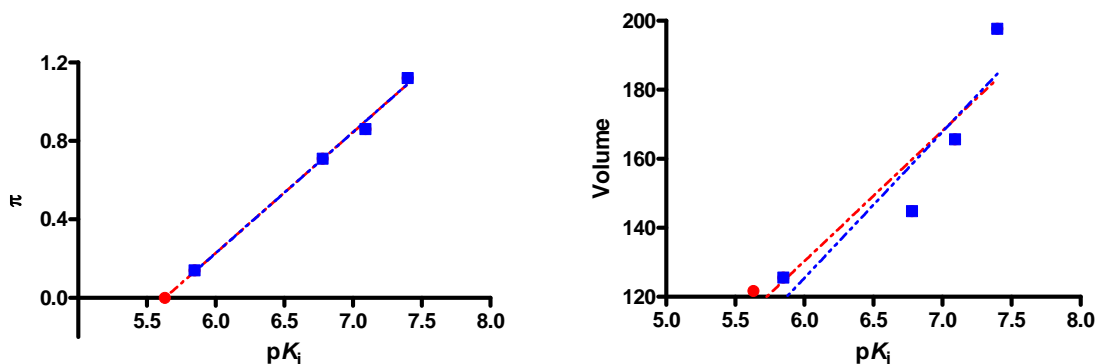


Figure 14. Linear regression plots of $\text{p}K_i$ versus π (left) and volume (right). The analyses including the unsubstituted compound **27** are shown in red, excluding the unsubstituted compound are shown in blue.

3. Hansch Analysis

A Hansch analysis was performed on the 3-position monosubstituted arylguanidines to better identify electronic and steric effects that might be influencing their binding to the 5-HT₃ receptor. The analysis was performed on the parameters (i.e., π , σ , L, B1, B5, MR, CMR, volume, MV, NVE, Pc, and polarizability) (Table 8) versus affinity (i.e., pK_i). A linear regression analysis (Table 9) of each of these individual parameters using GraphPad Prism against pK_i revealed statistically significant correlations ($p < 0.05$) with the electronic factor σ ($n = 11$, $r = 0.730$, $F = 10.25$; eq 2, Table 9; Figure 15), polarizability ($n = 11$, $r = 0.704$, $F = 8.86$; eq 12, Table 9; Figure 16), solvent accessible volume ($n = 11$, $r = 0.656$, $F = 6.80$; eq 7, Table 9; Figure 16), and complete molar refraction (CMR) ($n = 11$, $r = 0.670$, $F = 7.31$; eq 9, Table 9; Figure 17). These linear regression analyses indicate that the electronic effect of the substituent, the polarizability of the molecule, the solvent accessible volume of the substituent, or the complete molar refraction of the molecule may play a role in how well the arylguanidines bind to the 5-HT₃ receptor.

Internal correlations between parameters can lead to collinearity. Multicollinearity may be or is a problem for these compounds with volume and polarizability ($r = 0.742$, $n = 11$), CMR and polarizability ($r = 0.757$, $n = 11$), and volume and CMR ($r = 0.704$, $n = 11$)—since these three parameters are intercorrelated with each other it is expected that there is a problem with multicollinearity.

Table 8. Hansch analysis of the 5-HT₃ receptor binding of 3-substituted arylguanidines.

R	pK_i^a	π^b	σ_m^b	L^b	$B1^b$	$B5^b$	MR^b	Vol^b	NVE^b	CMR^b	MV^b	Pc^b	Polarizability ^b
27 H	5.631	0.00	0.00	2.1	1.0	1.0	1.03	122	52	4.08	115	304	15.51
2 Cl	6.780	0.71	0.37	3.5	1.8	1.8	6.03	145	58	4.57	124	333	17.33
30 NO ₂	7.071	-0.28	0.71	3.4	1.7	2.4	7.36	144	68	4.69	120	349	17.75
31 CH ₃	5.186	0.56	-0.07	3.0	1.5	2.0	5.65	138	58	4.54	130	335	17.26
32 CF ₃	5.613	0.88	0.43	3.3	2.0	2.6	5.02	151	76	4.59	145	358	17.39
39 OCH ₃	5.796	-0.02	0.12	4.0	1.4	3.1	7.87	146	64	4.70	137	354	17.81
40 CN	6.910	-0.57	0.56	4.2	1.6	1.6	6.33	139	60	4.56	128	350	18.10
41 OH	5.695	-0.67	0.12	2.7	1.4	1.9	2.85	127	58	4.15	112	310	15.85
42 F	5.484	0.14	0.34	2.7	1.4	1.4	0.92	126	58	4.10	118	304	15.46
43 Br	7.092	0.86	0.39	3.8	2.0	2.0	8.88	166	58	4.86	127	347	18.51
44 I	7.398	1.12	0.35	4.2	2.2	2.2	13.9	198	58	5.39	132	367	20.53

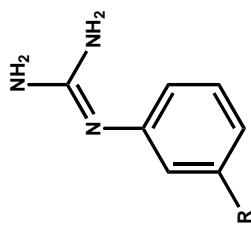
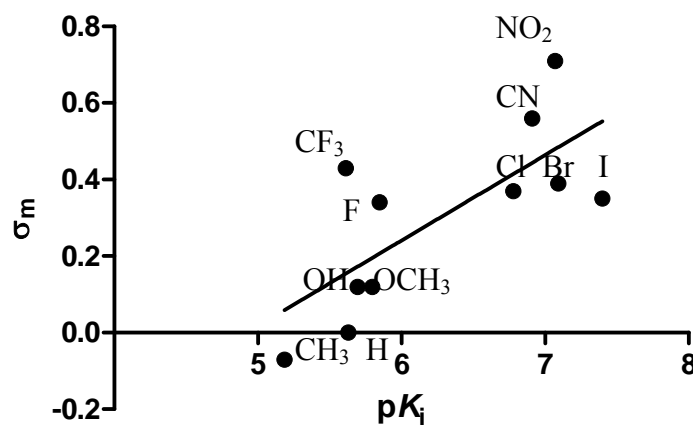
^a Binding data from Tables 5 and 7.^{7,100}^b See Table 4 for description of parameters.

Table 9. Linear regression analysis results ($n = 11$).

Equation	$pK_i =$	r
1	$0.1467(\pm 0.2599)\pi - 0.6721(\pm 1.642)$	0.185
2	$0.2230(\pm 0.06967)\sigma - 1.098(\pm 0.4401)$	0.730
3	$2.583(\pm 1.381)MR - 10.77(\pm 8.724)$	0.529
4	$0.2399(\pm 0.4358)L + 1.333(\pm 2.753)$	0.181
5	$0.3214(\pm 0.1425)B1 - 0.2826(\pm 0.9004)$	0.601
6	$1.085(\pm 0.7941)B5 - 3.850(\pm 5.017)$	0.414
7	$18.07(\pm 6.932)volume + 32.04(\pm 43.80)$	0.656
8	$-0.2806(\pm 2.779)NVE + 62.49(\pm 17.56)$	0.034
9	$0.3263(\pm 0.1207)CMR + 2.519(\pm 0.7624)$	0.670
10	$0.1198(\pm 4.232)MV + 125.5(\pm 26.74)$	0.009
11	$14.82(\pm 8.242)Pc + 244.3(\pm 52.07)$	0.514
12	$1.334(\pm 0.4484)polarizability + 9.036(\pm 2.833)$	0.704

**Figure 15.** Linear regression plot of pK_i versus σ_m ($r = 0.730$; eq 2; Table 9).

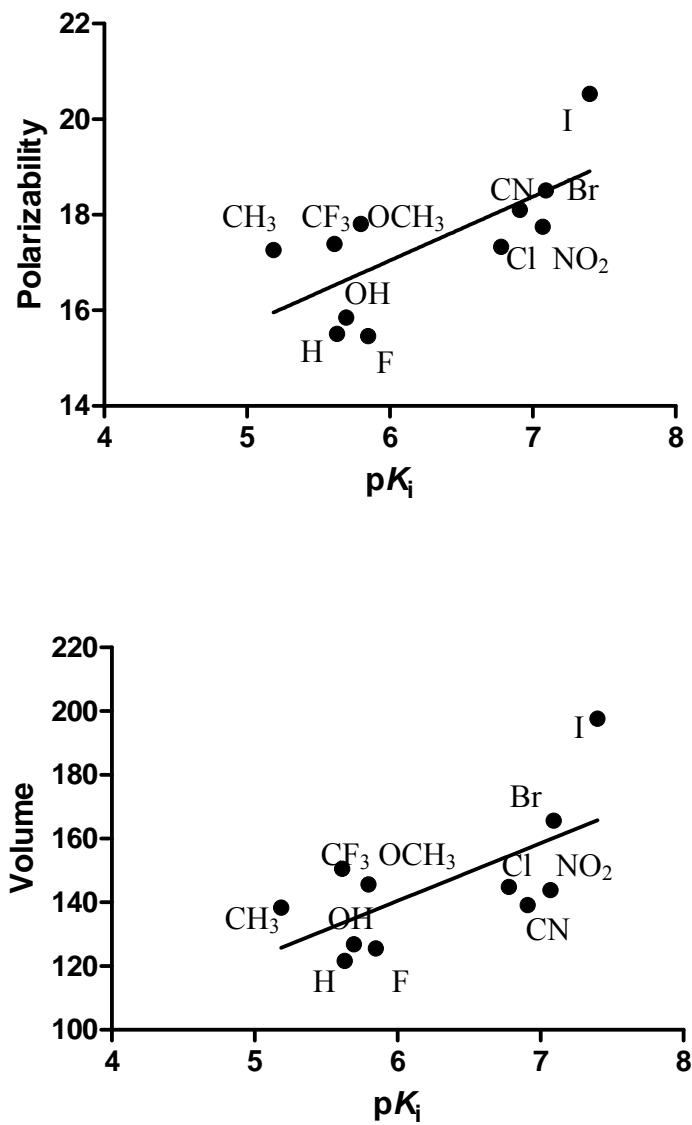


Figure 16. Linear regression plots of pK_i versus polarizability ($r = 0.704$; eq 12; Table 9) (top) and pK_i versus volume ($r = 0.656$; eq 7; Table 9) (bottom).

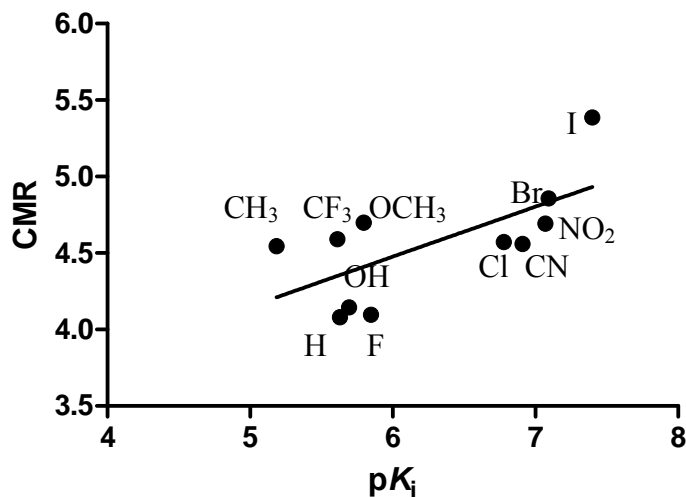


Figure 17. Linear regression plot of pK_i versus CMR ($r = 0.670$; eq 9; Table 9).

In order to obtain statistically relevant results for each parameter analyzed, data on at least six compounds are required. Using compounds **2**, **27**, **30-32**, **39-44**, there are only eleven compounds and, therefore, only one variable can be investigated with statistical significance. Despite lacking statistical rigor, inclusion of a second variable might provide some clues as to which variables are simultaneously affecting binding affinity. A multiple linear regression analysis was performed using GraphPad's InStat program on σ , volume, CMR, and polarizability versus pK_i (Table 10). There is no internal correlation between volume ($r = 0.851$, $n = 11$), CMR ($r = 0.855$, $n = 11$), or polarizability ($r = 0.867$, $n = 11$) and σ ; since they are independent of each other, any relationship of σ and the other three parameters may show an actual relationship together with the binding affinity. There is a good correlation ($p < 0.01$) with σ and polarizability

versus pK_i ($n = 11$, $r = 0.867$, $F = 12.05$; eq 15, Table 10), σ and volume versus pK_i ($n = 11$, $r = 0.851$, $F = 10.54$; eq 16, Table 10), and σ and CMR versus pK_i ($n = 11$, $r = 0.855$, $F = 10.86$; eq14, Table 10). Based on the results of these analyses, the electron-withdrawing nature and the size, polarizability, or volume of the substituent at the 3-position impact binding affinity. Since there are multiple linear regression correlations, the later three parameters are impacting binding affinity and not just one individual parameter.

Table 10. Multiple linear regression analysis results ($n = 11$).

Equation	$pK_i =$	r
13	$-2.010CMR + 0.9141polarizability - 0.4960$	0.757
14	$1.749\sigma + 1.118CMR + 0.6070$	0.855
15	$1.648\sigma + 0.3036polarizability + 0.4594$	0.867
16	$1.846\sigma + 0.01917volume + 2.893$	0.851
17	$-0.005657volume + 0.4817polarizability - 1.320$	0.742
18	$-0.001501volume + 1.578CMR - 0.7439$	0.704

In agreement with Glennon et al.,¹²⁴ this study has shown with different compounds that the electronic character at the 3-position is important for binding arylguanidines to the 5-HT₃ receptor. Dukat et al.¹⁰⁰ has shown previously that electronic effects account for nearly 20% and that steric effects account for nearly 80% of binding of arylguanidines and arylbiguanides at the 5-HT₃ receptor. This study is in agreement with Dukat and co-worker's¹⁰⁰ study as shown by the correlation between σ and binding affinity and it has been shown that the volume and complete molar refraction (CMR), both of which can be viewed as steric factors, provide statistically significant correlations

with binding affinity. In addition, the polarizability of the molecule, as shown by the polarizability factor and CMR, also display significant correlations. In this study the volume may be acting as a surrogate for the polarizability or the polarizability as a surrogate for the volume. One way to examine this possibility would be to synthesize and include in future analyses a compound with a substituent that has relatively low volume and relatively high polarizability (e.g., (3-cyclohexylphenyl)guanidine has a substituent volume of 201.3 and a polarizability of 25.46 or 2-(3-(prop-1-ynyl)phenyl)guanidine has a substituent volume of 154.1 and a polarizability of 20.92).

4. Log P Analysis

The retention times on a nitrile reversed-phase high performance liquid chromatography (HPLC) column of uracil, imidazole, acetanilide, benzophenone, naphthalene, and diphenylamine were determined in triplicate at various concentrations of aqueous acetonitrile (i.e., 40%, 50%, 60%, 70% acetonitrile). From the retention times of the above standards relative to uracil (i.e., $t_R - t_0$; where t_R = retention time of the standard and t_0 = retention time of uracil), the log of the capacity factor (i.e., $\log k' = \log[(t_R - t_0)/t_0]$) was determined for each of the standards. A plot of $\log k'$ versus the concentration of acetonitrile was constructed (shown for benzophenone in Figure 18) and a linear regression analysis performed. Using the equation for each plot the lines for each standard could be extrapolated and the log of the capacity factor at 0% acetonitrile could be determined ($\log k'_w$). The $\log k'_w$ values for each of the standards

(i.e., imidazole, $\log k'_w = -0.88$; acetanilide, $\log k'_w = 0.06$; benzophenone, $\log k'_w = 1.18$; naphthalene, $\log k'_w = 1.06$; and diphenylamine, $\log k'_w = 1.38$) were plotted against the literature shake-flask $\log P$ values ($\log P = -0.08, 1.16, 3.30, 3.18, 3.50$; respectively) giving a standard curve for this particular column (Figure 19). A linear regression analysis of this data calculated an equation for the line of $\log P = 1.660 \log k'_w + 1.285$ ($r = 0.996, F = 346.4$).

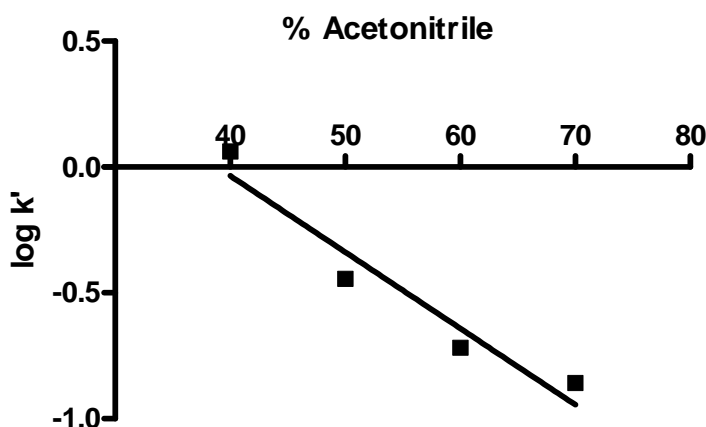


Figure 18. Plot of $\log k'$ of benzophenone versus concentration of aqueous CH_3CN .

The retention times of PG (**27**), MD-354 (**2**), 3-FPG (**42**), 3-BrPG (**43**), 3-IPG (**44**), 3,4,5-tri-Cl-PG (**35**), and mCPBG (**17**) were determined at various concentrations of aqueous acetonitrile (i.e., 55%, 65%, 75% acetonitrile). Based on the retention times relative to uracil, the log of the capacity factor was calculated for each of the compounds. The capacity factors were plotted against the concentration of acetonitrile and a linear

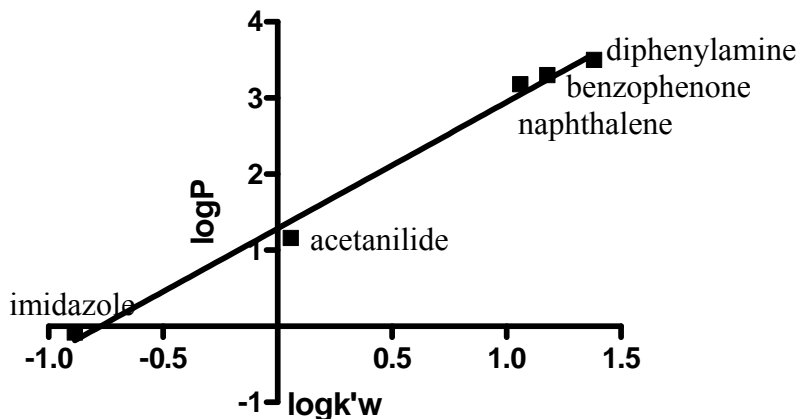


Figure 19. Plot of literature $\log P$ values from shake-flask data¹⁴⁴ versus $\log k'_w$ values.

regression analysis was performed (Figure 20). Based on this analysis the line from each plot could be extrapolated and the capacity factors at 0% acetonitrile (i.e., $\log k'_w$) could be determined (Table 11). As long as the same general range of concentration of acetonitrile was used the exact concentrations need not be the same with the standards and unknowns since the true value of interest is found based on the extrapolation to 0% acetonitrile—as if the compound was eluted in water only. The $\log k'_w$ value at 0% acetonitrile (i.e., $\log k'_w$) cannot actually be determined since running the HPLC column in pure water is ill-advised since it may destroy the column. Based on the capacity factors determined for 0% acetonitrile, the $\log P$ values for each of these compounds was calculated based on the standard curve (Table 11).

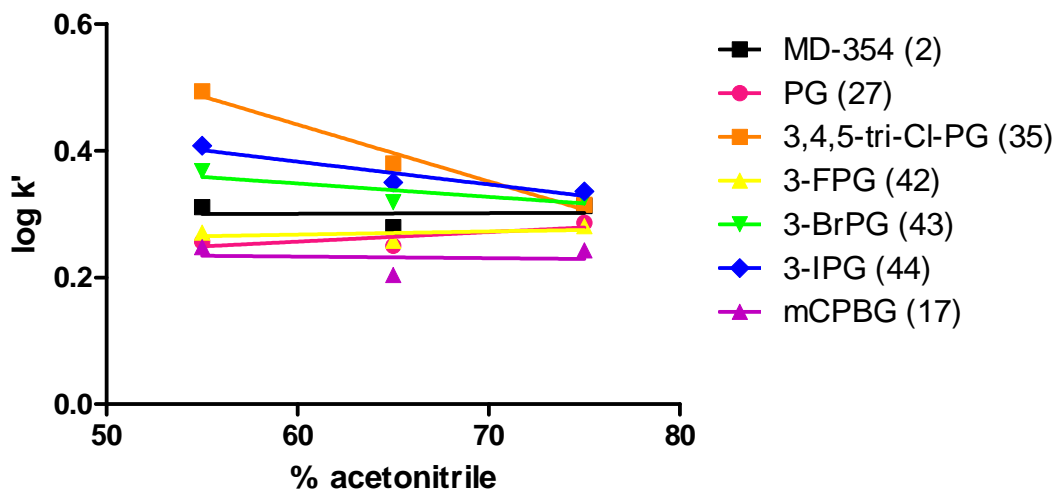


Figure 20. Plot of $\log k'$ of various arylguanidines and mCPBG versus concentration of aqueous CH_3CN .

Table 11. Capacity factors ($\log k'_w$) determined by linear regression and calculated/determined $\log P$ values for the selected arylguanidines and an arylbiguanide.

Compound	$\log k'_w$	Predicted $\log P^a$	Actual $\log P$ (shake-flask) ^b	Actual $\log P$ (HPLC)
27	0.1665 ± 0.0794	0.87	-1.32	1.56
2	0.2945 ± 0.1248	1.43	-0.64	1.77
42	0.2375 ± 0.0681	1.03	--	1.68
43	0.4742 ± 0.1059	1.70	--	2.07
44	0.5987 ± 0.0832	2.22	--	2.28
35	0.9781 ± 0.0927	2.54	1.16	2.91
17	0.2479 ± 0.1570	1.28	-0.38	1.70

^a Predicted using ChemDraw.

^b Results from a previously published study.⁹

As mentioned earlier, compounds with $\log P$ values ranging from 1.5 to 2.5 should readily penetrate the BBB.¹³⁸ Based on these results, most of these arylguanidines should be able to cross the BBB. The results obtained by relative retention times using

HPLC were consistent with the predicted log P values from ChemDraw ($r = 0.957$) and with the previous studies indicating that mCPBG (**17**) crosses the BBB.^{98,99} The study by Bachy et al.⁹⁷ that indicated mCPBG could not cross the BBB used a different radioligand (i.e., [³H]granisetron versus [³H]GR65630), a larger dose (i.e., 2 and 10 mg/kg versus 0.1-1.0 mg/kg), a longer time between injection and removal of the brains (i.e., 30 min versus 5 min), and a different species (i.e., mouse versus rat). Any of these differences may account for the difference in results between the two laboratories. Furthermore, given the evidence that mCPBG (**17**) can penetrate the BBB through ex vivo inhibition and radioligand binding, it would seem likely that the halogenated arylguanidines **2**, **42**, **43**, and **44** should also be capable of such. This method of determining log P values seems to be more accurate when compared to the predicted values than the shake-flask method.

5. Molecular Modeling

Homology models were constructed by two different methods (i.e., Method A and Method B). In both cases the models were developed from an alignment between the N-terminal domain of the h5-HT3A sequence and the sequence of three AChBP's, the N-terminal domain of a nACh receptor $\alpha 1$ subunit bound to α -bungarotoxin, the N-terminal domains of three different GABA_A receptor subunits, the N-terminal domains of two different GABA_C receptor subunits, the N-terminal domain of two different glycine receptor subunits, and the N-terminal domain of the mouse 5-HT3A receptor. This alignment was performed using ClustalX to identify conserved residues within the

different LGICs; specifically W90, W183, Y234, and the two cysteines forming the Cys-loop.

Method A. Using Sybyl's (version 7.3) Biopolymer package, the $\alpha 1$ subunit of a nACh receptor (PDB 2qc1)⁴² was mutated to the sequence of the h5-HT3A receptor using the conserved residue alignment to identify where insertions and deletions were needed. This single subunit was minimized using the Amber force field and Amber charges. The program, SCWRL, was used to optimize side chain orientations. ProCheck was run on the single subunit to create a Ramachandran plot (Figure 21) to identify amino acid residues in most favored (red field), additionally allowed (dark yellow), generously allowed (lighter yellow), and disallowed (white) regions. The Ramachandran plot indicated that 86.8% of amino acid residues were in the most favored regions, 12.6% of residues were in the additionally allowed regions, and only 0.5% of residues were in the disallowed regions. The one amino acid shown in the disallowed region is facing into the pore and does not interact with the binding pocket so it has no impact on the docking. Using the backbone of an AChBP (PDB 1i9b)³⁸ for orientation in space of two protomers, since it is a pentameric structure, a dimer of the h5-HT3A protomer was constructed.

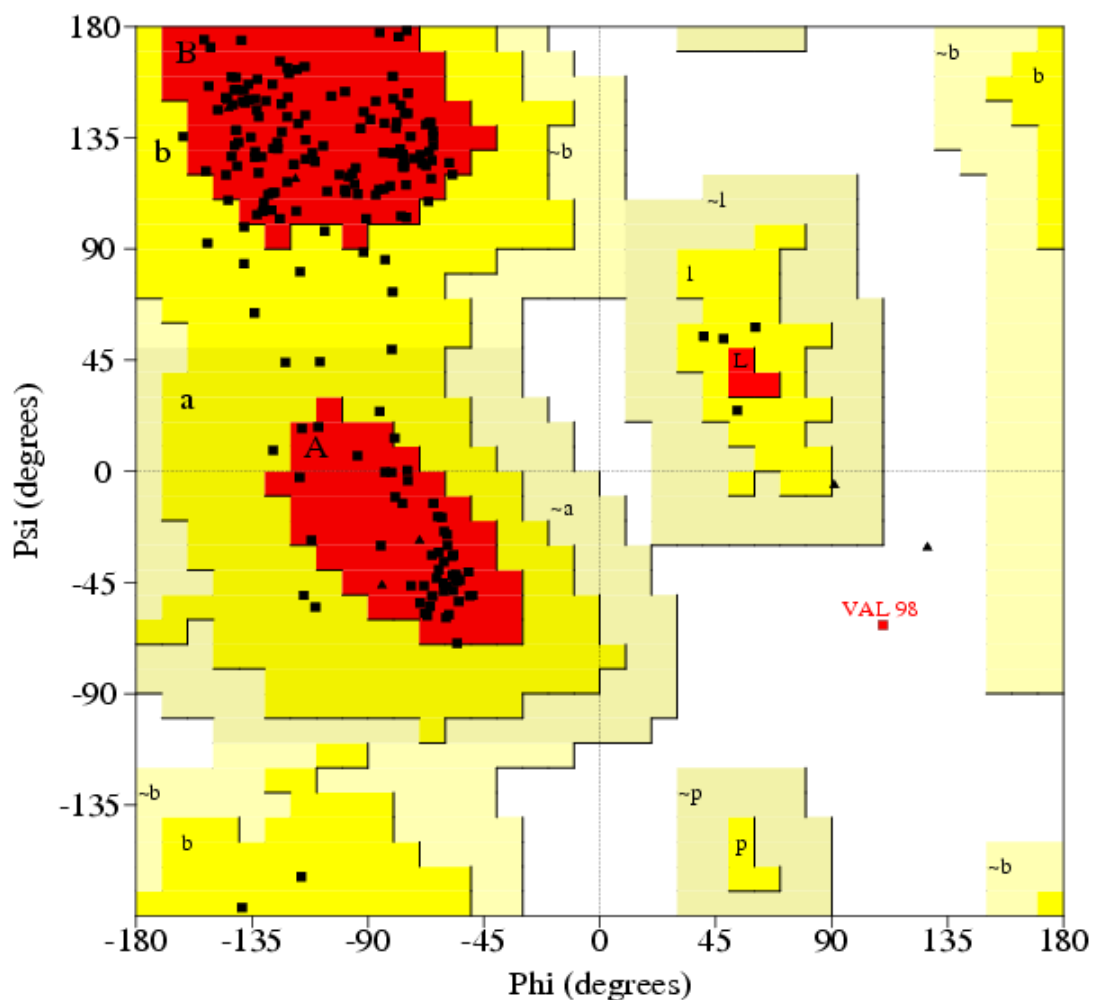


Figure 21. Ramachandran plot of a single subunit of the h5-HT3A receptor model developed using Sybyl's Biopolymer package (Method A).

The ligand 5-HT (**1**) was built in Sybyl 7.3 and given AM1-BCC charges and geometries from MOPAC. AM1-BCC charges are quantum mechanical charges that have bond correction charges (BCC) that allow for accurate charges of small molecules within the Amber force field. Using Gold 3.1, 5-HT was docked with 20 genetic algorithm runs in a 15 Å sphere around W183 to the interface between the two protomers. The proposed

binding mode of 5-HT (Figure 22) was consistent with the literature as the aliphatic amine is situated in the binding pocket in a way that it is directed towards the aromatic rings of W183 and Y234 and possibly capable of forming the cation- π bond as reported in the literature.^{101,145,146}

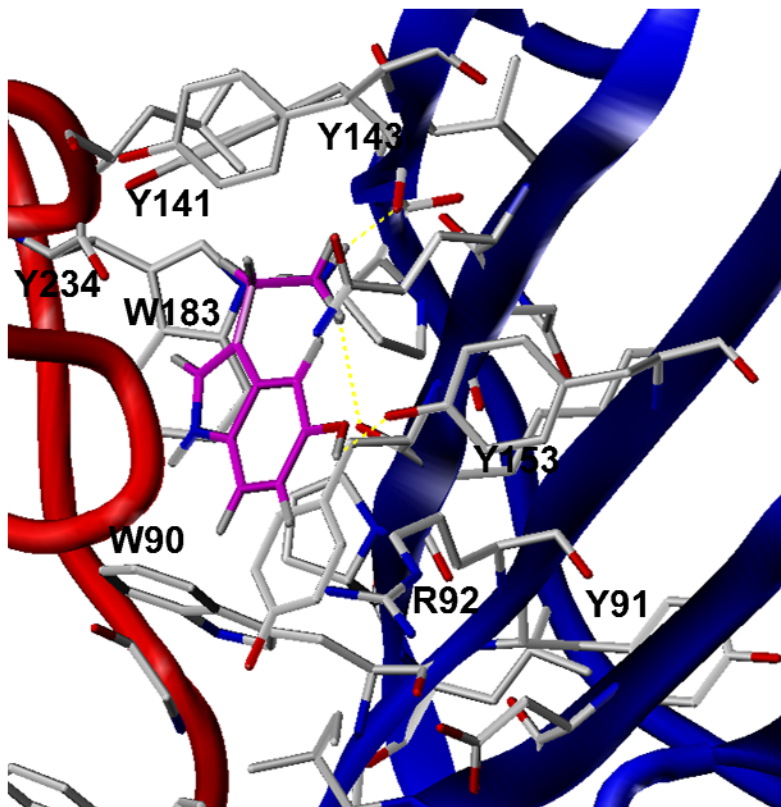


Figure 22. Proposed binding mode of serotonin (5-HT; **1**) in the h5-HT3A receptor model developed using Sybyl's Biopolymer package (Method A). 5-HT (**1**) is in magenta and the side chains of residues within 5 Å of the ligand are shown.

Since the proposed binding mode of 5-HT is relatively similar to that in the literature,^{101,145,146} MD-354 (**2**) was built and docked to the receptor model in the same manner as 5-HT (Figure 23). The proposed binding mode of MD-354 is similar to 5-HT

in that the guanidine portion of MD-354 overlaps with the aliphatic amine of 5-HT and is possibly interacting with W183, Y234, and Y143.

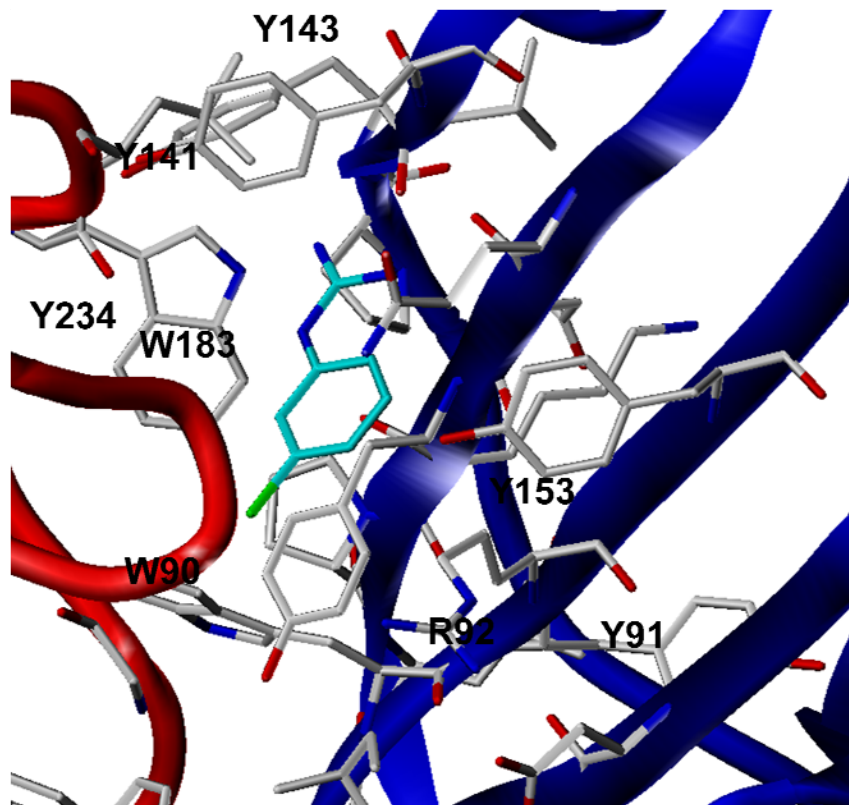


Figure 23. Proposed binding mode of MD-354 (**2**) to the h5-HT3A receptor using Sybyl's Biopolymer package (Method A). MD-354 (**2**) is in cyan and the side chains of residues within 5 Å of the ligand are shown.

The overlap of MD-354 (**2**) and 5-HT (**1**) is depicted in Figure 24; based on these proposed binding modes to this model, a new ligand was designed taking into account features both from 5-HT and MD-354. From the overlap of 5-HT and MD-354, it appears that the addition of a hydroxyl group to the aromatic ring of MD-354 in the 4-position

would enhance binding (Figure 24). The hydroxyl group of this designed ligand may be able to interact with Y153.

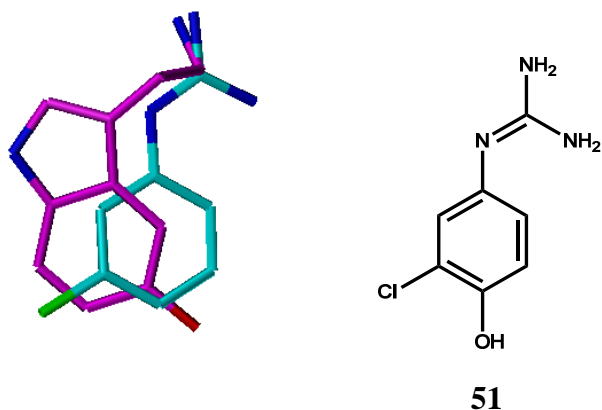


Figure 24. Overlap of 5-HT (**1**) and MD-354 (**2**) from the proposed binding modes to the h5-HT3A receptor developed using Sybyl's Biopolymer package (Method A) (left). The designed ligand *N*-(3-chloro-4-hydroxyphenyl)guanidine (right).

Method B. The homology model constructed through Sybyl (Method A) is crude and rigid, so another method for developing a homology model was explored. An alignment of AChBP (PDB 1i9b)³⁸, $\alpha 1$ nACh (2qc1)⁴², and h5-HT3A based on the conserved residue alignment was used to create ten initial pentameric models from five separate random seeds using the program Modeller 9.3. The program then generated ten loop models from each of the initial models, to create a total of 100 unique models. These models were given Kollman charges then minimized using NAMD, first with the backbone constrained then with the backbone unconstrained. Using AutoDock4, the ligand 5-HT (**1**), with the charges and geometries generated by MOPAC, was docked to

each of the five interfaces of each of the models with 20 genetic algorithm runs in a 40 Å x 40 Å x 40 Å region around the C-loop (Figure 25). Based on poses consistent with the

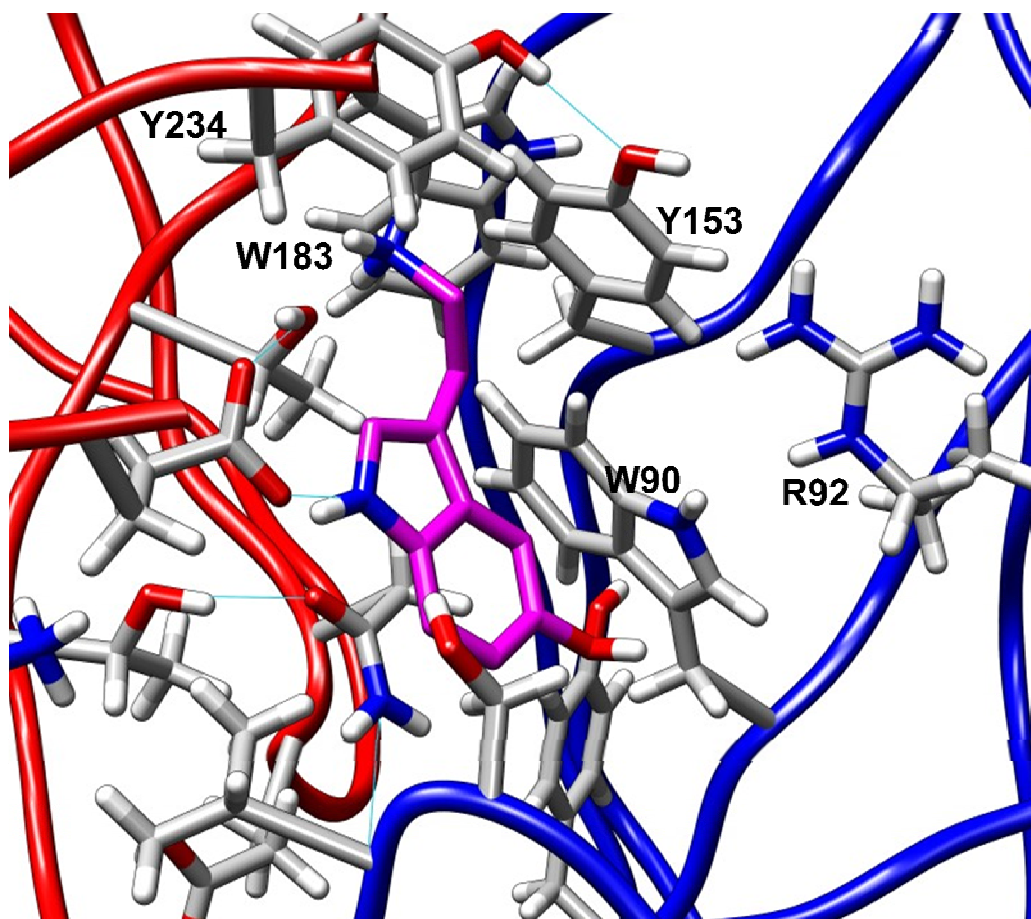


Figure 25. Proposed binding mode of 5-HT (**1**) in the h5-HT3A receptor agonist model developed using Modeller (Method B). 5-HT (**1**) is in magenta and the side chains of residues within 5 Å of the ligand are shown.

literature for 5-HT^{145,146} and the scoring function of AutoDock, one model was identified as the best model for agonists. ProCheck generated a Ramachandran plot in which 67.8% of residues were in most favored regions, 24.1% were in additionally allowed regions,

4.5% were in generously allowed regions, and 3.6% were in disallowed regions (Figure 26). Since multiple loop models were made by slight energy adjustments, the side chain conformations were not optimized using SCWRL; thus, there are more residues in the generously allowed and disallowed regions than with the model developed with Sybyl's Biopolymer package (i.e., Method A).

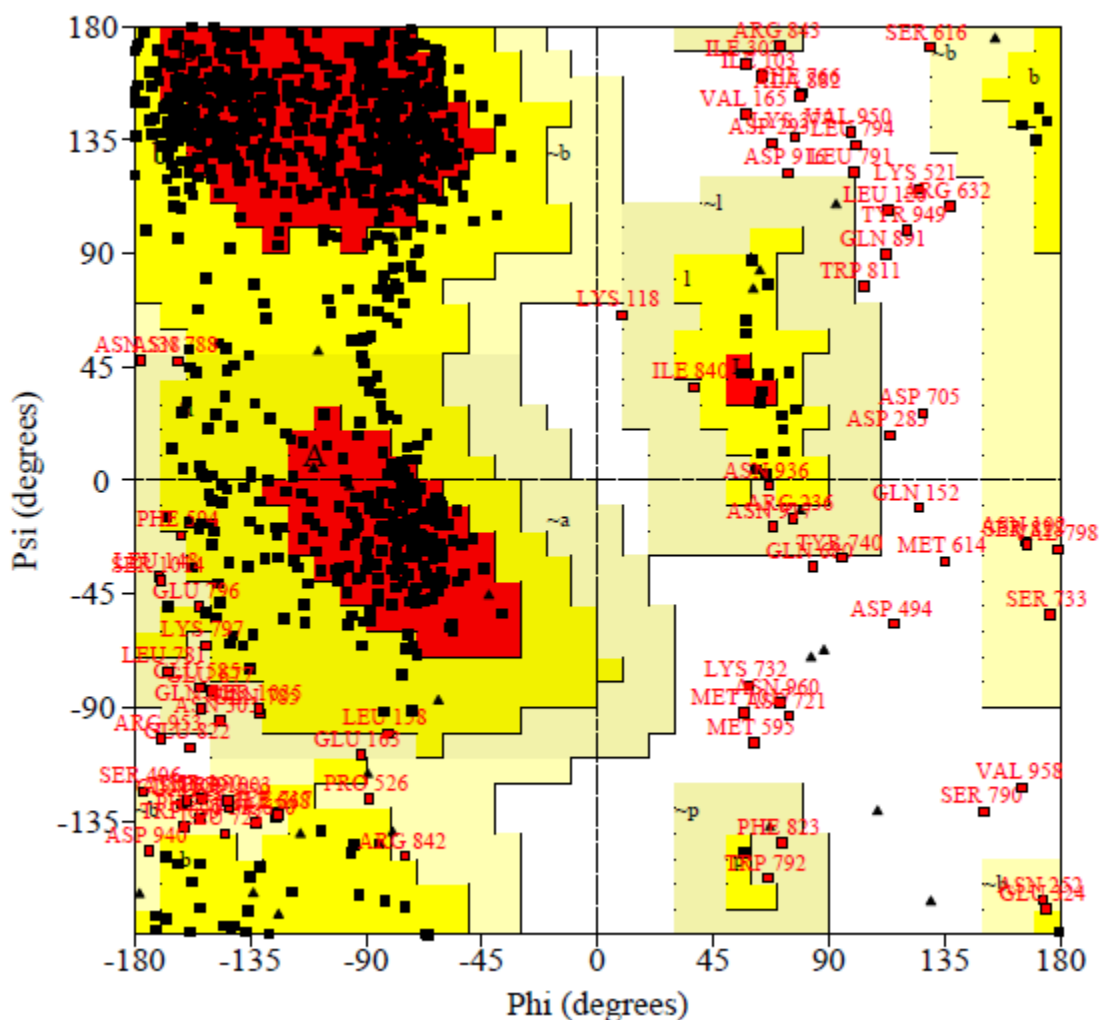


Figure 26. Ramachandran plot of the h5-HT3A receptor agonist model developed using Modeller (Method B).

Serotonin's indole ring is perpendicular to W90 and the aliphatic amine is situated between Y234 and W183 forming a possible cation- π bond. This pose is consistent with poses proposed by Reeves et al.¹⁴⁶ The indole amine is in close proximity to the hydroxyl group of Y153 and may form a H-bond.

Since this model was validated by docking 5-HT, MD-354 (**2**) was built and docked in the same manner as 5-HT. In the model, MD-354 docks in a manner in which the aromatic rings of 5-HT and MD-354 are in the same region of the binding pocket as are the aliphatic amine of 5-HT and the guanidine of MD-354 (Figure 27). The guanidine portion of MD-354 presumably forms a cation- π bond with W183 and Y234. The aromatic ring portion of MD-354 also may form a π - π interaction with Y153. However, the designed ligand (i.e., **51**) from the model developed using Method A (Figure 24) is no longer valid. The overlap using the model developed using Method B indicates a slightly different overlap of MD-354 and 5-HT. In the model developed using Method B, the overlap is such that the -OH group from 5-HT overlaps with the open *meta*-position of MD-354.

The newly synthesized halogen analogs were built and docked to this model following the same parameters. MD-354 (**2**), 3-BrPG (**43**), 3-IPG (**44**) overlapped very well; however, the aromatic ring and guanidine portion of 3-FPG (**42**) overlapped with the other halogenated analogs but the fluoro substituent was situated on the opposite side of the ring (Figure 28). This slight change may explain why **42** binds with decreased

affinity relative to MD-354, 3-BrPG, and 3-IPG. In fact, 3-FPG binds more closely to 5-HT, and both have lower binding affinities than MD-354, 3-BrPG, and 3-IPG.

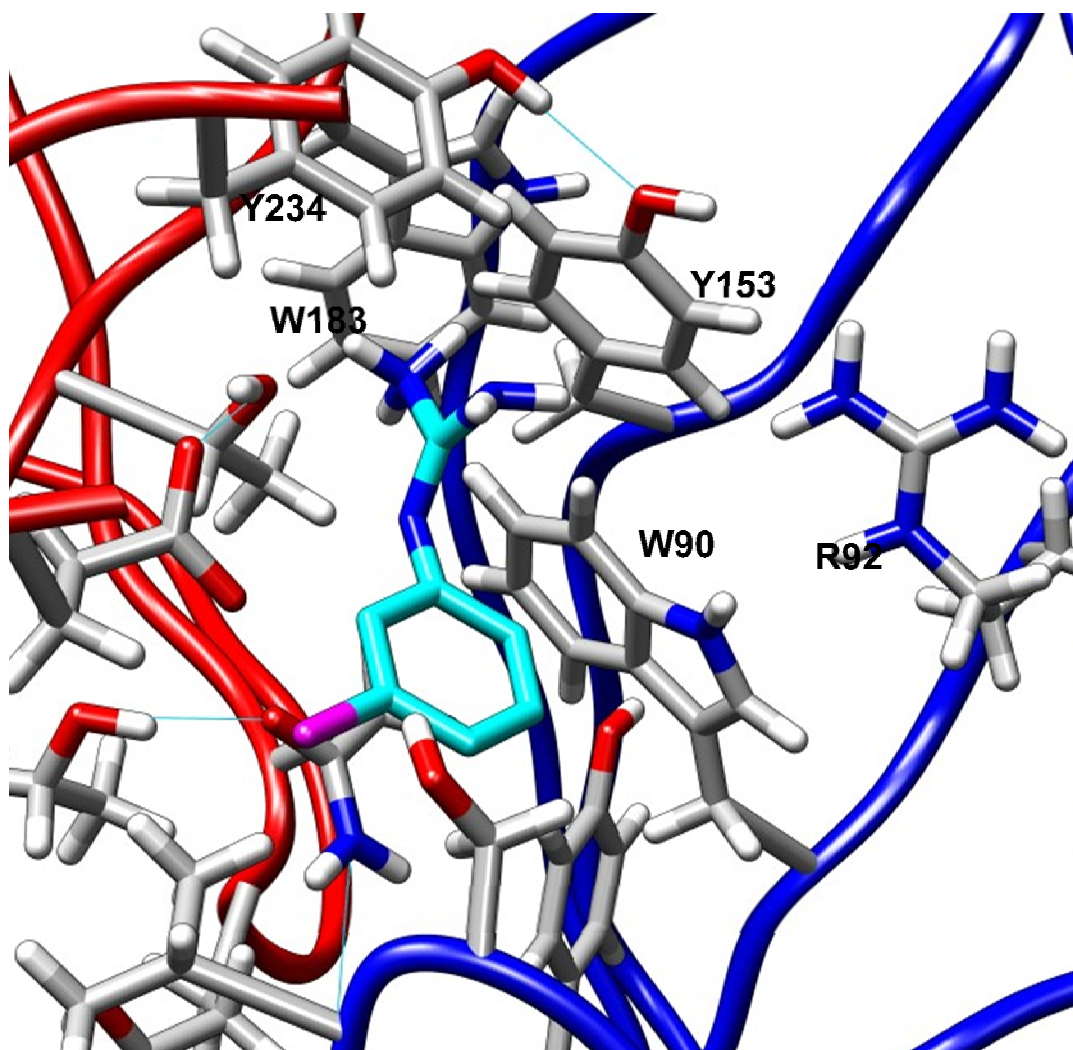


Figure 27. Proposed binding mode of MD-354 (2) to the h5-HT3A receptor agonist model developed using Modeller (Method B). MD-354 is shown in cyan and the side chains of residues within 5 Å of the ligand are shown.

The fluoro substituent affects the aromatic ring system more than the other halogen substituents. It is very electronegative and has orbitals similar in size to those of

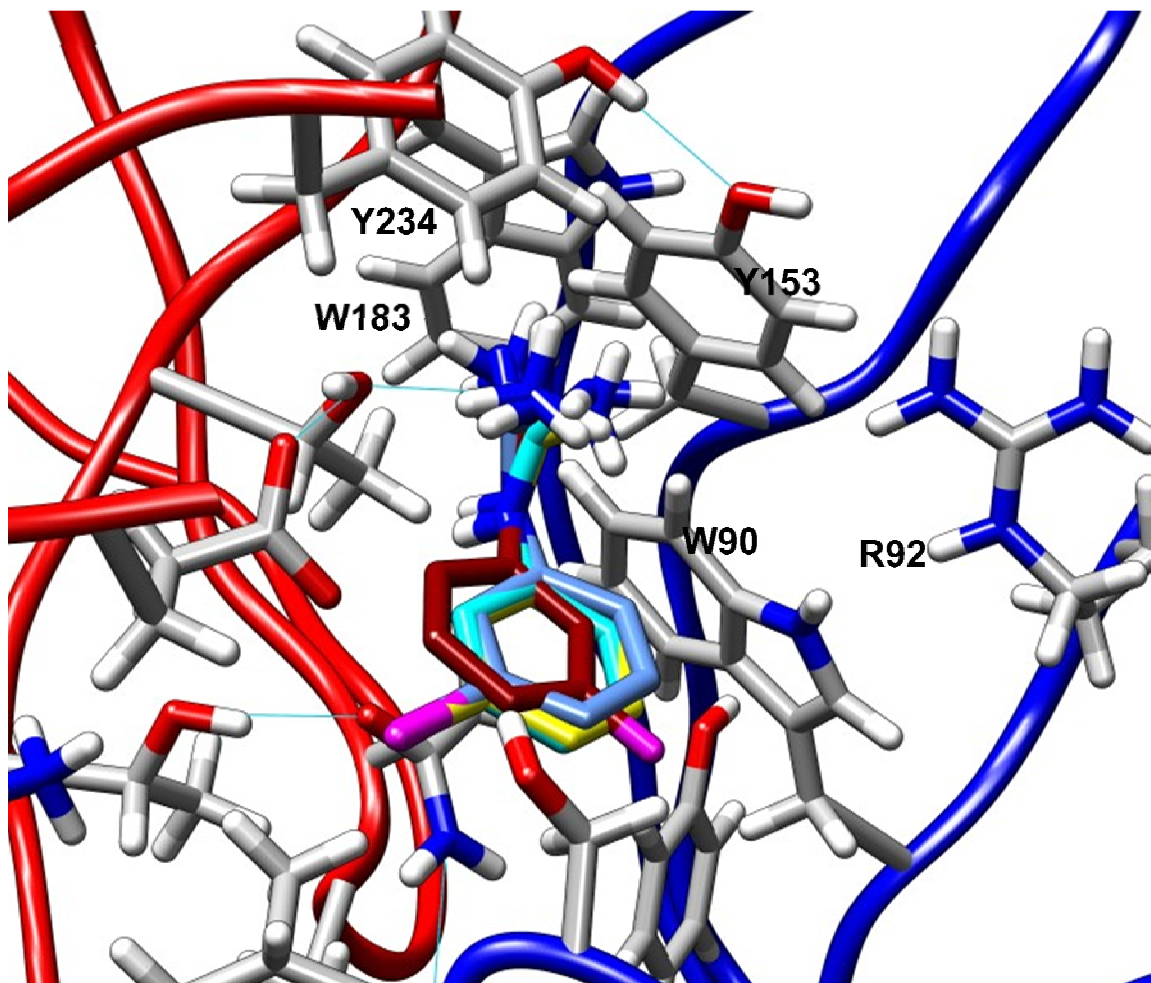


Figure 28. Proposed binding mode of MD-354 (cyan), 3-FPG (red), 3-BrPG (blue), 3-IPG (yellow) to the h5-HT3A receptor agonist model developed using Modeller (Method B).

carbon.¹⁴⁷ These two factors make the C—F bond the most energetic bond in which carbon can participate.¹⁴⁷ Because of the difference in electronegativity, the dipole moment that is created may contribute to the compound's ability to engage in intermolecular interactions since the physical properties and chemical reactivities are greatly affected. In addition, it has been shown through X-ray crystal structure data that

the fluoro group is actually closer in size sterically to an oxygen atom than a hydrogen atom.¹⁴⁸ The 3-OH substituted phenylguanidine (**41**; $K_i = 2020$ nM)¹⁰⁰ has been shown to have binding affinity slightly lower than 3-FPG (**42**; $K_i = 1420$ nM). Based on these data, the size of the substituent needs to be larger than a –F group or a –OH group to bind well to the 5-HT₃ receptors. Overall, the 3-substituted analogs analyzed earlier also follow this trend (Table 8).

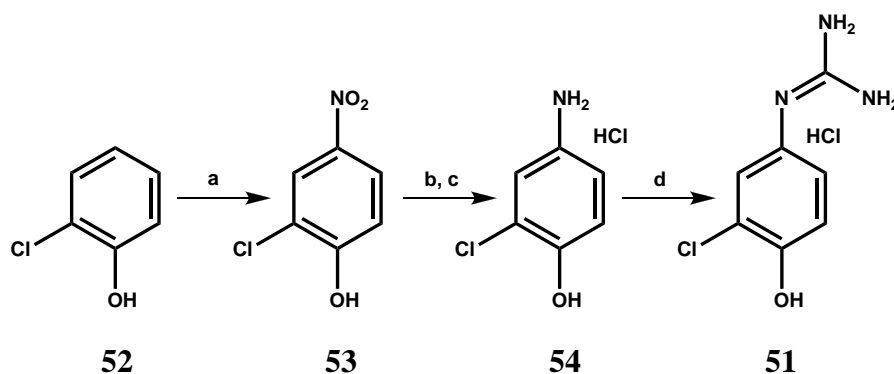
Very recent mutagenesis studies have suggested that E129 is involved in the hydrogen-bond with the –OH in 5-HT.¹⁴⁹ In the models created here E129 does not face into the binding pocket. This does not mean that the model is incorrect; however, it is just a model. Mutagenesis of E129 to A, D, G, H, N, K, or Q either decreased the pEC₅₀ value or there was no response. This may have also been because the mutations are not allowing the receptor binding pocket to form correctly. The model generated using Modeller (i.e., Method B) is a more reliable model than the model generated using Sybyl (i.e., Method A) because it has allowed for flexibility in not only building the receptor model but also in the docking algorithms. The rigidity of the model generated using Sybyl (i.e., Method A) does not allow the ligands to dock to the receptor as closely as those proposed in the literature.

6. Designed Ligand

The ligand designed on the basis of the Method A modeling studies (e.g., see Figure 22), *N*-(3-chloro-4-hydroxyphenyl)guanidine (**51**) (Figure 24), was synthesized by

the method outlined in Scheme 2. The target compound is a known compound.¹⁵⁰ The nitro intermediate (**53**) was obtained by sonication of 2-chlorophenol (**52**) with nitric acid (9% aqueous).¹⁵¹ The nitro group was then reduced using sodium hydrosulfite and aqueous sodium hydroxide.¹⁵² An ethanolic solution of the HCl salt of aniline **54** was heated at reflux with cyanamide (50% aqueous) to give **51**.¹⁵⁰ The structure was confirmed by IR, ¹H NMR, and melting point.

Scheme 2.^a



^a Reagents and conditions: a. HNO₃, 1,2-dichloroethane, sonication; b. Na₂S₂O₄, NaOH, H₂O, reflux; c. HCl, EtOAc; d. NH₂CN, EtOH, reflux.

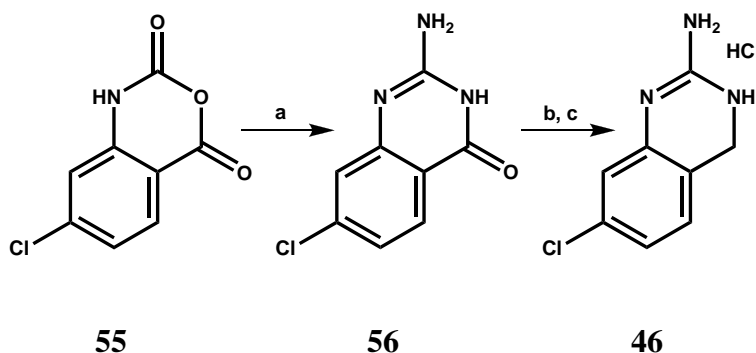
B. Conformationally-Constrained Analogs

1. Synthesis of 2-Amino-7-chloro-3,4-dihydroquinazoline (**46**)

The synthesis of 2-amino-7-chloro-3,4-dihydroquinazoline (**46**) was performed as described in Scheme 3. This was a novel compound at the time of its synthesis, and its method of preparation followed a literature procedure for the synthesis of 2-(alkylamino)-5,6- and 6,7-dihydroxy-3,4-dihydroquinazolines.¹⁵³ S-Methylisothiurea sulfate, sodium

carbonate, and 4-chloroisotoic anhydride (**55**) were heated at reflux in 80% aqueous acetonitrile. After cooling the reaction mixture to room temperature, 2-amino-7-chloroquinazolin-4-(3*H*)-one (**56**) precipitated from the solution and was collected by filtration. This intermediate (i.e., **56**) was reduced using borane in tetrahydrofuran and the HCl salt **46** was prepared. The structural assignment is consistent with IR, ¹H NMR, and elemental analysis.

Scheme 3.^a



^a Reagents and conditions: a. S-methylisothiurea sulfate, Na₂CO₃, CH₃CN (80%), reflux; b. BH₃-THF, reflux, c. HCl

2. Synthesis of 2-Amino-6-chloro-3,4-dihydroquinazoline (**47**)

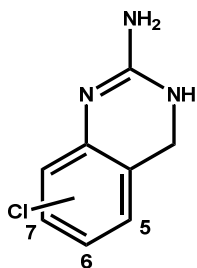
2-Amino-6-chloro-3,4-dihydroquinazoline (**47**) was re-synthesized for this study by the route outlined in Scheme 3 except that 5-chloroisotoic anhydride (**57**) was used in place of 4-chloroisotoic anhydride (**55**). It was found that the product yield was much higher (84% versus 19%) and the reaction time much shorter (6 h versus 20 h) using aqueous acetonitrile (80%) rather than 1,4-dioxane, which was used previously for the

synthesis of 2-amino-6-chloroquinazolin-4-(3*H*)-one (**58**).¹³² The physicochemical and spectral character of **47** was consistent with an authentic sample prepared earlier in this laboratory.¹³² A comparison of **46** and **47** on TLC showed little differences in R_f values regardless of eluant system (i.e., H₂O, CH₃OH, CH₂Cl₂:CH₃OH:NH₄OH 9:1:0.1).

3. Binding Studies

The new quinazoline analog **46** was evaluated, and the quinazoline analog **47** was re-evaluated for binding at the mouse 5-HT_{3A} receptor. Compound **47** was found to bind with the highest affinity out of the three quinazoline analogs (Table 12). This is interesting since it would be the equivalent of 4-chlorophenylguanidine (**29**; $K_i = 320$ nM) and thus indicating that neither *meta*-position is important for binding at the 5-HT₃

Table 12. Binding affinity of quinazoline series at 5-HT₃ receptors.

	-Cl position	K_i nM ^a	K_i nM ^b	K_i nM (SEM) ^c
		NG108-15 GR65630	HEK293 Granisetron	NIH3T3 LY 278,584
48	5		1148	1325 (257)
47	6	34	123	80 (11)
46	7			1975 (168)

^aNG108-15 mouse/rat recombinant receptors express 5-HT_{3A}; Previously reported by Rahman et al.⁹

^bHEK293 human native receptors express 5-HT_{3AB}; Dr. M. White (personal communication).

^cNIH3T3 mouse recombinant receptors express 5-HT_{3A}; K_i values were generously provided by the National Institute of Mental Health's Psychoactive Drug Screening Program, Contract # NO1MH32004 (NIMH PDSP)¹⁵⁴

receptor. But, since it has been shown that one of the *meta*-positions is important for the binding of arylguanidines (see previous section on halogen analogs), these constrained analogs might not bind in the same manner as MD-354 (**2**). The three sets of binding data presented in Table 12 were obtained from three different laboratories. The discrepancies in the binding data may be contributed to the different types of cells used (i.e., NG105-15, HEK293, NIH3T3) and thus variations in the population type of 5-HT₃ receptors (i.e., homomeric mouse 5-HT_{3A} or heteromeric human 5-HT_{3AB}). Or it may be the result of the radioligand used (i.e., GR65630, granisetron, and LY 278,584).

Analog **47** and **48** were submitted for functional assay and were identified as antagonists for 5-HT₃ receptors using whole cell patch-clamp experiments. MD-354 (**2**), **47**, and **48** were investigated using this functional assay. MD-354 was found to be an agonist in this assay with an EC₅₀ value of 3.24 (\pm 0.55) μ M. Quinazolines **47** and **48** were found to be antagonists with IC₅₀ values of 4.39 (\pm 0.78) and 16.53 (\pm 5.18) μ M, respectively (Dr. M. Schulte, personal communication, unpublished data). This functional data indicates that this quinazoline series is a novel class of 5-HT₃ receptor antagonists.

4. Log P Analysis

An analysis of the log P values for the quinazoline series of compounds was conducted in the same manner as with the arylguanidine series (Figure 29). Because these are positional isomers, it might be expected that their log P values would be very similar. The predicted log P value for each is 1.79 (Table 13). Constraining the guanidine by

introducing a methylene bridge between the terminal amine and the aromatic ring makes the compound more lipophilic than MD-354 (**2**; predicted $\log P = 1.43$; Table 11) so that it should more readily cross the BBB. The actual $\log P$ values as determined using HPLC for the three quinazolines are nearly identical; **46** had a $\log P$ value of 1.933, **47** has a $\log P$ value of 1.859, and **48** had a $\log P$ value of 1.889 (Table 13).

Table 13. Capacity factors ($\log k'_w$) determined by linear regression and calculated/determined $\log P$ values for the quinazolines.

Compound	Position of Cl	$\log k'_w$	Predicted $\log P^a$	$\log P$ (HPLC)
48	5	0.4388 ± 0.01562	1.79	1.89
47	6	0.4175 ± 0.00654	1.79	1.86
46	7	0.4712 ± 0.03175	1.79	1.93

^a Predicted using ChemDraw.

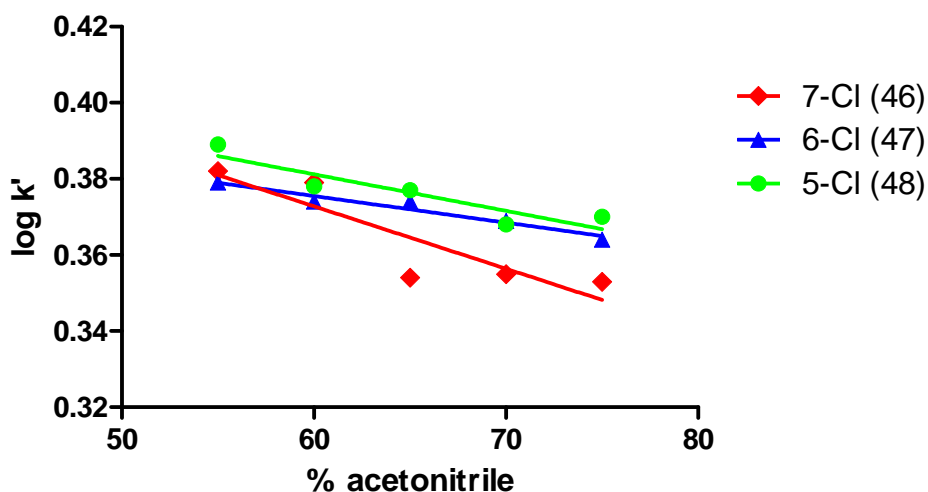


Figure 29. Linear regression analysis from the $\log k'_w$ values of **46**, **47**, **48** at various concentrations of acetonitrile for the quinzaoline analogs.

The log P values determined for the quinazoline analogs (i.e., approximately 1.9) fall within the range of log P values that are expected to cross the BBB (i.e., 1.5-2.5). Since they should be able to cross the BBB they should be able to act at centrally-located 5-HT₃ receptors.

5. Behavioral Studies

a. Tail Suspension Test

The partial agonist MD-354 (**2**) and quinazoline analogs **46-48** were tested for antidepressant activity using the mouse tail suspension assay (n = 8-11 mice/dose). Tricyclic antidepressants (i.e., desipramine and imipramine; 20 mg/kg), an SSRI (i.e., fluoxetine; 20 mg/kg), and a 5-HT₃ receptor antagonist (i.e., ondansetron; 0.1 µg/kg) were given by ip injection thirty minutes before the test and were used as controls. The doses of the controls (i.e., TCAs, SSRI, and ondansetron) and the length of the test were chosen based on literature studies.^{15,155} The tests were video recorded and the immobility times for each mouse were measured in triplicate. A one-way analysis of variance (ANOVA) showed that all of the standards displayed statistically lower immobility times when compared with saline (Figure 30). The strain of mice used in this study was the ICR strain; this strain has not typically been used in literature studies since ICR mice tend to be more active than other strains. In fact, van der Hayden et al.¹⁵⁶ and Nomura et al.¹⁵⁷ have shown imipramine to be inactive in ICR mice (i.e., 3, 10, 30 mg/kg and 10 mg/kg,

respectively). Both studies used automated devices to determine immobility rather than manual observation that was used in the present study.

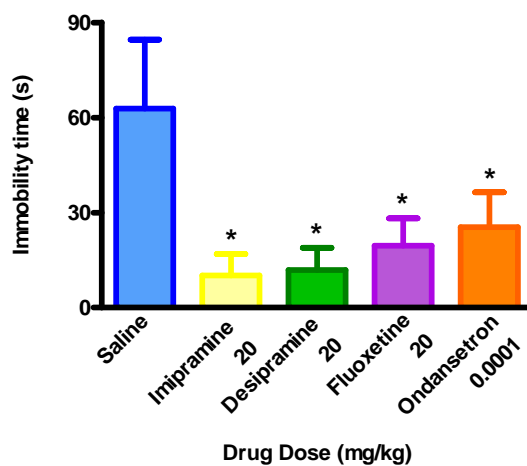


Figure 30. Effect (\pm SEM) of standards (ip) on duration of immobility in the mouse tail suspension test ($n = 8-11$ mice/treatment). The significance of the effect was evaluated with a one-way ANOVA test ($F_{4,41} = 3.256$, $p < 0.05$), Newman-Keuls post-hoc test ($p < 0.05$).

The quinazoline analogs (i.e., **46** and **47**) as HCl salts and MD-354 as a nitrate salt, were injected ip thirty minutes before the test at doses ranging from 0.1 to 30 mg/kg. The quinazoline analog (i.e., **48**) as HBr salt was injected ip thirty minutes before the test at doses ranging from 0.1 to 10 mg/kg. The 6-Cl and 7-Cl analogs (i.e., **47** and **46**, respectively) exhibited statistically lowered immobility times when compared to saline (Figure 31). Using a one-way ANOVA the 6-Cl analog (i.e., **47**; $K_i = 80$ nM) exhibited statistically significant lowered immobility times at the 1.0 and 3.0 mg/kg doses ($F_{6,58} = 3.232$, $p < 0.01$; Dunnett's post-hoc test $p < 0.01$, $p < 0.05$, respectively). Using a one-

way ANOVA the 7-Cl analog (i.e., **46**; $K_i = 1975$ nM) exhibited statistically significant lowered immobility times at the 0.1, 0.3, and 1.0 mg/kg doses ($F_{6,63} = 5.036$, $p < 0.01$; Dunnett's post-hoc test $p < 0.05$, 0.1 and 0.3 mg/kg doses; $p < 0.01$, 1.0 mg/kg dose). The

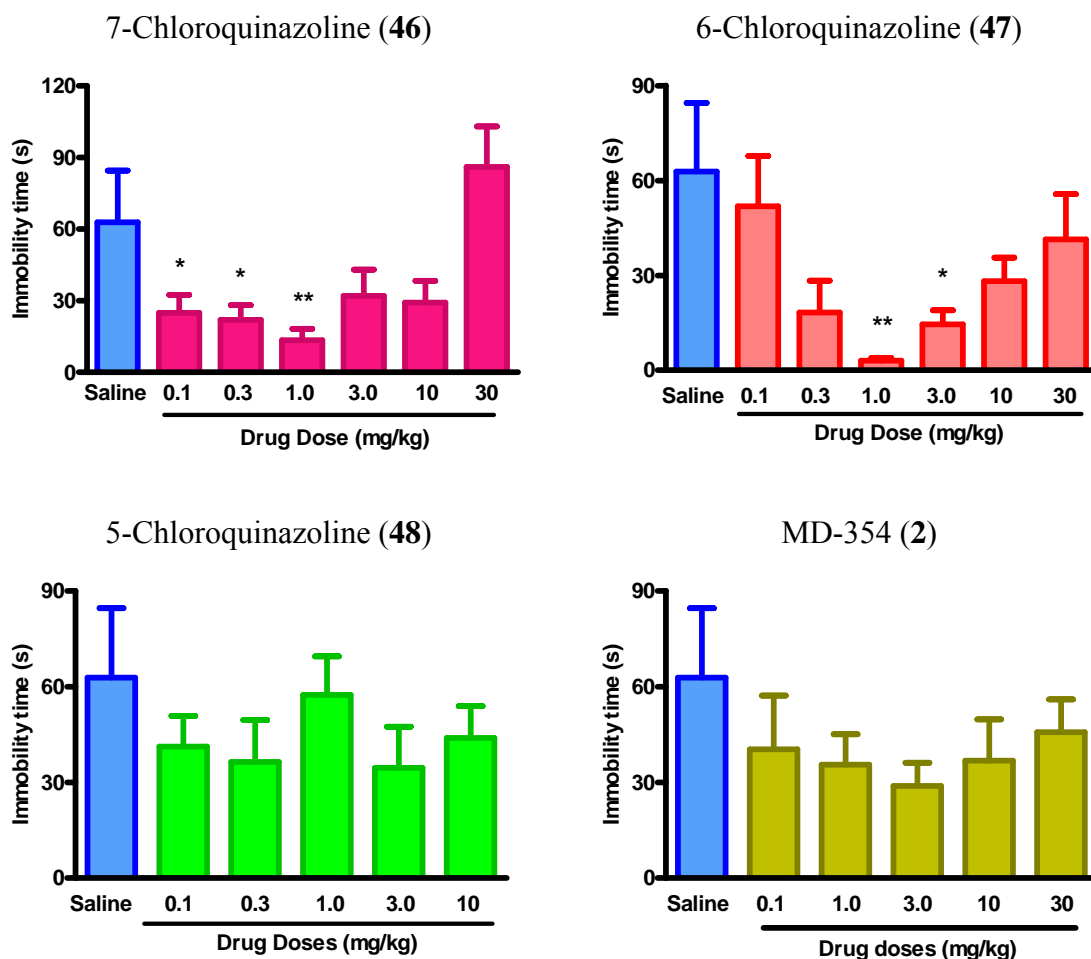


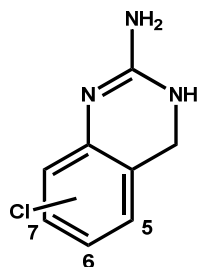
Figure 31. Effect (\pm SEM) of **46** (top left), **47** (top right), **48** (bottom left), and **2** (bottom right) (ip) on duration of immobility in the mouse tail suspension test ($n = 8-10$ mice/treatment). The significance of the effects were evaluated using one-way ANOVA tests. For **46** ($F_{6,63} = 5.036$, $p < 0.01$), Dunnett's post-hoc test (** $p < 0.01$, * $p < 0.05$). For **47** ($F_{6,58} = 3.232$, $p < 0.01$), Dunnett's post-hoc test (** $p < 0.01$, * $p < 0.05$).

5-Cl analog (i.e., **48**; $K_i = 1148$ nM) did not exhibit significantly lowered immobility time for any of the doses examined (Figure 31). MD-354 (**2**; $K_i = 166$ nM) exhibited reduced immobility times which were not significantly different than saline (Figure 31). MD-354 and **48** produce a saline-like effect in the mouse tail suspension test. The log P values determined for all four of these compounds suggest that they can easily cross the BBB. The decreased immobility time is the result of these compounds acting at a central receptor. Since these compounds were given by ip injection (i.e., injection into the body cavity) and some doses display a significant effect it can be assumed that they are crossing the BBB and acting at a centrally located receptor as the log P data suggested from the HPLC analysis.

As shown in Figure 31, 6-chloroquinazoline **47** seems to behave as antidepressant at 1.0 and 3.0 mg/kg doses. But the immobility time, while still reduced, is higher at doses greater than 3.0 mg/kg and less than 1.0 mg/kg resulting in a U-shaped dose-response curve. This curve can also be seen with the 7-chloroquinazoline analog (**46**) and MD-354 (**2**) but it is not as pronounced. The U-shape dose-response curve is characteristic for 5-HT₃ receptor ligands in biological assays.⁵ With regards to agonists, this type of dose-response curve can be explained by desensitization of the receptor. However, with regards to antagonists the underlying mechanism has yet to be explained. One possible explanation is that 5-HT₃ receptor antagonists may bind differently at the homomeric 5-HT_{3A} receptors and heteromeric 5-HT_{3AB} receptors.^{5,158}

The 7-Cl analog (**46**) does not bind with high affinity ($K_i = 1975$ nM) to 5-HT₃ receptors but displays lower immobility scores than saline; this may indicate that it acts via a non-5-HT₃ receptor mechanism to produce this effect. During the course of this investigation Peters et al.^{159,160} reported the synthesis of a number of cyclic guanidines, including **46-48**, through high throughput screening methods. They showed that some bind both to 5-HT_{5a} and 5-HT₇ receptors (Table 14). Peters et al. report prompted us to test our analogs for binding affinity at 5-HT_{5a} and 5-HT₇ receptors. We have found that the 7-Cl analog binds at 5-HT_{5a} and the 5-HT₇ receptors ($K_i = 302$ and 310 nM, respectively)¹⁵⁴ with 5-fold higher affinity than at 5-HT₃ receptors. Interestingly, the 5-HT₇ receptor has

Table 14. Binding profile of selected cyclic guanidines at 5-HT₃, 5-HT_{5a}, and 5-HT₇ receptors.



Compound	R	5-HT ₃		5-HT _{5a}		5-HT ₇	
48	5-Cl	1325 ± 257	1051 ^b	155 ^a	99 ^b	1109 ^a	793 ^b
47	6-Cl	80 ± 11 ^a	—	357 ± 38 ^a	807 ^b	1701 ± 242 ^a	—
46	7-Cl	1975 ± 168 ^a	—	302 ± 48 ^a	347 ^b	310 ± 43 ^a	—

^a K_i values were generously provided by the National Institute of Mental Health's Psychoactive Drug Screening Program, Contract # NO1MH32004 (NIMH PDSP)¹⁵⁴

^bPeters et al.¹⁵⁹

been implicated in depression.¹⁶¹ A recent review by Mnie-Filali et al. showed that 5-HT₇ receptor KO mice display antidepressant-like behavior in the FST and TST relative to

WT mice.¹⁶¹ In addition, the administration of the 5-HT₇ receptor antagonist SB-269970 also decreased immobility time.¹⁶¹ Therefore, the 5-HT₇ receptor mechanism in the antidepressant action of **46** cannot be excluded. The 5-ht_{5a} receptor's function is not fully understood because of the lack of selective agents. However, since it is located only in the CNS, primarily in the cerebral cortex, hippocampus, and cerebellum, it has been postulated that this receptor may be involved in schizophrenia or mood disorders.^{162,163} Based on this information **47** could be exhibiting its antidepressant effect through a 5-ht_{5a} or 5-HT₇ receptor mechanism. Interestingly, the 5-chloroquinazoline **48** seems to be more selective for the 5-ht_{5a} receptor over the 5-HT₃ and 5-HT₇ receptors. Optimization of this analog by Peters et al. has led to even more analogs that have increased binding affinity for 5-ht_{5a} receptors (e.g., 2-amino-5-chloro-4-methyl-3,4-dihydroquinazoline; 5-ht_{5a} K_i = 5.1 nM).^{159,160} The 5-Cl-4-CH₃ analog was also shown to be a competitive 5-ht_{5a} receptor antagonist through the [³⁵S]GTPγS assay with a pA₂ value of 8.52.¹⁵⁹ Most of their analogs had no more than a 4-fold selectivity over the 5-HT₇ receptors but because of the similar localization of the 5-ht_{5a} and 5-HT₇ receptors in the brain, Peters et al. continued to examine this series.¹⁵⁹ Their overall goal was to develop a pharmacological tool for behavioral studies to examine the role of the 5-ht_{5a} receptor's antipsychotic-like effects.¹⁶⁰ Although the involvement of a 5-HT₇ receptor mechanism in the antidepressant activity of **46** cannot be excluded at this time, it is unlikely to undermine the antidepressant activity of these quinazoline analogs because **47** binds with more than 20-fold lower affinity at 5-HT₇ receptors versus 5-HT₃ receptors.

b. Locomotor Activity Assay

Since hypermobility may also explain lowered immobility times relative to saline, the effective tail suspension test doses (**46**, 0.3 mg/kg; **47**, 1.0 and 3.0 mg/kg) were tested against saline for hyperactivity using the locomotor activity assay. The doses were injected ip with no pre-treatment time and their effect on locomotor activity was examined over 45 minutes. This time encompasses the 30 minutes pretreatment from the tail suspension test, the six minute tail suspension test, and nine minutes after the tail suspension test would be over; so any movements that have increased relative to saline during this time would have been increased during the antidepressant assay.

Using a one-way ANOVA there was no significant difference between any of the doses and saline for the 45 minute duration for total movement episodes, total movement time, total movement distance, number of jumps or average velocity (Figure 32). These parameters are usually used in the identification of stimulants. Stimulants generally increase the movement time, distance, and velocity but decrease the number of movement episodes (i.e., the drug increases the duration of motor activity but decreases the number of stops).¹⁶⁴ There was also no difference from saline for the retraced local movements, retraced local movement episodes (3 repeated local movements), and these movements'

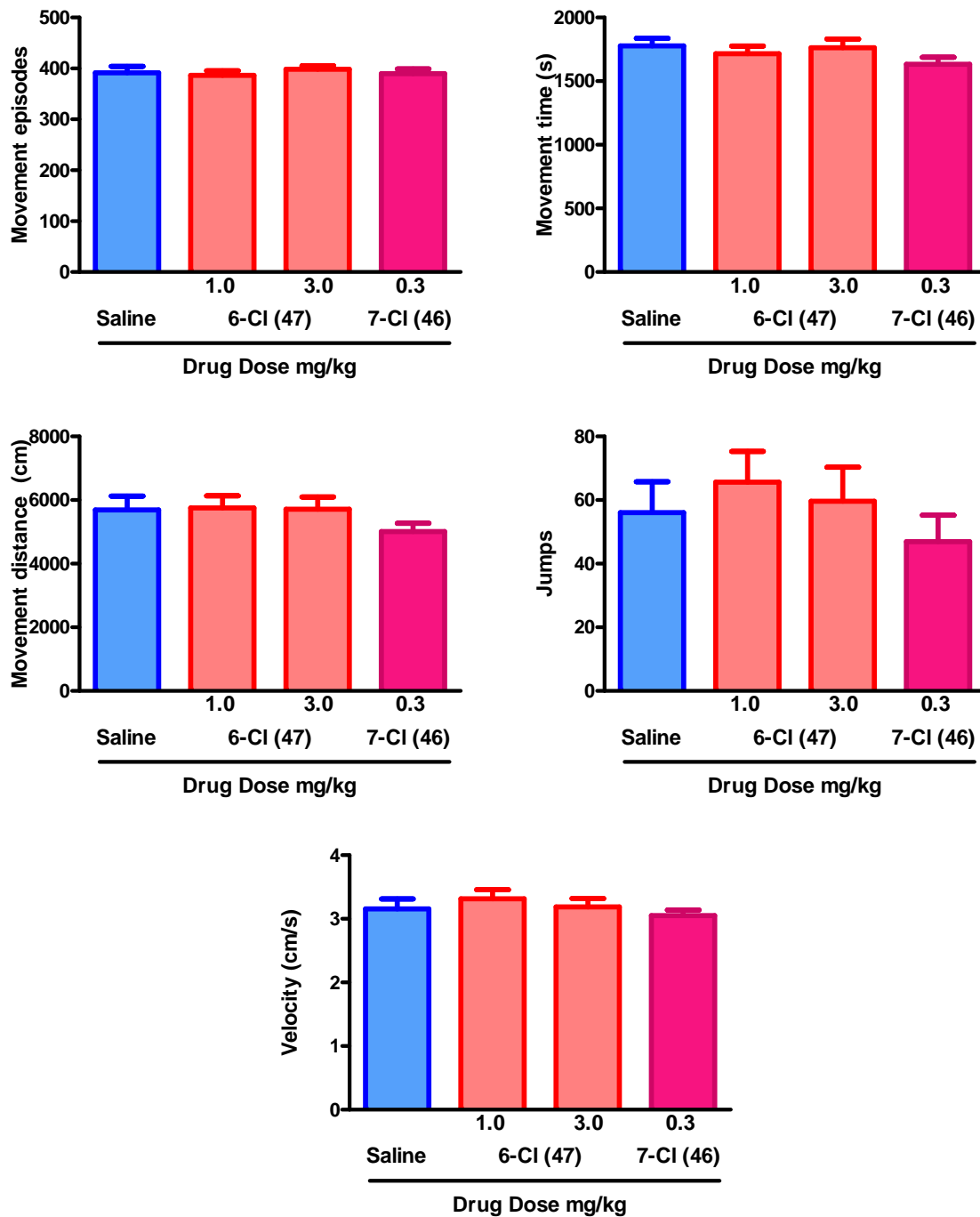


Figure 32. Effect (\pm SEM) of **47** (1.0 and 3.0 mg/kg) and **46** (0.3 mg/kg) on total number of movement episodes, total movement time, total movement distance, total number of jumps, and average velocity ($n = 12-13$ mice/treatment).

time which may indicate exploratory behavior (Figure 33). The term local refers to the fact that the animal's movement does not produce a large enough change in location from its starting point (i.e., less than ± 1.499 beam spaces from the starting point). As with all of the other parameters examined there was no difference using a one-way ANOVA between the doses evaluated and saline for margin distance traveled, time spent in the margin, center distance traveled, time spent in the center, number of center entries, and the number of vertical entries (Figure 34). Increased margin activity or decreased central activity is generally viewed as an anxiogenic-like effect. Vertical entries may indicate the "nonspecific excitability level" of the animal.

The 5-HT₃ receptor antagonist ondansetron (**3**) and the 5-HT₃ receptor partial agonist MD-354 (**2**) showed no effect on locomotor activity in previous studies.^{15,132} Based on those results, there was no reason to expect a change in locomotor activity for the quinazoline analogs **46** and **47** unless these compounds cause hyperactivity. Since there was no difference in activity from saline using a one-way ANOVA with any of the doses examined, the lowered immobility scores from the tail suspension test should be from an antidepressant-like action of the compounds and not from hyperactivity. However, **46** displayed a decreased number of center entries, a decreased amount of time spent in the center of the arena, and a decreased distance traveled in the center of the

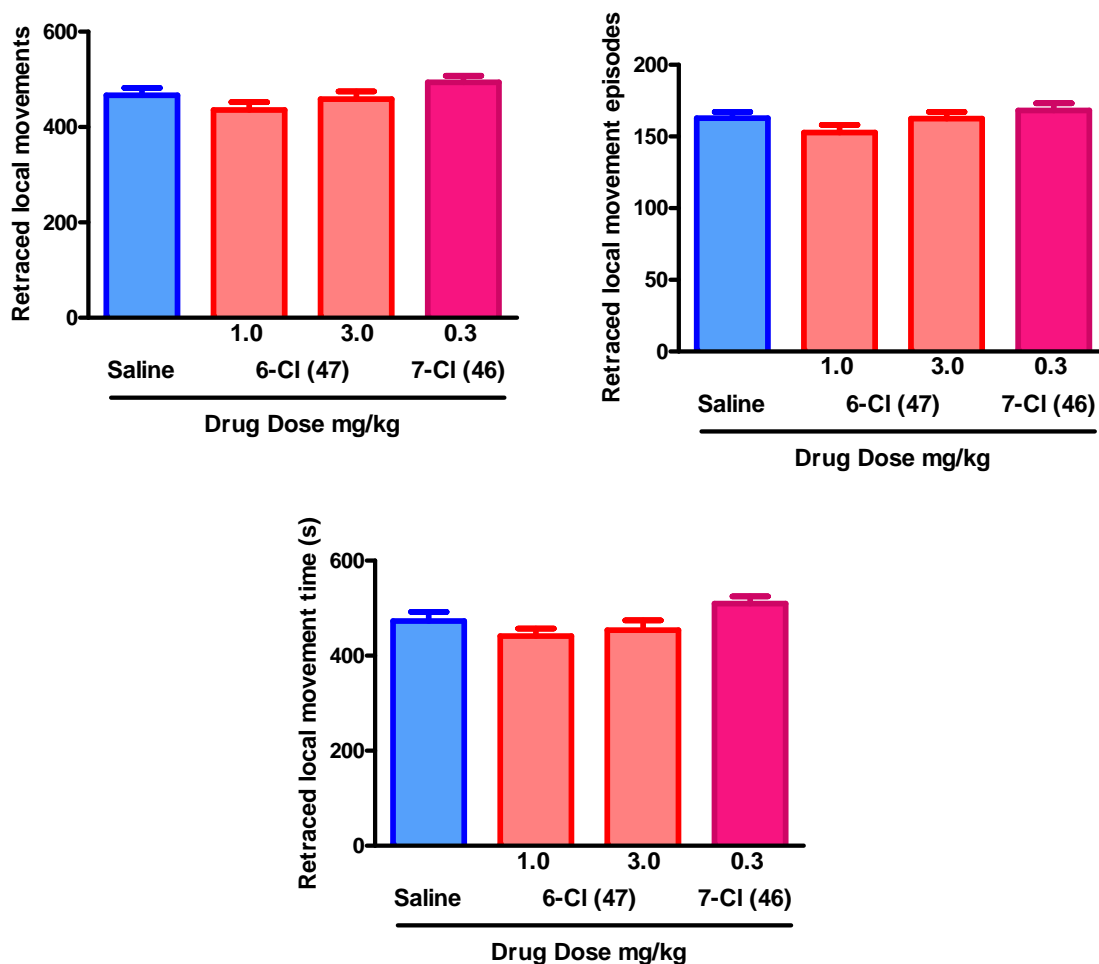


Figure 33. Effect (\pm SEM) of **47** (1.0 and 3.0 mg/kg) and **46** (0.3 mg/kg) on total number of retraced local movements, total number of retraced local movement episodes, and total time spent on retraced local movements ($n = 12-13$ mice/treatment).

arena, but they were not found to be significantly different from saline using a one-way ANOVA. A significant decrease in center activities may have indicated anxiogenic-like properties. Because these parameters were not significantly different than saline using a one-way ANOVA, this may be because of variation and not a true example of anxiogenic properties. If it is because of anxiogenic properties, it is most likely the result of acute

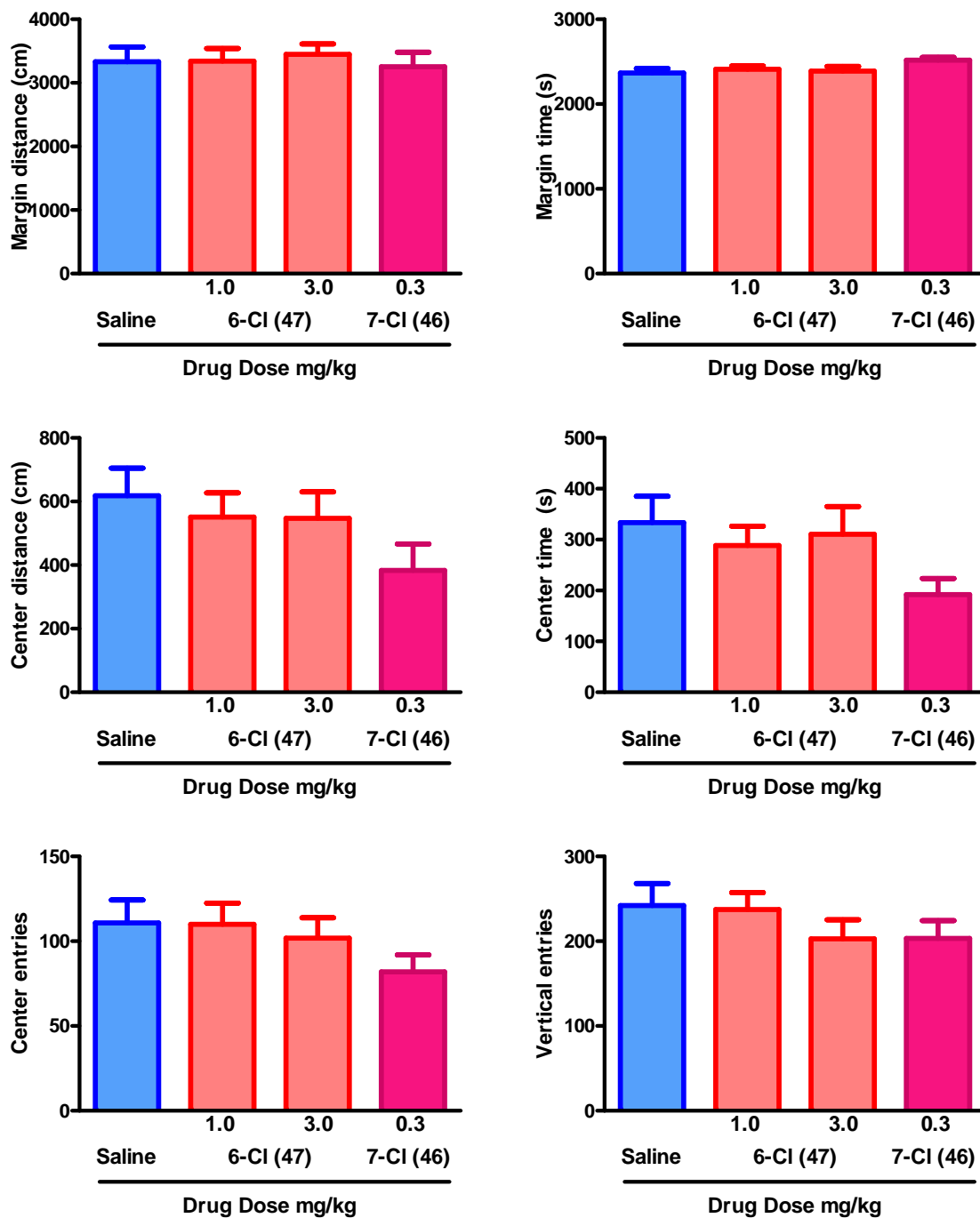


Figure 34. Effect (\pm SEM) of **47** (1.0 and 3.0 mg/kg) and **46** (0.3 mg/kg) on total distance traveled in the margin, total time spent in the margin, total distance traveled in the center, total time spent in the center, the number of center entries, and the number of vertical entries ($n = 12-13$ mice/treatment).

administration; there have been reports indicating that some antidepressants increase anxiety levels when administered acutely.^{165,166}

6. Molecular Modeling

Since the constrained analogs **47** and **48** were found to be antagonists for the 5-HT₃ receptor, it would be of value to identify the docking poses of these constrained analogs to a 5-HT₃ receptor homology model. Using the same set of models generated using Modeller (Method B) and AutoDock4, the 5-HT₃ receptor antagonist granisetron (**4**), with the charges and geometries generated by MOPAC, was docked to each of the five interfaces of each of the 100 models with 20 genetic algorithms in a 40 Å x 40 Å x 40 Å region around the C-loop. A different model than the model identified by the agonist 5-HT, was identified through the proposed binding mode of the antagonist granisetron. This proposed binding mode is similar to that in the literature for granisetron (Figure 35).^{167,168} The azabicyclic ring is located towards W90 and F226, while the aromatic ring is located towards W183 and Y234. ProCheck was used to create a Ramachandran plot of the pentamer; it was found that 64.8% of residues were in favored regions, 28% in additionally allowed regions, 4.8% in generously allowed regions and 2.5% in disallowed regions (Figure 36). Since the loop models are generated by small changes in energies, the side chains were not optimized with SCRWL leading to residues found in the generously allowed and disallowed regions as seen with the 5-HT₃ receptor agonist model also developed by Modeller. In addition, AutoDock allowed for flexibility

in the backbone atoms during the docking process to allow for the best possible interactions.

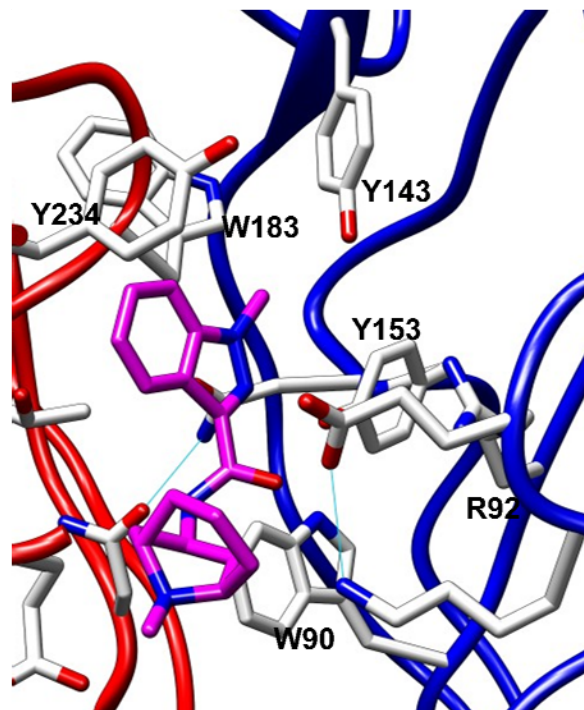


Figure 35. Proposed binding mode of granisetron (**4**) to the h5-HT₃A receptor antagonist model developed using Modeller (Method B). Granisetron is shown in magenta and residues within 5 Å are shown.

Since this antagonist model could be validated by granisetron (**4**), the quinazoline analogs **46-48** and the 5-HT₃ receptor partial agonist MD-354 (**2**) were built and given geometries and charges according to MOPAC. They were docked to the antagonist validated receptor model using AutoDock and the same parameters as before. The

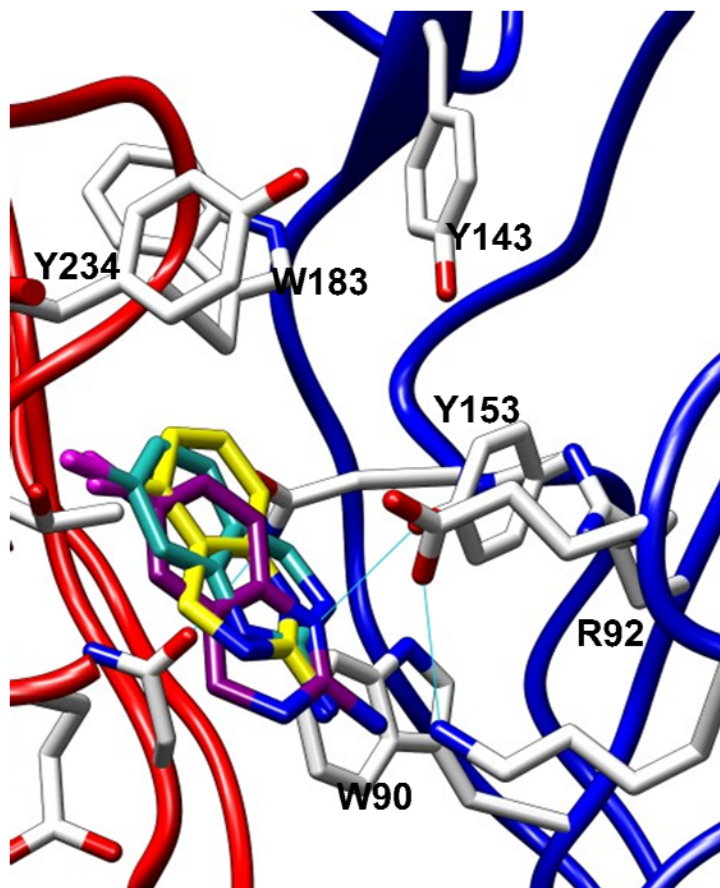


Figure 37. Proposed binding mode of the quinazoline analogs **46-48** to the h5-HT3A receptor antagonist model developed using Modeller (Method B). The 5-Cl analog (**48**) is shown in cyan, the 7-Cl analog (**46**) is shown in yellow, and the 6-Cl analog (**47**) is shown in purple. Residues within 5 Å are also shown.

Based on the structures of the quinazolines and MD-354, it was assumed that the quinazolines should be able to bind overlapping MD-354. However, based on the proposed binding modes, the quinazoline analogs do not bind in the same manner as the partial agonist MD-354. But bind in the opposite direction as MD-354 (Figure 38). The

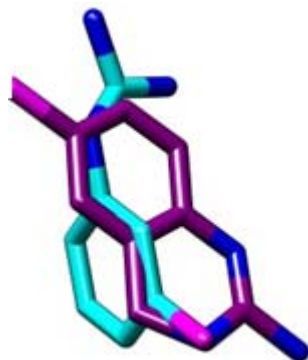


Figure 38. Overlap of the proposed binding modes of MD-354 (**2**; cyan) and the highest binding affinity analog, 6-Cl quinazoline **47** (purple).

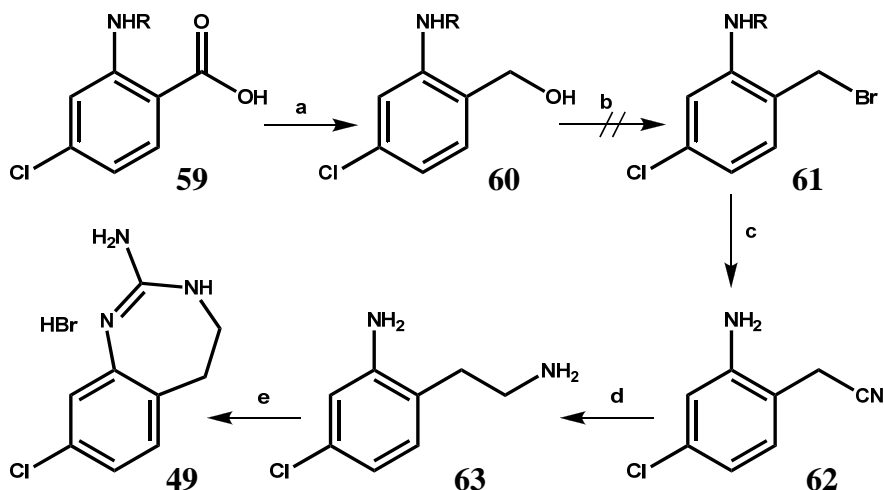
guanidine of the quinazolines may be interacting with W90 instead of W183 as seen with the proposed binding mode of MD-354. These changes in proposed binding modes may explain why the quinazolines are antagonists and MD-354 is merely a partial agonist. The constrained guanidine cannot make the same interactions (W183 and Y234) with its nitrogen atoms as the free guanidine of MD-354. This may also explain why neither of the two rotameric constrained analogs of MD-354 (i.e., **46** and **48**) bind with the same affinity as MD-354.

7. Synthesis of 2-Amino-8-chloro-1,3-benzodiazepine (**49**)

The synthesis of this constrained analog of MD-354 (**2**) would allow for a longer centroid-to-amine distance, closer to that of MD-354, and a larger height of the primary amine above the plane of the aromatic ring (Table 6). The first attempted synthesis followed the reaction outlined in Scheme 4. The benzoic acid **59** was reduced to the benzyl alcohol **60**.¹⁶⁹ An attempt was made to convert the benzyl alcohol to the benzyl

bromide **61**.¹⁷⁰ However, the benzyl bromide was unable to be isolated and characterized with and without first protecting the amine (i.e., (Boc)₂O or trifluoroacetic anhydride).

Scheme 4.^a



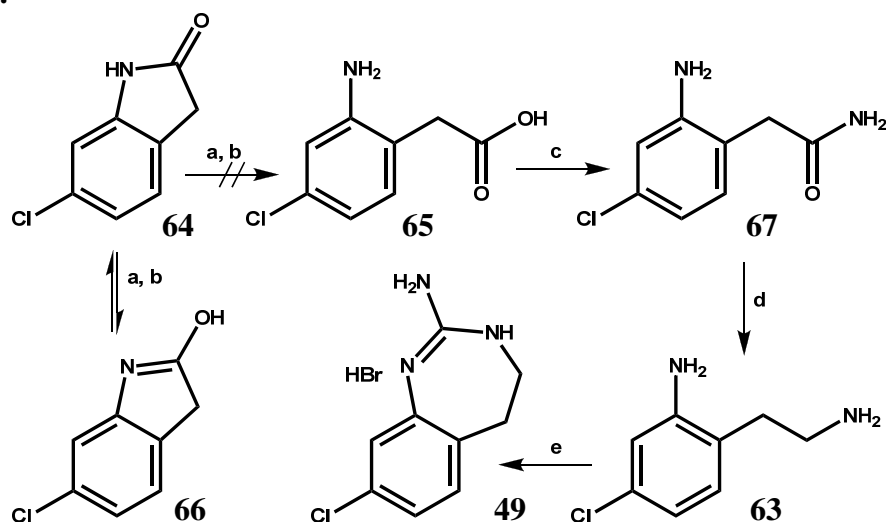
R = H, Boc, TFA

^aReagents and conditions: a. LiAlH₄, THF (R = H); b. PBr₃, CH₂Cl₂ or Et₂O; c. NaCN, isopropanol, H₂O, d. Raney Ni, e. BrCN, EtOH

The second route of synthesis involved the opening of the oxindole ring **64** to obtain the carboxylic acid **65**.¹⁷¹ Under the conditions described in Scheme 5 the desired ring-opened intermediate was not isolated. Either it was formed, and then recycled to the starting material (i.e., **64**), as the use of acid is typically employed to prepare oxindoles from the 2-aminophenylacetic acids,¹⁷² or only tautomer **66** of the starting material was formed which then reverts back to starting material. The NMR and IR

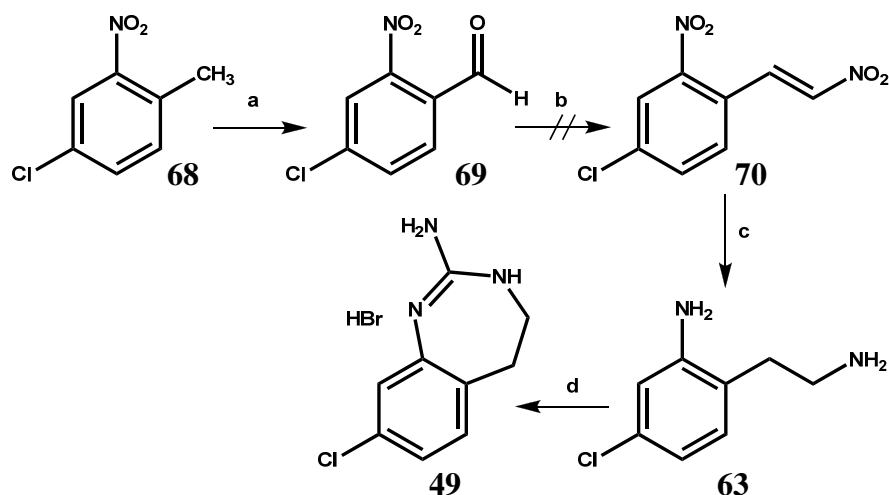
analysis of the product from the reaction could not conclusively be identified as either **65** or **66** but was different from **64** on TLC.

Scheme 5.^a



^aReagents and conditions: a. NaOH, H₂O, reflux; b. HCl, H₂O; c. carbonyldiimidazole, NH₃, CH₃OH, d. BH₃-THF, e. BrCN, EtOH

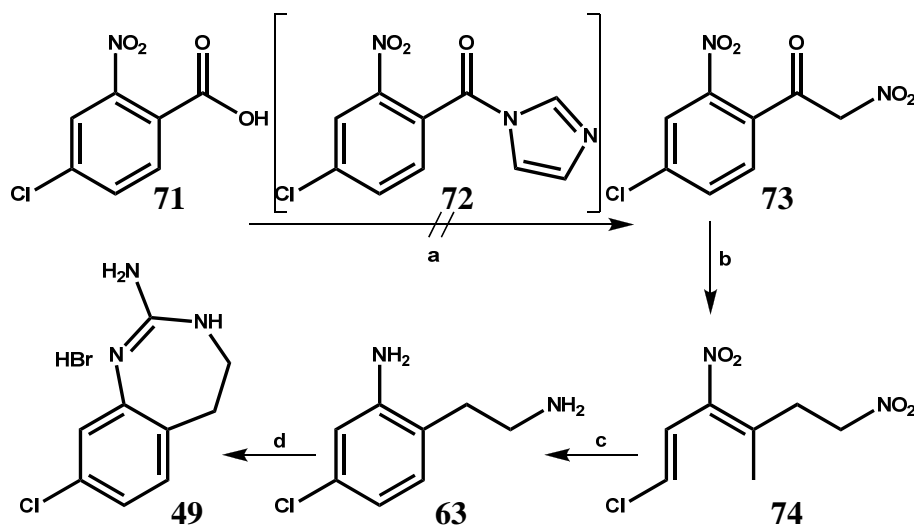
The third route of synthesis involved the conversion of nitrotoluene **68** to benzaldehyde **69** with DMF-DMA,¹⁷³ then converting the benzaldehyde to a nitrostyrene **70** with nitromethane¹⁷⁴ as outlined in Scheme 6. The benzaldehyde **69** could not be purified from bi-products formed during the reaction.

Scheme 6.^a

^aReagents and conditions: a. 1. DMF-DMA, 140 °C, 2. NaIO₄; b. CH₃NO₂, NH₄OAc, reflux, c. SnCl₂, HCl, d. BrCN, EtOH

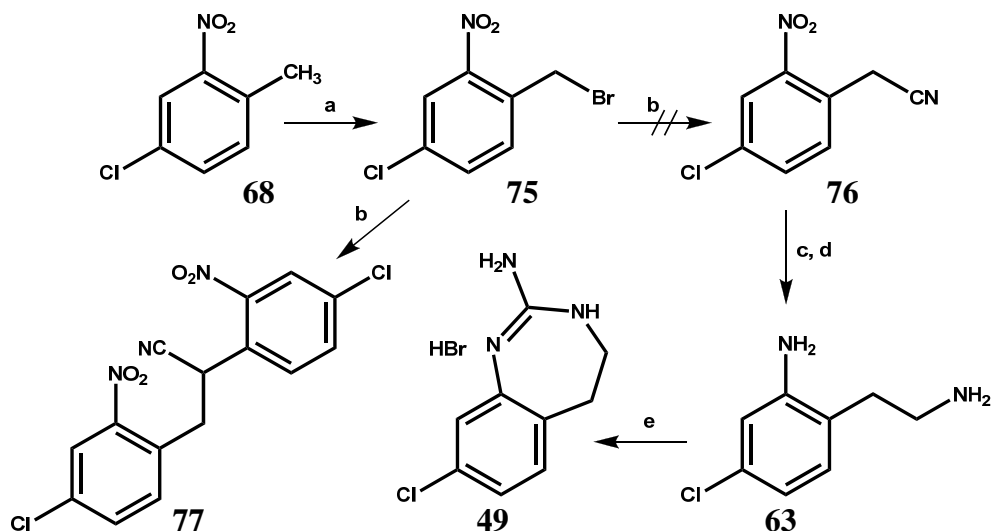
The fourth route of synthesis attempted to convert benzoic acid **71** to nitrophenylethanone **73** going through intermediate **72** as outlined in Scheme 7.¹⁷⁵ However, only the intermediate **72** was formed and isolated; the nitrophenylethanone **73** was not. It appears that the intermediate does not react as easily with the nitromethane as suggested in the literature.

The fifth route of synthesis involved the reaction of nitrotoluene **68** with N-bromosuccinamide and benzoyl peroxide to form benzyl bromide **75** (Scheme 8).¹⁷⁶ The benzyl bromide was slightly more polar than the starting material and has a very similar melting point making separation difficult. An attempt to convert benzyl bromide **75** to (nitrophenyl)acetonitrile **76** using hydrogen cyanide formed in situ from sodium cyanide

Scheme 7.^a

^aReagents and conditions: a. carbonyldiimidazole, K₂CO₃, THF, CH₃NO₂, reflux; b. BH₃-THF; c. SnCl₂, HCl; d. BrCN, EtOH

and strong acid resulted in the formation of a dimer complex (i.e., **77**). This type of dimerization was seen by Kalir and Mualem with the reaction of 2-nitrobenzylbromide using this reaction.¹⁷⁷ Another attempt to convert the benzyl bromide **75** to (nitrophenyl)acetonitrile **76** was made using liquid-liquid phase transfer catalysis. Sodium cyanide ionizes in water into a sodium ion and cyanide ion. The cyanide reacts with **75** to form **76**, and then quickly reacts with another equivalent of **75** to form 2,3-bis(4-chloro-2-nitrophenyl)propanenitrile (**77**). Adjusting the pH to be acidic to increase the ionization of the cyanide completely halted the reaction. Using solid-liquid phase transfer catalysis with potassium cyanide, 18-crown-6 ether, in acetonitrile still produced **77** and not **76** as desired.

Scheme 8.^a

Reagents and conditions: a. N-bromosuccinamide, benzoyl peroxide, CCl₄, light, reflux; b. NaCN, H₂O, TBAB, CH₂Cl₂; c. BH₃-(CH₃)₂S, reflux; d. Raney Ni; e. BrCN, EtOH, reflux

Given that the height of the amine above the plane and the aromatic centroid to primary amine distances of **49** are closer to that of MD-354 (**2**) relative to the other constrained analogs (i.e., **45-48**), **49** may bind with enhanced affinity. Since the synthesis of **49** was unsuccessful, binding data is not available. If **49** binds with higher affinity than **46**, the longer amine to centroid distance and/or the out-of-plane character of **49** might explain the difference in binding affinities.

V. Conclusions

Two novel series of MD-354 (**2**) analogs were synthesized as part of this investigation. The intended purpose of evaluating these series was to identify *what* characteristics of the *meta*-position are necessary for binding to the 5-HT₃ receptor and *which meta*-position is important for binding.

The first series of analogs developed was the mono-substituted halogen analogs of MD-354. By purely examining the binding affinity of PG (**27**), 3-FPG (**42**), MD-354 (**2**), 3-BrPG (**43**), and 3-IPG (**44**) it appears that smaller substituents do not bind very well at the 5-HT₃ receptors. The receptor may need a substituent at the 3-position of a particular size or larger to have high affinity; the -H or -F groups may be too small to fit this requirement. However, the 3-CF₃ analog binds with even lower affinity than PG or 3-FPG and is much larger in terms of solvent accessible volume than any of the halogenated analogs, suggesting that something more than just size plays a role in binding affinity. A Hansch analysis indicated that size in the form of volume (i.e., surface accessible volume and CMR), polarizability (i.e., CMR and polarizability) and electronic character (i.e., π) are important components in binding affinity. However, volume and polarizability are intercorrelated and can therefore act as surrogates for each other. But a multiple linear regression analysis has shown that π and either CMR, volume, or polarizability impact binding affinity. All of this information is consistent with a prior

QSAR analysis^{100,124} of arylguanidines and supports the current pharmacophore for arylguanidines and arylbiguanides⁸³ that at one of the *meta*-positions an electron-withdrawing group of a certain volume or polarizability is needed for optimal binding affinity.

Two distinct homology models of the h5-HT_{3A} receptor were developed by different methods (i.e., Method A and Method B) and validated by docking the 5-HT₃ receptor agonist serotonin. Upon validation of the models, the docking of the halogenated analogs to a homology model (Method B) of the h5-HT_{3A} receptor was investigated. The results suggested that these analogs bind in the same manner as MD-354. However, 3-FPG (**42**) is suggested to dock in an orientation in which the fluorine atom does not overlap with the other halogens but is on the opposite side of the aromatic ring. This can be explained by the effects of a fluorine atom attached to an aromatic ring. The electronegativity of the fluorine atom might affect the electronic character of not only the ring but also of the guanidine.

Based on the proposed docking poses of MD-354 and serotonin (Method A) a new analog was designed and synthesized, (3-chloro-4-hydroxyphenyl)guanidine (**51**). The guanidine portion should be able to interact with W183 and Y234 as the aliphatic amine in serotonin does and the hydroxyl group should be able to interact with Y153. The -Cl group from this compound should be able to sit in the same pocket as the -Cl group from MD-354. In theory **51** should bind with higher affinity than 5-HT or MD-354 because it should be able to interact with the receptor similar to both 5-HT and MD-354.

The second series of analogs developed were constrained analogs of MD-354 (**2**); in which the guanidine was constrained by a methylene group to form a series of quinazolines (i.e., **46-48**). This series was initially developed to determine which *meta*-position was important for binding affinity. However, binding data at the 5-HT₃ receptor of these three analogs indicated that neither position was important. Since it has been shown previously that there is an electronic effect for a *meta*-substituent (*vide supra*), at least one *meta*-position is important and necessary for binding to the 5-HT₃ receptor if the compounds are binding in the same manner. Based on this data, the quinazoline series does not seem to be binding to the 5-HT₃ receptor in the same manner as the arylguanidines. A functional assay has also shown that some of these quinazolines are antagonists for the 5-HT₃ receptor (**47**; IC₅₀ = 4.39 ± 0.78 μM and **48**; IC₅₀ = 16.53 ± 5.18 μM; Dr. M. Schulte, personal communication, unpublished data).

Molecular modeling of the possible binding modes of the quinazolines to a homology model (Method B) of the h5-HT_{3A} receptor validated by the docking of the 5-HT₃ receptor antagonist granisetron, indicates that the quinazolines do not bind in the same manner as MD-354. The quinazolines seem to bind upside-down relative to MD-354 in which their guanidine portion interacts with W90 and not W183. Since this series has been shown to be functionally different than MD-354 and does not seem to bind in the same manner, it should be considered a novel class of 5-HT₃ receptor ligands.

Some of the newly synthesized analogs (e.g., **43**, **44**, and **47**) have higher binding affinity for the 5-HT₃ receptors than MD-354. But, having higher binding affinity had no

effect on the ability of the compound to cross the BBB. The evidence for mCPBG (**17**) to penetrate the BBB has been controversial. A newer method of determining partition coefficients was employed using HPLC. With this method, mCPBG was shown to have a log P value consistent with its being able to cross the BBB. The log P values determined for PG (**27**), 3-FPG (**42**), MD-354 (**2**), 3-BrPG (**43**), 3-IPG (**44**), 3,4,5-tri-Cl-PG (**35**), 5-Cl quinazoline **48**, 6-Cl quinazoline **47**, and 7-Cl quinazoline **46** also indicate that they should be able to readily cross the BBB.

Considering the log P values of the quinazoline series indicates that these compounds should be able to readily cross the BBB and interact with central 5-HT₃ receptors and, considering that this is a novel series of 5-HT₃ receptor ligands, their ability to treat depression was evaluated with the mouse tail suspension test. Results from the study indicated that some of the doses of two of the quinazolines (1.0 and 3.0 mg/kg of **47** and 0.1, 0.3, and 1.0 mg/kg of **46**) decrease immobility time relative to saline. Whereas, the other quinazoline analog (i.e., **48**) and MD-354 (**2**) did not statistically decrease immobility time. Furthermore, the lowered immobility scores are not because of increased movements of the mice as shown by saline-like effects on the locomotor parameters assessed. However, the lack of selectivity for the 5-HT₃ receptor may indicate that the antidepressive action seen may or may not be because of a 5-HT₃ receptor mechanism. If the antidepressive action that is observed is not because of a 5-HT₃ receptor mechanism, then these compounds being antagonists is not relevant. But, if the antidepressive action that is observed is because of a 5-HT₃ receptor mechanism, then

these compounds are behaving similarly to the other 5-HT₃ receptor antagonists, ondansetron and bemesetron; if that is the case, the 5-HT₃ receptor agonist SR 57227A may be desensitizing the receptor and producing its antidepressive effect. If the antidepressant action of the agonist SR 57227A is from desensitization it may explain why MD-354, a partial agonist, is inactive and that the antidepressant action is because of an antagonist effect at the 5-HT₃ receptors. However, since 5-HT₃ receptors have been implicated in anxiety, the SR 57227A could be anxiogenic and the lowered immobility scores due to tremors from anxiety.

In conclusion, two novel series of MD-354 analogs were synthesized. The first series, halogen analogs, was used to determine that an electronic effect at a *meta*-position is essential for binding. Furthermore, the polarizability or the volume of the substituent is important as well for the binding of arylguanidines and arylbiguanides. It is most likely a combination of both the electronic effect and the polarizability, or the electronic effect and the volume, that affect binding together rather than just one individually. While the second series, quinazoline analogs, was developed to determine which *meta*-position was important, it has instead been shown to be a novel class of 5-HT₃ receptor ligands. Two of the analogs (i.e., **46** and **47**) have been shown to behave as antidepressants in the mouse tail suspension test. They may or may not be acting through a 5-HT₃ receptor mechanism since **46** binds with higher affinity to the 5-HT₅ and 5-HT₇ receptors and **47** only has a 4-fold selectivity over the 5-HT₅ receptor. Overall the current pharmacophore for arylguanidines and arylbiguanides has been validated for unconstrained

arylguanidines. And a novel class of 5-HT₃ receptor ligands, which are conformationally-constrained arylguanidines, has been developed which do not fit the pharmacophore for arylguanidines and arylbiguanides.

VI. Experimental

A. Synthesis

Melting points were taken on one of two melting point apparatuses in glass capillary tubes and are uncorrected. Unless otherwise noted melting points were taken on a Thomas-Hoover melting point apparatus. When noted, the melting points were taken on a Büchi B-545 melting point apparatus. ¹H NMR spectra were recorded with a Varian EM-390 spectrometer with tetramethylsilane (TMS) as an internal standard. Peak positions are given in parts per million (δ). Infrared spectra were obtained on a Nicolet Avatar 360 FT-IR spectrophotometer. Microanalyses were performed by Atlantic Microlab Inc. (Norcross, GA) for the indicated elements and results are within 0.4% of calculated values. Chromatographic separations were performed on silica gel columns (Silica Gel 62, 60-200 mesh, Sigma-Aldrich). Flash chromatography was performed on a CombiFlash Companion/TS (Teledyne Isco Inc. Lincoln, NE). Reactions were monitored by thin-layer chromatography (TLC) on silica gel GHLF plates (250 μ , 2.5 X 10 cm; Analtech Inc. Newark, DE).

***N*-(3-Fluorophenyl)guanidine Nitrate (42).** Compound **42** was prepared according to a literature procedure.¹⁴³ A solution of 3-fluoroaniline hydrochloride (**50**) (1.00 g, 6.78 mmol) and cyanamide (0.38 g, 9.04 mmol) in abs EtOH (5 mL) was heated at reflux for 6

h. The solvent was removed under reduced pressure to give a pale yellow oil. The crude product was dissolved in H₂O (2 mL) and NH₄NO₃ (1.00 g, 12.5 mmol) was added in excess. The solvent was removed under reduced pressure and the residue was crystallized from H₂O. The light brown crystals were collected by filtration and washed with cold Et₂O (3 x 5 mL) to yield 0.81 g (55%) of **42**: mp 145-146 °C (H₂O), 146-147 °C (EtOH) (lit¹⁷⁸ 165 °C, EtOH); IR (KBr, cm⁻¹): 3342, 3330, 3195, 1669, 1597, 1493, 1369, 1143; ¹H NMR (DMSO-d₆) δ 7.21-7.04 (m, 3H, ArH), 7.53-7.45 (m, 5H, ArH, NH₂, ex with D₂O), 9.72 (s, 1H, NH, ex with D₂O). Anal. calcd for C₇H₈FN₃ · HNO₃: C, 38.89; H, 4.20; N, 25.92 Found: C, 39.08; H, 4.15; N, 25.89.

2-Amino-7-chloro-3,4-dihydroquinazoline, Hydrochloride (46). Compound **46** was prepared using a literature procedure for a similar compound.¹⁵³ BH₃-THF complex (12.2 mL, 1 M, 12.2 mmol) was added in a dropwise manner to **56** (0.60 g, 3.06 mmol) under a N₂ atmosphere. The orange mixture was heated at reflux for 2.5 h. After cooling the reaction mixture to room temperature, a 6 N solution of HCl (3 mL) was added in a dropwise manner releasing gas. Then a 6 N solution of NaOH (12 mL) was added in a dropwise manner to basify the reaction mixture. The solution was concentrated under vacuum, and hot CHCl₃ (3 x 10 mL) was added. The solid at the interface was collected and dried under reduced pressure for 4 h to give a white solid 0.15 g, (24%): mp 183-185 °C; ¹H NMR (DMSO-δ₆): 3.45 (br s, 1H, NH, D₂O ex), 4.30 (s, 2H, CH₂), 6.12 (br s, 1H, NH, D₂O ex), 6.60 (s, 1H, ArH), 6.73 (d, 1H, ArH), 6.89 (d, 1H, ArH). A solution of the crude product (0.13g, 0.72 mmol) in abs EtOH was cooled in an ice/water bath.

Concentrated HCl was added in a dropwise manner to a pH \approx 3. The solvent was removed under reduced pressure and the process repeated twice more to give a white solid. The solid was recrystallized from hot EtOH to give a white solid 0.08 g (53%) of **46**: mp 249-251°C; IR (KBr, cm^{-1}): 3300, 3190, 2979, 2927, 2855, 1700, 1618, 1493, 1091; ^1H NMR (DMSO- δ_6): 4.45 (s, 2H, CH_2), 7.07 (d, 1H, ArH), 7.17 (dd, 1H, ArH), 7.25 (d, 1H, ArH), 7.77 (s, 2H, NH_2 , 1H D_2O ex), 8.63 (s, 1H, NH, D_2O ex), 11.02 (s, 1H, NH, D_2O ex). Anal calcd for $\text{C}_8\text{H}_8\text{N}_3\text{Cl} \cdot \text{HCl} \cdot 0.25 \text{H}_2\text{O}$: C, 43.17; H, 4.30; N, 18.88 Found C, 43.37; H, 4.07; N, 18.55.

2-Amino-6-chloro-3,4-dihydroquinazoline, Hydrochloride (47). Compound **47** was prepared according to a literature procedure for a similar compound.¹⁵³ BH_3 -THF complex (11.6 mL, 1 M, 11.6 mmol) was added in a dropwise manner to **58** (0.65 g, 3.33 mmol) under a N_2 atmosphere. The orange mixture was heated at reflux for 2 h. After cooling the reaction mixture to room temperature, a 6 N solution of HCl (3 mL) was added in a dropwise manner releasing gas. Then a 6 N solution of NaOH (12 mL) was added to basify the mixture. The solution was concentrated under vacuum, and extracted with hot CHCl_3 (20 mL x 3). The solvent was removed under reduced pressure to give a white solid 0.28 g (46%): mp 227-230 °C (lit¹³² 225-230 °C, EtOH). A solution of the crude product (0.28 g, 1.51 mmol) in abs EtOH was cooled in an ice/water bath. Concentrated HCl was added in a dropwise manner to pH \approx 3. The solvent was removed under reduced pressure and the process repeated twice more to give a white solid. The

solid was recrystallized from EtOH to afford a white crystalline solid 0.26 g (80%) of **47**: mp 237-240 °C (lit¹³² 237-238 °C, EtOH).

N-(3-Chloro-4-hydroxyphenyl)guanidine, Hydrochloride (51). Compound **51** was prepared according to a literature procedure.¹⁵⁰ A solution of **54** (0.13 g, 0.72 mmol) and cyanamide (0.046 g, 1.08 mmol, 50% aq solution) in abs EtOH was heated at reflux for 18 h. After allowing the purple solution to cool to room temperature, it was cooled further to -25 °C (in the freezer). A purple precipitate formed and was collected by filtration and washed with cold EtOH. The solid was dried under reduced pressure for 2 h over toluene to give **51** (0.080 g, 0.36 mmol, 50%) as a purple solid: mp 239-241 °C, 251-254 °C (Büchi melting point apparatus) (lit¹⁵⁰ 244-246 °C dec, EtOH); ¹H (DMSO-d₆): 2.53 (s, 1H, OH), 7.05 (s, 1H, ArH), 7.26-7.40 (d, 2H, ArH); IR (KBr, cm⁻¹) 3370, 1287.

2-Chloro-4-nitrophenol (53). Compound **53** was prepared according to a literature procedure.¹⁵¹ Nitric acid (10.9 mL H₂O, 9% wt) was added in a dropwise manner to a solution of 2-chlorophenol (**52**) (0.50 g, 3.89 mmol) in 1,2-dichloroethane (12.5 mL). The reaction mixture was sonicated for 3 h, then washed with H₂O (3 x 25 mL) and extracted with CH₂Cl₂ (3 x 25 mL). The combined organic portion was dried (Na₂SO₄), and the solvent was evaporated under reduced pressure to give a yellow, oily residue. Purification by flash chromatography on a silica gel column using hexanes/EtOAc (9:1) as eluent gave a crude yellow solid. The product was recrystallized from petroleum ether

to afford yellow crystals 0.24 g (35%) of **55**: mp 106-108 °C (lit¹⁵² 106-110 °C, H₂O and AcOH).

3-Chloro-4-hydroxyaniline, Hydrochloride (54). The free base of compound **54** was prepared according to a literature procedure.¹⁵² Sodium hydrosulfite (1.20 g, 6.91 mmol) was added in ten equal portions (0.12 g) over 10 min to a solution of **53** (0.30 g, 1.73 mmol) in H₂O (2 mL with 0.83 g, 20.74 mmol NaOH) heated at reflux. The reaction mixture was heated at reflux until the red color disappeared (approximately 20-30 min). After cooling to room temperature, a precipitate formed and was filtered then washed with cold H₂O. The filtrate was extracted with Et₂O (3 x 15 mL), the organic layer was dried (Na₂SO₄), and the solvent was removed under reduced pressure to afford a gray powder 0.13 g (50%) (which turned brown over time) of the free base of **54**: mp 149-151 °C (lit¹⁵² 150-151 °C, H₂O). The free base (0.125g, 0.87 mmol) was dissolved in EtOAc, cooled in an ice/water bath, and charged with N₂ (g). HCl (g) was bubbled in for 10 min. After 30 min of standing on ice the suspension was filtered to give **54** (0.13 g, 83%) as a pale gray solid: mp > 250 °C.

2-Amino-7-chloro-quinazolin-4-(3H)-one (56). Compound **56** was prepared according to a literature procedure for a similar compound.¹⁵³ S-Methylisothiurea sulfate (1.4 g, 5.06 mmol) and Na₂CO₃ (0.58 g, 5.47 mmol) were added to a solution of 4-chloroisatoic anhydride (**55**) (1.00 g, 5.06 mmol) in CH₃CN (24 mL, 80%) and heated at reflux for 5 h. The reaction mixture was allowed to cool to room temperature over 30 min and the precipitate was collected by filtration. The solid was washed with CH₃CN (80%, 3 x 25

mL) then dried under reduced pressure over toluene for 16 h to give **56** (0.64 g, 65%) as a pale pink solid: mp > 300 °C (lit¹⁷⁹ > 300 °C); IR (KBr, cm⁻¹) 3401, 2133, 1597, 1442, 1101; ¹H NMR (DMSO- δ_6): 6.58 (br s, 2H, NH₂, D₂O ex), 7.11 (dd, 1H, ArH), 7.21 (d, 1H, ArH), 7.87 (d, 1H, ArH), 11.10 (br s, 1H, NH, D₂O ex).

2-Amino-6-chloro-quinazolin-4-(3H)-one (58). This compound was prepared according to a literature procedure for a similar compound.¹⁵³ 5-Chloroisatoic anhydride (**57**) (1.00 g, 5.06 mmol) was dissolved in CH₃CN (24 mL, 80%), then S-methylisothiurea sulfate (1.4 g, 5.06 mmol) and Na₂CO₃ (0.58 g, 5.47 mmol) were added to the solution. The resulting solution was heated at reflux for 6 h. The reaction was allowed to cool to room temperature over 0.5 h. The suspension was filtered and washed with CH₃CN (80%, 25 mL x 3). The solid was dried under reduced pressure for 16 h to give a pale pink solid 0.67 g (67%): mp >300 °C (lit⁹ >300 °C).

2-Amino-4-chlorobenzylalcohol (60, R = H). Compound **60**, R = H, was prepared according to a literature procedure.¹⁶⁹ A suspension of LiAlH₄ (0.33 g, 8.74 mmol) in anhydrous THF (50 mL) was cooled to 0 °C in an ice/water bath under N₂ atmosphere. 2-Amino-4-chlorobenzoic acid (**59**, R = H) (1.0 g, 5.83 mmol) in THF (25 mL) was added in a dropwise manner. The mixture was allowed to stir in an ice/water bath for 30 min, room temperature for 30 min, then heated at reflux for 40 min. The mixture was cooled to 0 °C in an ice/water bath and an aqueous solution of THF (THF:H₂O, 2:1) was added. The precipitate was removed by filtration and washed with THF (3 x 10 mL). The filtrate was dried (MgSO₄) and the solvent was removed under reduced pressure. The resulting

solid was purified by column chromatography (hexanes:EtOAc, 2:1; hexanes:EtOAc, 1:1; EtOAc). The crude product was recrystallized from *i*-PrOH to give white crystals 0.80 g (87%) of the title compound: mp 139-140 °C (Lit¹⁶⁹ 140-142 °C).

2-Amino-4-chlorobenzylbromide (61, R = H). Method A. Compound **61** (R = H) was attempted to be prepared according to the literature procedure for a similar compound.¹⁸⁰ Phosphorous tribromide (0.09 g, 0.33 mmol) was added to a suspension of **60** (R = H) (0.10 g, 0.63 mmol) in Et₂O (3 mL) while stirring in an ice/water bath. The solution was stirred for 1 h then NH₄Cl (saturated, 5 mL) was added and gas evolved. Water (5 mL) was added, and the reaction mixture was extracted with Et₂O (3 x 5 mL). The Et₂O layer was washed with brine (5 mL) and dried (MgSO₄). The solvent was removed under reduce pressure. Compound **61** (R = H) could not be isolated.

Method B. Compound **61** (R = H) was attempted to be prepared according to the literature procedure for a similar compound.¹⁸¹ Phosphorous tribromide (0.34 g, 1.27 mmol) was added to a stirred solution of **60** (R = H) (0.10 g, 0.63 mmol) in CH₂Cl₂ (10 mL). The solution was stirred at room temperature for 4 h then quenched by the addition of H₂O (10 mL). The reaction mixture was extracted with CH₂Cl₂ (3 x 10 mL), washed with brine (10 mL), and dried (MgSO₄). The solvent was removed under reduced pressure. Compound **61** could not be isolated.

2-(2-Amino-4-chlorophenyl)acetic Acid (65). Attempts were made to prepare this compound according to a literature procedure.¹⁷¹ 6-Chlorooxindole (0.20 g, 1.19 mmol)

was suspended in 4 M NaOH (3 mL). The mixture was heated at reflux for 4.5 h, then cooled to room temperature. The precipitate was removed by filtration and washed with Et₂O. The solid was dissolved in H₂O (5 mL) and 6 N HCl was added in a dropwise manner while the solution was allowed to stir in an ice bath until a precipitate formed. The pale brown precipitate was collected: mp 195-197 °C. The filtrate was basified with 6 N NaOH and extracted with Et₂O (3 x 20 mL) and dried (Na₂SO₄). The solvent was removed to give a pale brown solid: mp 192-195 °C. The melting points of both solids matched the melting point of the starting material **64**: mp 195-199 °C; ¹H NMR (DMSO- δ_6) 3.44-3.54 (t, 2H), 3.94 (br s), 6.84 (s, 1H), 6.97-7.00 (d, 1H), 7.21-7.24 (d, 1H), 10.57 (s, 1H); IR (KBr, cm⁻¹) 3370, 1555, 1483, 1390, 1091. The literature¹⁷¹ melting point for **65**: 251-254 °C.

4-Chloro-2-nitrobenzaldehyde (69). Compound **69** was prepared according to a literature procedure.¹⁷³ A solution of **68** (2.5 g, 12.2 mmol) and DMF-DMA (4.36 g, 36.6 mmol) was allowed to stir in a 135 °C (oil bath) for 11 h then cooled to room temperature. The reaction mixture was added in a dropwise manner to a solution of NaIO₄ (7.8 g, 36.5 mmol) in H₂O (25 mL) and DMF (12.5 mL). After 3 h the suspension was filtered and the precipitate washed with toluene. The layers were separated and the organic portion was extracted with H₂O (3 x 15 mL) and solvent was removed under reduced pressure. The resulting oil was purified by column chromatography (hexanes:EtOAc, 5:1). The starting material **68** was recovered (1.4 g) and compound **69** was precipitated from the column fractions using hexanes to give 0.12 g (5%): mp 60-61

°C (lit¹⁸² 50-60 °C, lit¹⁸³ 67-68 °C); ¹H NMR (DMSO-d₆) δ 7.95-8.05 (m, 2H, ArH), 8.31 (s, 1H, ArH), 10.19 (s, 1H, OH).

4-Chloro-2-nitro-1-(2-nitrovinyl)benzene (70). Compound **70** was attempted to be synthesized by a literature procedure for a similar compound.¹⁷⁴ Ammonium acetate (0.02 g, 0.30 mmol) was added to a solution of **69** (0.10 g, 0.54 mmol) in CH₃NO₂ (1.0 mL). The reaction mixture was heated at reflux for 5.5 h then allowed to cool to room temperature. The solution was concentrated under reduced pressure and the crude product was triturated in cold CH₃OH (1 mL) and the solid removed by filtration. The filtrate was concentrated under reduced pressure. Neither column chromatography (hexanes:EtOAc, 4:1) nor Kugelrohr distillation could purify the product.

(4-Chloro-2-nitrophenyl)(1H-imidazol-1-yl)methanone (72). Compound **72** was synthesized according to a literature procedure.¹⁷⁵ Carbonyldiimidazole (1.2 g, 7.5 mmol) was added to a suspension of **71** (1.5 g, 7.5 mmol) in THF (10 mL); CH₃NO₂ (2.0 mL) and K₂CO₃ (1.1 g, 8.2 mmol) were added in THF (8 mL). The reaction mixture was allowed to stir and heated at reflux for 4 h then allowed to cool to room temperature and the solvent removed under reduced pressure. The oily residue was dissolved in EtOAc (25 mL) and extracted with H₂O (3 x 25 mL), washed with brine (10 mL), and dried (Na₂SO₄). The solvent was removed under reduced pressure and the residue was purified by column chromatography (EtOAc:CH₃OH, 9:1) to give a solid compound **72**: mp 139-140 °C; ¹H NMR (DMSO-d₆) δ 7.18 (s, 1H), 7.73 (s, 1H), 8.04-8.23 (m, 3H), 8.505 (s, 1H).

4-Chloro-2-nitrobenzylbromide (75). This compound was prepared according to a literature procedure.¹⁸⁴ Benzoyl peroxide (0.54 g, 2.2 mmol) was slowly added to a stirred solution of 4-chloro-2-nitrotoluene (**68**) (22.3 g, 130.0 mmol) and *N*-bromosuccinamide (23.1 g, 130.0 mmol) in CCl₄ (200 mL). The reaction mixture was heated at reflux for 4 h, then irradiated with a 250 W light bulb for an additional 65 h. After cooling to room temperature the suspension was filtered and the filtrate was washed with H₂O (2 x 50 mL). The organic portion was dried (MgSO₄) and the solvent was removed under reduced pressure to give a brown oil. Crystals formed upon the addition of Et₂O and petroleum ether. The remaining oil was purified by column chromatography (hexanes:EtOAc, 30:1) to give yellow crystals 14.5 g (45%): mp 38-39 °C (lit¹⁸⁴ 40-41 °C, hexanes).

2,3-Bis(4-chloro-2-nitrophenyl)propanenitrile (77). Method A. Compound **77** was prepared according to a literature procedure for a similar compound.¹⁷⁷ Sodium cyanide (0.37 g, 7.5 mmol) was dissolved in anhydrous DMSO (2.4 mL) under N₂ atmosphere at 10-15 °C. Concentrated H₂SO₄ (0.25 g, 2.5 mmol) was added by pipette and the mixture was allowed to stir for 10 min. A solution of **75** (0.63 g, 2.5 mmol) in anhydrous DMSO (1.1 mL) was added at -5 °C. The frozen suspension was allowed to warm to 5 °C. A blue precipitate formed then the solution turned brown. The solution was allowed to stir at 5 °C for 3 h. The reaction mixture was poured into ice water (25 mL). The suspension was extracted with EtOAc (3 x 15 mL). The organic portion was washed with brine (15 mL), dried (Na₂SO₄) and the solvent removed under reduced pressure. A crude brown oily

solid (0.50 g) was recrystallized from a mixture of Et₂O and CH₃OH to give 0.1 g of a beige solid: mp 155-157 °C; ¹H NMR (CDCl₃) δ 3.45-3.51 (d, 1H), 3.78-3.82 (d, 1H), 5.12-5.16 (t, 1H), 7.29 (s, 2H), 7.42 (d, 1H), 7.63-7.73 (m, 3H), 8.08 (s, 2H).

Method B. Sodium cyanide (23.48 g, 490 mmol) was dissolved in H₂O (133 mL). Compound **75** (12 g, 49.01 mmol) was added as a solution in CH₂Cl₂ (30 mL) with tetrabutylammonium bromide (0.05 g). The biphasic solution was allowed to vigorously stir for 30 min then separated. The organic portion was washed with H₂O (3 x 100 mL), dried (Na₂SO₄), and the solvent evaporated. The crude product was separated by flash chromatography (hexanes:EtOAc, 10:1; hexanes:EtOAc, 4:1, hexanes:EtOAc, 1:1). The collected fractions solvent was removed under reduced pressure and the product was recrystallized from a mixture of hexanes and Et₂O to give a pale, yellow solid: mp 149-150 °C.

Method C. Sodium cyanide (1.0 g) was dissolved in H₂O (5 mL). Hydrobromic acid was added in a dropwise manner until approximately pH 1-2. Compound **75** (0.1 g) was added as a solution in CH₂Cl₂ (10 mL). Addition of tetrabutylammonium bromide did not initiate the reaction.

Method D. Potassium cyanide (0.2 g) was suspended in acetonitrile (2 mL) and 18-crown-6 (~0.05 g) was added. Compound **75** (0.05 g) was added and the solution immediately turned blue then dark brown. After 1 h the starting material was consumed

and TLC comparison of the product was consistent with products from both Methods A and B.

B. Log P Analysis

High-performance liquid-chromatography was performed on a Varian ProStar (Model 210, Varian Inc. Palo Alto, CA). Compounds were dissolved in aqueous acetonitrile (~0.7 mg/mL; ~85%). Each solution was filtered a total of four times; twice through two separate 0.45 μm Teflon filters. An ammonium acetate buffer was made using HPLC-grade water (Spectrum, Gardena, CA) and ammonium hydroxide (28% NH_3 in H_2O ; Sigma-Aldrich) and acetic acid (99.5%; Sigma-Aldrich), the pH was measured using a pH meter and the pH was adjusted to 6.93-7.40. A Microsorb-MV 100 CN column (particle size 5 μm , 4.6 mm i.d. x 250 mm l.; Varian Inc., Palo Alto, CA), was equilibrated with HPLC-grade acetonitrile and the ammonium acetate buffer solution until a standard baseline and constant pressure were achieved. The column was set to run in isocratic mode for 30 min and detect at a wavelength of 254 nm.

1. Standards

A sample (30 μL) of one of the standards (i.e., acetanilide, benzophenone, naphthalene, diphenylamine, imidazole) or uracil was injected into a 20 μL loop and the retention time from the elution peak was recorded. At the end of 30 min cycle another 30 μL sample was run. This was repeated a third time then the column was washed by running it without a sample in graduated mode 80% to 20% acetonitrile. This process of

running three samples at one concentration of acetonitrile then washing the column was repeated for each sample at each concentration of acetonitrile used (40%, 50%, 60%, and 70%).

The average retention time for each standard and uracil was calculated for each concentration of acetonitrile (40%, 50%, 60%, and 70%). The relative retention time (RRT) to uracil was calculated for each compound at each concentration of acetonitrile by subtracting the average retention time of uracil from the average retention time of the standard (See Appendix A).

The log of the capacity factor ($\log k'$) was calculated for each compound at each concentration of acetonitrile by taking the log of RRT divided by the average retention time of uracil (See Appendix A).

The $\log k'$ values were plotted on the y-axis and the concentration of acetonitrile was plotted on the x-axis separately for each standard. Linear regression analyses were performed using GraphPad Prism (GraphPad Software Inc. La Jolla, CA) to give a linear equation for each compound. The $\log k'_w$ value is the y-intercept or the value when the concentration of acetonitrile is 0%.

The $\log k'_w$ values for each standard were plotted on the x-axis and their experimental log P values from a shake-flask experiment were plotted on the y-axis.

Linear regression analysis of this plot gave a standard curve equation (e.g., $\log P = 1.660 (\log k'_w) + 1.285$).

2. Halogen Series

The average retention time for each compound in the halogen series (i.e., **27, 2, 42-44, 35, 17**) was calculated for each concentration of acetonitrile (55%, 65%, and 75%). The relative retention time (RRT) to uracil was calculated for each compound at each concentration of acetonitrile by subtracting the average retention time of uracil from the average retention time of each compound tested. The log capacity factor ($\log k'$) was calculated for each compound at each concentration of acetonitrile by taking the log of the RRT divided by the average retention time of uracil (See Appendix A).

The $\log k'$ values were plotted on the y-axis and the concentration of acetonitrile was plotted on the x-axis separately for each compound. Linear regression analyses were performed using GraphPad Prism to give a linear equation for each compound. The $\log k'_w$ value is the y-intercept or the value when the concentration of acetonitrile is 0%. By substituting their $\log k'_w$ values into the standard curve equation the log P values were obtained.

3. Quinazoline Series

The average retention time for each compound in the quinazoline series (i.e., **46-48**) was calculated for each concentration of acetonitrile (55%, 60%, 65%, 70% and

75%). The relative retention time (RRT) to uracil was calculated for each compound at each concentration of acetonitrile by subtracting the average retention time of uracil from the average retention time of each compound tested. The log capacity factor ($\log k'$) was calculated for each compound at each concentration of acetonitrile by taking the log of the RRT divided by the average retention time of uracil (See Appendix A).

The $\log k'$ values were plotted on the y-axis and the concentration of acetonitrile was plotted on the x-axis separately for each compound. Linear regression analyses were performed using GraphPad Prism to give a linear equation for each compound. The $\log k'_w$ value is the y-intercept or the value when the concentration of acetonitrile is 0%. By substituting their $\log k'_w$ values into the standard curve equation the log P values were obtained.

C. Behavioral Studies

1. Animals

Male ICR mice (19-30 g) were used throughout the study (Harlan Laboratories, Indianapolis, IN). Mice were housed in groups of 5-6 in solid-bottom plastic cages in a temperature (~22 °C)- and humidity (~50%)-controlled room. A standard 12:12 h dark:light cycle (lights on at 0700 h) was used, and food and water were available *ad lib*. The experiments were conducted according to standards set by the Institutional Animal Care and Use Committee (IACUC) of Virginia Commonwealth University and the NIH Guide for Care and Use of Laboratory Animals. Mice were allowed to adapt to the testing

environment at least 1 h prior to any treatment, and weighed 30 min prior to the start of the experiments.

2. Drugs

Ondansetron hydrochloride (Zofran[®], Lot CO99723; GlaxoSmithKline) was purchased from MCVH-Pharmacy. Fluoxetine hydrochloride (Prozac[®], Batch 4A/80352; Eli Lilly) was purchased from Tocris. Desipramine hydrochloride (Norpramin[®], Lot 86H0942; Aventis Pharm) and imipramine hydrochloride (Tofranil[®], Lot 27H1380; Novartis) were purchased from Sigma. Compound **2** was used as a nitrate salt, compounds **46** and **47** were used as HCl salts, and compound **48** was used as an HBr salt; these four compounds were synthesized in our laboratory. Solutions were prepared fresh daily; all drugs were dissolved in 0.9% saline and administered to mice in a total volume of 10 mL/kg body weight by intraperitoneal (ip) injections. One exception was that solutions of compound **48** were not made fresh daily but were refrigerated overnight and used over a two-day period since very little of this compound was in stock and the synthesis is more extensive than the other quinazoline analogs.¹³³

3. Tail Suspension Test

The mice were allowed to adapt to the room and to a white noise generator (to block out ambient noises from the surrounding hallways) for at least 2 h prior to the test; tests were conducted between 1000 and 1500 h. Mice, naïve to the test apparatus, were suspended ~1.5 cm from the tip of their tail with industrial grade Duct Tape to a bar 60

cm above a flat bench. The experimenter/rater was unaware of the experimental conditions (drug, drug dose) for individual animals. A random number table was used to determine the order the drugs were administered to the mice.¹⁸⁵ The mice were treated with either saline (30 min pre-injection time), imipramine (20 mg/kg; 30 min pre-injection time), desipramine (20 mg/kg; 30 min pre-injection time), fluoxetine (20 mg/kg, 30 min pre-injection time), ondansetron (0.1 µg/kg, 30 min pre-injection time), MD-354 (0.1, 1.0, 3.0, 10, or 30 mg/kg; 30 min pre-injection time), **46** (0.1, 0.3, 1.0, 3.0, 10, or 30 mg/kg; 30 min pre-injection time), **47** (0.1, 0.3, 1.0, 3.0, 10, or 30 mg/kg; 30 min pre-injection time), or **48** (0.1, 0.3, 1.0, 3.0, or 10 mg/kg; 30 min pre-injection time). Drug doses and pre-injection times for the standard agents were identical with what has been previously reported.^{15,155} The mice were only tested once and each dose of test agent was studied in 8-11 mice ($n = 8-11$ mice/treatment). The six minute suspension test was captured by video recording either with a Logitech Quickcam Pro for Notebooks or Nikon Coolpix S210 and Pinnacle USB-video capture device. The immobility time for each mouse was determined by viewing each mouse's 6 min trial and recording the immobility time; each trial was reviewed and scored in triplicate and the mean of the three scores was used. A mouse was considered immobile when it was making no active escape movements but included passive swaying. A mouse was considered mobile when it was making running motions, body jerks, or attempting to catch its tail.

4. Locomotor Activity Assay

The mice were allowed to adapt to the room for at least 1 h prior to the test; tests were conducted between 0800 and 1630 h. Mice, naïve to the test apparatus, were placed in individual TruScan Activity System (Coulbourn Instruments, Allentown, PA) photocell arena chambers (model E63-10; 26 cm x 26 cm x 39 cm). The walls of the chamber were transparent and surrounded by two rings of infrared photodetectors (model E63-12). Each ring contained an array of 16 x 16 infrared detectors (spaced 1.524 cm (0.6 in) apart). These rings were interfaced to a computer for the monitoring of the coordinates of each mouse's location. A random number table was used to determine the order the drugs were administered.¹⁸⁵ The mice were treated with saline (0 min pre-injection time), **46** (0.3 mg/kg; 0 min pre-injection time), or **47** (1.0 or 3.0 mg/kg; 0 min pre-injection time). The mice were only tested once and each dose of test agent was studied in 12-13 mice ($n = 12-13$ mice/treatment). The behavioral analysis examined 14 measures of activity: movement episodes, movement time (s), movement distance (cm), jumps, retraced local movements, retraced local movement episodes, retraced local movement time (s), margin distance traveled (cm), margin time (s), center arena entries, center distance (cm), center time (s), velocity (cm/s), and vertical plane entries.

5. Statistical Analysis

Data for immobility times and for each measure of locomotor activity were analyzed statistically by a one-way analysis of variance (ANOVA) followed by either the Dunnett's t-test or the Newman-Keuls post-hoc comparison test using GraphPad Prism

(GraphPad Software Inc. La Jolla, CA). A Grubb's test for outliers was used to identify outliers with an $\alpha = 0.05$.

D. Molecular Modeling

The homology model studies were performed on a Silicon Graphics workstation using Sybyl (Version 7.3.3; Tripos Inc. St. Louis, MO), Modeller (Version 9.3; University of California San Francisco, San Francisco, CA), Chimera (Version 1, Build 2422; University of California San Francisco, San Francisco, CA), GOLD (Version 3.1; Cambridge Crystallographic Data Centre, Cambridge, UK), and AutoDock (Version 4; Scripps Research Institute, La Jolla, CA). All ligands were built in Sybyl and given AM1 charges and geometries based on MOPAC. The alignment of several LGICs and AChBPs was performed in Clustal X¹⁸⁶ using the following accession numbers: 47519841 (5-HT3A; *Homo sapiens*), 7305175 (5-HT3A; *Mus musculus*), 38327554 (GABA_A α 1; *Homo sapiens*), 4503863 (GABA_A β 1; *Homo sapiens*), 34734071 (GABA_A δ ; *Homo sapiens*), 12314059 (GABA_A ρ 2; *Homo sapiens*), 119372310 (Gly α 1; *Homo sapiens*), and 1346173 (Gly β ; *Homo sapiens*). PDBs used for alignment are 1i9b (AChBP; *Lymnaea stagnalis*), 2bg9 (nAChR; *Torpedo marmorata*), 2bj0 (AChBP; *Bulinus truncates*), 2byn (AChBP; *Aplysia californica*), and 2qc1 (nAChR α 1 and α -bungarotoxin; *Bungarus multicinctus*).

Bibliography

Bibliography

1. Twarog, B. M. Responses of a molluscan smooth muscle to acetylcholine and 5-hydroxytryptamine. *J. Cell Comp. Physiol.* **1954**, *44*, 141-163.
2. Gaddum, J. H.; Picarelli, Z. P. Two kinds of tryptamine receptors. *Br. J. Pharmacol.* **1957**, *12*, 323-328.
3. Funahashi, M.; Mitoh, Y.; Matsuo, R. Activation of presynaptic 5-HT₃ receptors facilitates glutamatergic synaptic input to area postrema neurons in rat brain slices. *Methods Find. Exp. Clin. Pharmacol.* **2004**, *26*, 615-622.
4. Greenshaw, A. J.; Silverstone, P. H. The non-antiemetic uses of serotonin 5-HT₃ receptor antagonists. *Drugs* **1997**, *53*, 20-39.
5. Faerber, L.; Drechsler, S.; Ladenburger, S.; Gschaimmeier, H.; Fischer, W. The neuronal 5-HT₃ receptor network after 20 years of research—evolving concepts in management of pain and inflammation. *Eur. J. Pharmacol.* **2007**, *560*, 1-8.
6. Glennon, R. A.; Dukat, M. Serotonin receptors and drugs affecting serotonergic neurotransmission. In *Foye's Medicinal Chemistry*, 5 ed.; Williams, D. A.; Lemke, T. L., Eds. Lippincott Williams & Wilkins: Baltimore, 2002; pp 315-337.
7. Dukat, M.; Abdel-Rahman, A. A.; Ismaiel, A. M.; Ingher, S.; Teitler, M.; Gyermek, L.; Glennon, R. A. Structure-activity relationships for the binding of arylpiperazines and arylbiguanides at 5-HT₃ serotonin receptors. *J. Med. Chem.* **1996**, *39*, 4017-4026.
8. Dukat, M.; Young, R.; Darmani, N. N.; Ahmed, B.; Glennon, R. A. The 5-HT₃ agent N-(3-chlorophenyl)guanidine (MD-354) serves as a discriminative stimulus in rats and displays partial agonist character in a shrew emesis assay. *Psychopharmacology* **2000**, *150*, 200-207.
9. Rahman, A. A.; Daoud, M. K.; Dukat, M.; Herrick-Davis, K.; Purohit, A.; Teitler, M.; Taveres do Amaral, A.; Malvezzi, A.; Glennon, R. A. Conformationally-restricted analogues and partition coefficients of the 5-HT₃ serotonin receptor ligands meta-chlorophenylbiguanide (mCPBG) and meta-chlorophenylguanidine (mCPG). *Bioorg. Med. Chem. Lett.* **2003**, *13*, 1119-1123.

10. Massie, M. J. Prevalence of depression in patients with cancer. *J. Natl. Cancer. Inst. Monogr.* **2004**, *32*, 57-71.
11. Pirl, W. F. Evidence report on the occurrence, assessment, and treatment of depression in cancer patients. *J. Natl. Cancer. Inst. Monogr.* **2004**, *32*, 32-39.
12. Bourin, M.; Hascoet, M.; Colombel, M. C.; Redrobe, J. P.; Baker, G. B. Differential effects of clonidine, lithium, and quinine in the forced swimming test in mice for antidepressants: possible roles of serotonergic systems. *Eur. Neuropsychopharmacol.* **1996**, *136*, 226-234.
13. Kos, T.; Popik, P.; Pietraszek, M.; Shchäfer, D.; Danysz, W.; Dravolina, O.; Blokhina, E.; Galankin, T.; Bernalov, A. Y. Effect of 5-HT₃ receptor antagonist MDL 72222 on behaviors induced by ketamine in rats and mice. *Eur. Neuropsychopharmacol.* **2006**, *16*, 297-310.
14. Poncelet, M.; Pério, A.; Simiand, J.; Gout, G.; Soubrié, P.; Le Fur, G. Antidepressant-like effects of SR 57227A, a 5-HT₃ receptor agonist, in rodents. *J. Neural Transm.* **1995**, *102*, 83-90.
15. Ramamoorthy, R.; Radhakrishnan, M.; Borah, M. Antidepressant-like effects of serotonin type-3 antagonist, ondansetron: an investigation in behaviour-based rodent models. *Behav. Pharmacol.* **2008**, *19*, 29-40.
16. Redrobe, J. P.; Bourin, M. Partial role of 5-HT₂ and 5-HT₃ receptors in the activity of antidepressants in the mouse forced swimming test. *Eur. J. Pharmacol.* **1997**, *325*, 129-135.
17. Srivastava, S. K. Antidepressant activity of ondansetron, a 5-HT₃ antagonist. *Indian J. Pharmacol.* **1998**, *30*, 411-412.
18. Rapport, M. M. The discovery of serotonin. *Perspect. Biol. Med.* **1997**, *40*, 260-273.
19. Erspamer, V.; Vialli, M. Ricerche sul secreto delle cellule enteroromaffini. *Boll. Soc. Med. Chir. di Pavia* **1937**, *51*, 357-363.
20. Rapport, M. M.; Green, A. A.; Page, I. H. Serum vasoconstriction (serotonin) III. Chemical inactivation. *J. Biol. Chem.* **1948**, *176*, 1237-1251.
21. Rapport, M. M. Serum vasoconstrictor (serotonin). V. The presence of creatinine in the complex: a proposed structure of the vasoconstrictor principle. *J. Biol. Chem.* **1949**, *180*, 961-969.

22. Erspamer, V.; Asero, B. Identification of enteramine, the specific hormone of the enterchromaffin cell system, as 5-hydroxytryptamine. *Nature* **1952**, *169*, 800-801.
23. Twarog, B. M.; Page, I. H. Serotonin content of some mammalian tissues and urine and a method for its determination. *Am. J. Physiol.* **1953**, *175*, 157-161.
24. Woolley, D. W.; Shaw, E. A. A biochemical and pharmacological suggestion about certain mental disorders. *Proc. Natl. Acad. Sci. USA* **1954**, *40*, 228-231.
25. Gaddum, J. H.; Hameed, K. A. Drugs which antagonize 5-hydroxytryptamine. *Br. J. Pharmacol.* **1954**, *9*, 240-248.
26. Peroutka, S. J.; Snyder, S. H. Multiple serotonin receptors: differential binding of [³H]5-hydroxytryptamine, [³H]lysergic acid diethylamide, and [³H]spiropiperidol. *Mol. Pharmacol.* **1979**, *16*, 687-699.
27. Kenakin, T. P.; Bond, R. A.; Bonner, T. I. Definition of pharmacological receptors. *Pharmacol. Rev.* **1992**, *44*, 351-362.
28. Hoyer, D.; Clarke, D. E.; Fozard, J. R.; Hartig, P. R.; Martin, G. R.; Mylecharane, E. J.; Saxena, P. R.; Humphrey, P. P. A. VII. International union of pharmacology classification of receptors for 5-hydroxytryptamine (serotonin). *Pharmacol. Rev.* **1994**, *46*, 157-203.
29. Green, A. R. Neuropharmacology of 5-hydroxytryptamine. *Br. J. Pharmacol.* **2006**, *147*, 5145-5152.
30. Kitson, S. L. 5-Hydroxytryptamine (5-HT) receptor ligands. *Curr. Pharm. Des.* **2007**, 2621-2637.
31. Lagerström, M. C.; Schiöth, H. B. Structural diversity of G protein-coupled receptors and significance for drug discovery. *Nat. Rev. Drug Design* **2008**, *7*, 339-357.
32. Boess, F. G.; Lummis, S. C. R.; Martin, I. L. Molecular properties of 5-hydroxytryptamine₃ receptor-type binding sites purified from NG108-15 cells. *J. Neurochem.* **1992**, *59*, 1692-1701.
33. Mukerji, J.; Haghghi, A.; Seguela, P. Immunological characterization and transmembrane topology of 5-hydroxytryptamine₃ receptors by functional epitope tagging. *J. Neurochem.* **1996**, *66*, 1027-1032.
34. Spier, A. D.; Wotherspoon, G.; Nayak, S. V.; Nichols, R. A.; Priestley, J. V.; Lummis, S. C. R. Antibodies against the extracellular domain of the 5-HT₃

- receptor label both native and recombinant receptors. *Mol. Brain Res.* **1999**, *67*, 221-230.
35. Eisele, J.-L.; Bertrand, S.; Galzi, J.-L.; Devillers-Thiery, A.; Changeux, J.-P.; Bertrand, D. Chimaeric nicotinic serotonergic receptor combines distinct ligand binding and channel specificities. *Nature* **1993**, *366*, 479-483.
 36. Reeves, D. C.; Lummis, S. C. R. The molecular basis of the structure and function of the 5-HT₃ receptor: a model ligand gated ion channel (Review). *Mol. Memb. Biol.* **2002**, *19*, 11-26.
 37. Ortells, M. O.; Lunt, G. G. Evolutionary history of the ligand-gated ion-channel superfamily of receptors. *Trends in Neurosciences* **1995**, *18*, 121-127.
 38. Brejc, K.; van Dijk, W. J.; Klaassen, R. V.; Schuurmans, M.; van der Oost, J.; Smith, A. B.; Sixma, T. K. Crystal structure of an ACh-binding protein reveals the ligand-binding domain of nicotinic receptors. *Nature* **2001**, *411*, 269-276.
 39. Celie, P. H.; Klaassen, R. V.; van Rossum-Fikkert, S. E.; van Elk, R.; van Nierop, P.; Smith, A. B.; Sixma, T. K. Crystal structure of acetylcholine-binding protein from *Bulinus truncatus* reveals the conserved structural scaffold and sites of variation in nicotinic acetylcholine receptors. *J. Biol. Chem.* **2005**, *280*, 26457-26466.
 40. Hansen, S. B.; Talley, T. T.; Radic, Z.; Taylor, P. Structural and ligand recognition characteristics of an acetylcholine-binding protein from *Aplysia californica*. *J. Biol. Chem.* **2004**, *279*, 24197-24202.
 41. Unwin, N. Refined structure of the nicotinic acetylcholine receptor at 4 Å resolution. *J. Mol. Biol.* **2005**, *346*, 967-989.
 42. Dellisanti, C. D.; Yao, Y.; Stroud, J. C.; Wang, Z. Z.; Chen, L. Crystal structure of the extracellular domain of nAChR α 1 bound to α -bungarotoxin at 1.94 Å resolution. *Nature Neurosci.* **2007**, *10*, 953-962.
 43. Bouzat, C.; Gumilar, F.; Spitzmaul, G.; Wang, H. I.; Rayes, D.; Hansen, S. B. Coupling of agonist binding to channel gating in an ACh-binding protein linked to an ion channel. *Nature* **2004**, *430*, 896-900.
 44. Bradley, P. B.; Engel, G.; Feniuk, W.; Fozard, J. R.; Humphrey, P. P. A.; Middlemiss, D. N.; Mylecharane, E. J.; Richardson, B. P.; Saxena, P. R. Proposal for the classification and nomenclature of functional receptors for 5-hydroxytryptamine. *Neuropharmacology* **1986**, *25*, 563-576.

45. Maricq, A. V.; Peterson, A. S.; Brake, A. J.; Myers, R. M.; Julius, D. Primary structure and functional expression of the 5-HT₃ receptor, a serotonin-gated ion channel. *Science* **1991**, *254*, 432-437.
46. Belelli, D.; Balcarek, J. M.; Hope, A. G.; Peters, J. A.; Lambert, J. J.; Blackburn, T. P. Cloning and functional expression of a human 5-hydroxytryptamine type 3A subunit. *Mol. Pharmacol.* **1995**, *48*, 1054-1062.
47. Miyake, A.; Mochizuki, S.; Takemoto, Y.; Akusawa, S. Molecular cloning of human 5-hydroxytryptamine₃ receptor: heterogeneity in distribution and function among species. *Mol. Pharmacol.* **1995**, *48*, 407-416.
48. Weiss, B.; Mertz, A.; Schröck, E.; Koenen, M.; Rappold, G. Assignment of a human homolog of the mouse *HTR3* receptor gene to chromosome 11q23.1-q23.2. *Genomics* **1995**, *29*, 304-305.
49. Jensen, T. N.; Nielsen, J.; Frederiksen, K.; Ebert, B. Molecular cloning and pharmacological characterization of serotonin 5-HT_{3A} receptor subtype in dog. *Eur. J. Pharmacol.* **2006**, *538*, 23-31.
50. Lankiewicz, S.; Lobitz, N.; Wetzel, C. H.; Rupprecht, R.; Gisselmann, G.; Hatt, H. Molecular cloning, functional expression, and pharmacological characterization of 5-hydroxytryptamine₃ receptor cDNA and its splice variants from the guinea pig. *Mol. Pharmacol.* **1998**, *399*, 97-106.
51. Mochizuki, S.; Watanabe, T.; Miyake, A.; Saito, M.; Furuichi, K. Cloning expression, and characterization of ferret 5-HT₃ receptor subunit. *Eur. J. Pharmacol.* **2000**, *399*, 97-106.
52. Bruss, M.; Barann, M.; Hayer-Zillgen, M.; Eucker, T.; Gothert, M.; Bonisch, H. Modified 5-HT_{3A} receptor function by co-expression of alternatively spliced human 5-HT_{3A} receptor isoforms. *Naunyn-Schmiedeberg's Arch. Pharmacol.* **2000**, *362*, 392-401.
53. Davies, P. A.; Pistis, M.; Hanna, M. C.; Peters, J. A.; Lambert, J. J.; Hales, T. G.; Kirkness, E. F. The 5-HT_{3B} subunit is a major determinant of serotonin-receptor function. *Nature* **1999**, *397*, 359-363.
54. Dubin, A. E.; Huva, R.; D'Andrea, M. R.; Pyati, J.; Zhu, J. Y.; Joy, K. C.; Wilson, S. J.; Galindo, J. E.; Glass, C. A.; Luo, L.; Jackson, M. R.; Lovenberg, T. W.; Erlander, M. G. The pharmacological and functional characteristics of the serotonin 5-HT_{3A} receptor are specifically modified by a 5-HT_{3B} receptor subunit. *J. Biol. Chem.* **1999**, *274*, 30779-30810.

55. Hanna, M. C.; Davies, P. A.; Hales, T. G.; Kirkness, E. F. Evidence for expression of heteromeric serotonin 5-HT₃ receptors in rodents. *J. Neurochem.* **2000**, *75*, 240-247.
56. Niesler, B.; Frank, B.; Kapeller, J.; Rappold, G. Cloning, physical mapping and expression analysis of the human 5-HT₃ serotonin receptor-like genes *HTR3C*, *HTR3D*, *HTR3E*. *Gene* **2003**, *310*, 101-111.
57. Karnovsky, A. M.; Gotow, L. F.; McKinley, D. D.; Piechan, J. L.; Ruble, C. L.; Mills, C. J.; Schellin, K. A.; Slightom, J. L.; Fitzgerald, L. A.; Benjamin, C. W.; Roberds, S. L. A cluster of novel serotonin receptor 3-like genes on human chromosome 3. *Gene* **2003**, *319*, 137-148.
58. Holbrook, J. D.; Gill, C. H.; Zebda, N.; Spencer, J. P.; Leyland, R.; Rance, K. H.; Trinh, H.; Balmer, G.; Kelly, F. M.; Yusaf, S. P.; Courtenay, N.; Luck, J.; Rhodes, A.; Modha, S.; Moore, S. E.; Sanger, G. J.; Gunthorpe, M. J. Characterisation of 5-HT_{3C}, 5-HT_{3D}, 5-HT_{3E} receptor subunits: evolution, distribution and function. *J. Neurochem.* **2009**, *108*, 384-396.
59. Niesler, B.; Walstab, J.; Combrink, S.; Moeller, D.; Kapeller, J.; Rietdorf, J.; Bonisch, H.; Gothert, M.; Rappold, G.; Bruss, M. Characterization of the novel human serotonin receptor subunits 5-HT_{3C}, 5-HT_{3D}, and 5-HT_{3E}. *Mol. Pharmacol.* **2007**, *72*, 8-17.
60. Barnes, N. M.; Hales, T. G.; Lummis, S. C. R.; Peters, J. A. The 5-HT₃ receptor—the relationship between structure and function. *Neuropharmacology* **2009**, *56*, 273-284.
61. Niesler, B.; Kapeller, J.; Hammer, C.; Rappold, G. Serotonin type 3 receptor genes: *HTR3A*, *B*, *C*, *D*, *E*. *Pharmacogenomics* **2008**, *9*, 501-504.
62. Barrera, N. P.; Herbert, P.; Henderson, R. M.; Martin, I. L.; Edwardson, J. M. Atomic force microscopy reveals the stoichiometry and subunit arrangement of 5-HT₃ receptors. *Proc. Natl. Acad. Sci. USA* **2005**, *102*, 12595-12600.
63. Pratt, G. D.; Bowery, N. G. The 5-HT₃ receptor ligand, [³H]BRL 43694, binds to presynaptic sites in the nucleus tractus solitarius of the rat. *Neuropharmacology* **1989**, *28*, 1367-1376.
64. Pratt, G. D.; Bowery, N. G.; Kilpatrick, G. J.; Leslie, R. A.; Barnes, N. M.; Naylor, R. J.; Jones, B. J.; Nelson, D. R.; Palacios, J. M.; Slater, P.; Reynolds, D. J. M. Consensus meeting agrees distribution of 5-HT₃ receptors in mammalian hindbrain. *Trends Pharmacol. Sci.* **1990**, *11*, 135-137.

65. Tecott, L. H.; Maricq, A. V.; Julius, D. Nervous system distribution of the serotonin 5-HT₃ receptor mRNA. *Proc. Natl. Acad. Sci. USA* **1993**, *90*, 1430-1434.
66. Abi-Dargham, A.; Laruelle, M.; Wong, D. R.; Roberston, D. W.; Weinberger, D. R.; Kleinman, J. E. Pharmacological and regional characterization of [³H]LY278584 binding sites in human brain. *J. Neurochem.* **1993**, *60*, 730-737.
67. Bufton, K. E.; Steward, L. J.; Barber, P. C.; Barnes, N. M. Distribution and characterization of the [³H]granisetron-labelled 5-HT₃ receptor in the human forebrain. *Neuropharmacology* **1993**, *32*, 1325-1331.
68. Parker, R. M.; Barnes, J. M.; Ge, J.; Barber, P. C.; Barnes, N. M. Autoradiographic distribution of [³H]-(s)-zacopride-labelled 5-HT₃ receptors in the human brain. *J. Neurol. Sci.* **1996**, *144*, 119-127.
69. Aviado, D. M.; Aviado, D. G. The Bezold-Jarisch reflex: a historical perspective of cardiopulmonary reflexes. *Annals NY Acad. Sci.* **2001**, *940*, 48-58.
70. Sam, T. S.; Cheng, J. T.; Johnston, K. D.; Dan, K. k.; Ngan, M. P.; Rudd, J. A.; Wai, M. K.; Yeung, J. H. K. Action of 5-HT₃ receptor antagonists and dexamethasone to modify cispatin-induced emesis in *Suncus murinus* (house musk shrew). *Eur. J. Pharmacol.* **2003**, *472*, 135-145.
71. Gozlan, H. 5-HT₃ Receptors. In *Serotonin Receptors and Their Ligands*, Olivier, B.; van Wijngaarden, I.; Soudijn, W., Eds. Elsevier Science B. V.: Amsterdam, 1997; pp 221-258.
72. Zhang, Y.; Vaenkatachalan, S. P.; Xu, H.; Xu, X.; Joshi, P.; Ji, H.-F.; Schulte, M. Michromechanical measurement of membrane receptor binding for label-free drug discovery. *Biosens. Bioelectron.* **2004**, *19*, 1473-1478.
73. Tang, Y.; Fang, F.; Yan, X.; Ji, H.-F. Fabrication and characterization of SiO₂ microcantilever for microsensor application. *Sens. Actuators* **2004**, *97*, 109-113.
74. Greenshaw, A. J. Behavioral pharmacology of 5-HT₃ receptor antagonists: a critical update on therapeutic potential. *Trends Pharmacol. Sci.* **1993**, *14*, 265-270.
75. Chey, W. D.; Cash, B. D. Cilansetron: a new serotonergic agent for the irritable bowel syndrome with diarrhoea. *Exp. Opin. Invest. Drug* **2005**, *14*, 185-193.
76. Sato, Y.; Yamada, M.; Yoshida, S.; Soneda, T.; Ishikawa, M.; Nizato, T.; Suzuki, K.; Konno, F. Benzoxazole derivatives as novel 5-HT₃ receptor partial agonists in the gut. *J. Med. Chem.* **1998**, *41*, 3015-3021.

77. Ito, H.; Kiso, T.; Miyata, K.; Kamato, T.; Yuki, H.; Akuzawa, S.; Nagakura, Y.; Yamano, M.; Suzuki, M.; Naitoh, Y.; Sakai, H.; Iwaoka, K.; Yamaguchi, T. Pharmacological profile of YM-31636, a novel 5-HT₃ receptor agonists, in vitro. *Eur. J. Pharmacol.* **2000**, *409*, 195-201.
78. Hamon, M.; Gallissot, M. C.; Menard, F.; Gozlan, H.; Bourgoin, S.; Verge, D. 5-HT₃ receptor binding sites are on capsiacin-sensitive fibres in the rat spinal cord. *Eur. J. Pharmacol.* **1989**, *164*, 315-322.
79. Wesolowska, A.; Young, S.; Dukat, M. MD-354 potentiates the antinociceptive effect of clonidine in the mouse tail-flick but not hot-plate assay. *Eur. J. Pharmacol.* **2004**, *495*, 129-136.
80. Costall, B.; Naylor, N. J. 5-HT₃ Receptors. *Curr. Drug Targets—CNS Neurological Disorders* **2004**, *3*, 27-37.
81. Bhatnagar, S.; Nowak, N.; Babich, L.; Bok, L. Deletion of the 5-HT₃ receptor differentially affects behavior of males and females in the Porsolt forced swim and defensive withdrawal tests. *Behav. Brain Res.* **2004**, *153*, 527-535.
82. Yamada, K.; Hattori, E.; Iwayama, Y.; Ohnishi, T.; Ohba, H.; Toyota, T.; Takao, H.; Minabe, Y.; Nakatani, N.; Higuchi, T.; Detera-Wadleigh, S. D.; Yoshikawa, T. Distinguishable haplotype blocks in the *HTR3A* and *HTR3B* region in the Japanese reveal evidence of association of *HTR3B* with femal major depression. *Biol. Psychiatry* **2006**, *60*, 192-201.
83. Dukat, M. 5-HT₃ Serotonin receptor agonists: a pharmacophoric journey. *Curr. Med. Chem.—Central Nervous System Agents* **2004**, *4*, 77-94.
84. Richardson, B. P.; Engel, G.; Donatsch, P.; Stadler, P. A. Identification of serotonin M-receptor subtypes and their specific blockade by a new class of drugs. *Nature* **1985**, *316*, 126-131.
85. Kilpatrick, G. J.; Bunce, K. T.; Tyers, M. B. 5-HT₃ Receptors. *Med. Res. Rev.* **1990**, *10*, 441-475.
86. Dukat, M.; Miller, K.; Teitler, M.; Glennon, R. A. Binding of amine-substituted and quaternary amine analogs of serotonin at 5-HT₃ serotonin receptors. *Med. Chem. Res.* **1991**, *1*, 271-276.
87. Wallis, D. I.; Nash, H. Relative activities of substances related to 5-hydroxytryptamine as depolarizing agents of superior cervical ganglion cells. *Eur. J. Pharmacol.* **1981**, *70*, 381-392.

88. Glennon, R. A.; Ismaiel, A. M.; McCarthy, B. G.; Peroutka, S. J. Binding of arylpiperazines to 5-HT₃ serotonin receptors: results of a structure-affinity study. *Eur. J. Pharmacol.* **1989**, *168*, 387-392.
89. Kilpatrick, G. J.; Jones, B. J.; Tyers, M. B. Identification and distribution of 5-HT₃ receptors in rat brain using radioligand binding. *Nature* **1987**, *330*, 746-748.
90. Campiani, G.; Cappelli, A.; Nacci, V.; Anzini, M.; Vomero, S.; Hamon, M.; Cagnotto, A.; Fracasso, C.; Uboldi, C.; Caccia, S.; Consol, S.; Mennuni, T. Novel and highly potent 5-HT₃ receptor agonists based on a pyrroloquinoxaline structure. *J. Med. Chem.* **1997**, *40*, 3670-3678.
91. Cappelli, A.; Anzini, M.; Vomero, S.; Canullo, L.; Mennuni, T.; Makovec, F.; Doucet, E.; Hamon, M.; Menziani, M. C.; De Benedetti, P. G.; Bruni, G.; Romeo, M. R.; Giorgi, G.; Donati, A. Novel potent and selective central 5-HT₃ receptor ligands provided with different intrinsic efficacy. 2. Molecular basis of the intrinsic efficacy of arylpiperazine derivatives at the central 5-HT₃ receptors. *J. Med. Chem.* **1999**, *42*, 1556-1575.
92. Cappelli, A.; Anzini, M.; Vomero, S.; Mennuni, T.; Makovec, F.; Doucet, E.; Hamon, M.; Bruni, G.; Romeo, M. R.; Menziani, M. C.; De Benedetti, P. G.; Langer, T. Novel potent and selective central 5-HT receptor ligands provided with different intrinsic efficacy. 1. Mapping the central 5-HT receptor binding site by arylpiperazine derivatives. *J. Med. Chem.* **1998**, *41*, 728-741.
93. Glennon, R. A.; Dukat, M. Serotonin receptors and their ligands. A lack of selective agents. *Pharmacol. Biochem. Behav.* **1991**, *40*, 1009-1017.
94. Zifa, E.; Fillion, G. 5-Hydroxytryptamine receptors. *Pharmacol. Rev.* **1992**, *44*, 401-458.
95. Cappelli, A.; Giuliani, G.; Gallelli, A.; Valenti, S.; Anzini, M.; Mennuni, T.; Makovec, F.; Cupello, A.; Vomero, S. Structure-affinity relationship studies on arylpiperazine derivatives related to quipazine as serotonin transporter ligands. Molecular basis of the selectivity SERT/5-HT₃ receptor. *Bioorg. Med. Chem.* **2005**, *13*, 3455-3460.
96. Kilpatrick, G. J.; Butler, A.; Burridge, J.; Oxford, A. W. 1-(m-Chlorophenyl)-biguanide, a potent high affinity 5-HT₃ receptor agonist. *Eur. J. Pharmacol.* **1990**, *182*, 193-197.
97. Bachy, A.; Héalme, M.; Giudice, A.; Michaud, J.-C.; Lefevre, I. A.; Souilhac, J.; Manara, L.; Emerit, M. B.; Gozlan, H.; Hamon, M.; Keane, P. E.; Soubrie, P.; Le Fur, G. SR 57227A: a potent and selective agonist at central and peripheral 5-HT₃ receptors in vitro and in vivo. *Eur. J. Pharmacol.* **1993**, *237*, 299-309.

98. Kilpatrick, G. J.; Rogers, H. 5-HT₃ Receptors. In *Serotonin*, Vanhoutte, P. M., Ed. Kluwer Academic Publisher and Fondazione Giovanni Lorenzini: Netherlands, 1993; pp 99-106.
99. Steward, L. J.; West, K. E.; Kilpatrick, G. J.; Barnes, N. M. Labelling of 5-HT₃ receptor recognition sites in the rat brain using the agonist radioligands [³H]meta-chlorophenylbiguanide. *Eur. J. Pharmacol.* **1993**, *243*, 13-18.
100. Dukat, M.; Choi, Y.; Teitler, M.; Du Pre, A.; Herrick-Davis, K.; Smith, C.; Glennon, R. A. The binding of arylguanidines at 5-HT₃ serotonin receptors: a structure-affinity investigation. *Bioorg. Med. Chem. Lett.* **2001**, *11*, 1599-1603.
101. Morain, P.; Abraham, C.; Portevin, B.; De Nanteuil, G. Biguanide derivatives: agonist pharmacology at 5-hydroxytryptamine type 3 receptors in vitro. *Mol. Pharmacol.* **1994**, *46*, 732-742.
102. Glennon, R. A. Pharmacophore identification for sigma-1 (σ_1) receptor binding: application of the "deconstruction - reconstruction - elaboration" approach. *Mini Rev. Med. Chem.* **2005**, *5*, 927-940.
103. Daveu, C.; Bureau, R.; Baglin, I.; Prunier, H.; Lancelot, J.-C.; Rault, S. Definition of a pharmacophore for partial agonists of serotonin 5-HT₃ receptors. *J. Chem. Inf. Comput. Sci.* **1999**, *39*, 362-369.
104. Yamada, M.; Sato, Y.; Kobayahi, K.; Konno, F.; Soneda, T.; Watanabe, T. A new 5-HT₃ receptor ligand. II. Structure-activity analysis of 5-HT₃ receptor agonist activity in the gut. *Chem. Pharm. Bull.* **1998**, *46*, 445-451.
105. Fozard, J. R.; Mobarak Ali, A. T. M.; Newgroush, G. Blockade of serotonin receptors on autonomic neurons by (-)-cocaine and some related compounds. *Eur. J. Pharmacol.* **1979**, *59*, 195-210.
106. Fozard, J. R.; Gittos, M. W. Selective blockade of 5-hydroxytryptamine neuronal receptors by benzoic acid esters of tropine. *Br. J. Pharmacol.* **1983**, *80*, 511P.
107. Kilpatrick, G. J.; Tyers, M. B. The pharmacological properties and functional roles of central 5-HT₃ receptors. In *Central and peripheral 5-HT₃ receptors*, Hamon, M., Ed. Academic Press: San Diego, 1992; pp 33-58.
108. King, F. D. Structure activity relationships of 5-HT₃ receptor antagonists. In *5-Hydroxytryptamine-3 receptor antagonists*, King, F. D.; Jones, B. J.; Sanger, G. J., Eds. CRC Press: Boca Raton, 1994; pp 1-66.

109. Richardson, B. P.; Buchheit, K. H. The pharmacology, distribution and function of 5-HT₃ receptors. In *Neuronal Serotonin*, Osborne, N. N.; Hamon, M., Eds. John Wiley & Sons: New York, 1988; pp 465-506.
110. Sanger, G. J.; Wootton, G. Benzamide and anilide derivatives. EP0158265(A2), 1985.
111. Barnes, J. M.; Barnes, N. M.; Costall, B.; Ironside, J. W.; Naylor, R. J. Identification and characterisation of 5-hydroxytryptamine₃ recognition sites in human brain tissue. *J. Neurochem.* **1989**, *53*, 1787-1793.
112. Oxford, A. W.; Bell, J. A.; Kilpatrick, G. J.; Ireland, S. J.; Tyers, M. B. Ondansetron and related 5-HT₃ antagonists: recent advances. In *Progress in Medicinal Chemistry*, Ellis, G. P.; Luscombe, D. K., Eds. Elsevier Science Publishers: 1992; Vol. 29, pp 239-270.
113. Hansch, C. A quantitative approach to biochemical structure-activity relationships. *Acc. Chem. Res.* **1969**, *2*.
114. Hansch, C. On the structure of medicinal chemistry. *J. Med. Chem.* **1976**, *19*, 1-6.
115. Hansch, C.; Leo, A.; Unger, S. H.; Kim, K. H.; Nikaitani, D.; Lien, E. J. "Aromatic" substituent constants for structure-activity correlations. *J. Med. Chem.* **1973**, *16*, 1207-1216.
116. Lien, E. J.; Guo, Z. R.; Li, R. L.; Su, C. T. Use of dipole moment as a parameter in drug-receptor interaction and quantitative structure-activity relationship studies. *J. Pharm. Sci.* **1982**, *71*, 641-655.
117. Taft, R. W. Steric Effects. In *Organic Chemistry*, Newman, M. S., Ed. Wiley: New York, 1956; pp 556-675.
118. Verloop, A.; Hoogerstraaten, W.; Tipker, J. Development and application of new steric parameters. In *Drug Design*, Ariens, Ed. Academic Press: New York, 1976; Vol. VII, pp 165-207.
119. Tipker, J.; Verloop, A., The chemistry of excitation at interfaces. In *American Chemical Society*, Washington DC, 1984.
120. Verma, R. P.; Kurup, A.; Hansch, C. On the role of polarizability in QSAR. *Bioorg. Med. Chem.* **2005**, *13*, 237-255.
121. Quayle, O. R. The parachors of organic compounds. *Chem. Rev.* **1953**, *53*, 439-589.

122. Kubinyi, H. QSAR and 3D QSAR in drug design part 1: methodology. *Drug Discov. Today* **1997**, *2*, 457-467.
123. Cramer, R. D.; Patterson, D. E.; Bunce, J. D. Comparative molecular field analysis (CoMFA). 1. Effect of shape on binding steroids to carrier proteins. *J. Am. Chem. Soc.* **1988**, *110*, 5959-5967.
124. Glennon, R. A.; Daoud, M. K.; Dukat, M.; Teitler, M.; Herrick-Davis, K.; Purohit, A.; Syed, H. Arylguanidine and arylbiguanide binding at 5-HT₃ serotonin receptors: a QSAR study. *Bioorg. Med. Chem.* **2003**, *11*, 449-454.
125. Porsolt, R. D.; Le Pichon, M.; Jalfre, M. Depression: a new animal model sensitive to antidepressant treatments. *Nature* **1977**, *266*, 730-732.
126. Porsolt, R. D. Behavioral despair. In *Antidepressants: neurochemical, behavioral and clinical perspectives*, Enna, S. J.; Malick, J.; Richelson, E., Eds. Raven Press: New York, 1981; pp 121-139.
127. Liu, X.; Peprah, D.; Gershenfield, H. K. Tail-suspension induced hypothermia: a new measure of stress reactivity. *J. Psychiatr. Res.* **2003**, *37*, 249-259.
128. Cryan, J. F.; Mombereau, C.; Vassout, A. The tail suspension test as a model for assessing antidepressant activity: Review of pharmacological and genetic studies in mice. *Neurosci. Biobehav. Rev.* **2005**, *29*, 571-625.
129. Bourin, M.; Chen, F.; Ripoll, N.; David, D. J. P. A proposal of decision tree to screen putative antidepressants using forced swim and tail suspension tests. *Behav. Brain Res.* **2005**, *164*, 266-269.
130. Porsolt, R. D.; Lenegre, A. Behavioral models of depression. In *Experimental approaches to anxiety and depression*, Elliot, J.; Heal, D.; Mardesh, C., Eds. Wiley: London, 1992; pp 73-85.
131. Steru, L.; Chermat, R.; Thierry, B.; Simon, P. The tail suspension test: a new method for screening antidepressants in mice. *Psychopharmacology* **1985**, *85*, 367-370.
132. Worsham, J. N. 5-HT₃ Receptor ligands and their effect on psychomotor stimulants. Virginia Commonwealth University, Richmond, 2008.
133. Young, S. Dual mechanism analgesia-enhancing agents. Virginia Commonwealth University, Richmond, 2005.
134. Lodge, N. J.; Li, Y.-W. Ion channels as potential targets for the treatment of depression. *Curr. Opin. Drug Discov. Devel.* **2008**, *11*, 633-641.

135. Gaynes, B. N.; Rush, A. J.; Trivedi, M. H.; Wisniewski, S. R.; Spenser, D.; Fava, M. The STAR*D study: treating depression in the real world. *Cleveland Clin. J. Med.* **2008**, *75*, 57-66.
136. Nestler, E. J. Antidepressant treatments in the 21st century. *Biol. Psychiatry* **1988**, *44*, 526-533.
137. Ressler, K. J.; Nemeroff, C. B. Role of norepinephrine in the pathophysiology and treatment of mood disorders. *Biol. Psychiatry* **1999**, *46*, 1219-1233.
138. Hansch, C.; Björkroth, J. P.; Leo, A. Hydrophobicity and central nervous system agents: on the principle of minimal hydrophobicity in drug design. *J. Pharm. Sci.* **1987**, *76*, 663-687.
139. Brent, D. A.; Sabatka, J. J.; Minick, D. J.; Henry, D. W. A simplified high-pressure liquid chromatography method for determining lipophilicity for structure-activity relationships. *J. Med. Chem.* **1983**, *26*, 1014-1020.
140. Valko, K. General approach for the estimation of octanol/water partition coefficient by reversed-phase high-performance liquid chromatography. *J. Liq. Chromatogr.* **1984**, *7*, 1405-1424.
141. Mirrless, M. S.; Multon, S. J.; Murphy, C. T.; Taylor, P. J. Direct measure of octanol-water partition coefficients by high-pressure liquid chromatography. *J. Med. Chem.* **1976**, *19*, 615-619.
142. Lombardo, F.; Shalaeva, M. Y.; Tupper, K. A.; Gao, F.; Abraham, M. H. ElogP: a tool for lipophilicity determination in drug discovery. *J. Med. Chem.* **2000**, *43*, 2922-2928.
143. King, H.; Tokin, I. M. 235. Antiplasmodial action and chemical constitution. Part VIII. Guanidines and diguanides. *J. Chem. Soc.* **1946**, 1063-1069.
144. Hansch, C.; Leo, A.; Hoekman, D. *Exploring QSAR: Hydrophobic, electronic, and steric constants*. American Chemical Society: Washington DC, 1995; Vol. II.
145. Maksay, G.; Simonyi, M.; Bikádi, Z. Subunit rotation models activation of serotonin 5-HT_{3AB} receptors by agonists. *J. Comput. Aided Mol. Des.* **2004**, *18*, 651-664.
146. Reeves, D. C.; Sayed, M. F. R.; Chau, P.-L.; Price, K. L.; Lummis, S. C. R. Prediction of 5-HT₃ receptor agonist-binding residues using homology modeling. *Biophys. J.* **2003**, *84*, 2338-2344.
147. Razgulin, A. V.; Mecozzi, S. Binding properties of aromatic carbon-bound fluorine. *J. Med. Chem.* **2006**, *49*, 7902-7906.

148. Smart, B. E. Characteristics of C-F systems. In *Organofluorine Chemistry: Principles and Commercial Applications*, Banks, R. E.; Smart, B. E.; Tatlow, J. C., Eds. Plenum Press: New York, 1994; pp 57-88.
149. Price, K. L.; Bower, K. S.; Thompson, A. J.; Lester, H. A.; Dougherty, D. A.; Lummis, S. C. R. A hydrogen bond in loop A is critical for the binding and function of the 5-HT₃ receptor. *Biochemistry* **2008**, *47*, 6370-6377.
150. Hughes, J. L.; Liu, R. C.; Enkoji, T.; Smith, C. M.; Bastian, J. W.; Luna, P. D. Cardiovascular activity of aromatic guanidine compounds. *J. Med. Chem.* **1975**, *18*, 1077-1088.
151. Nandurkar, N. S.; Bhor, M. D.; Samant, S. D.; Bhanage, B. M. Ultrasound-assisted regioselective nitration of phenols using dilute nitric acid in a biphasic medium. *Ind. Eng. Chem. Res.* **2007**, *46*, 8590-8596.
152. Christiansen, W. G. *N*-Methyl-para-amino-ortho-chlorophenol sulfate, a new photographic developer. *J. Am. Chem. Soc.* **1923**, *45*, 2192-2194.
153. Grosso, J. A.; Nichols, D. E.; Kohli, J. D.; Glock, D. Synthesis of 2-(alkylamino)-5,6- and -6,7-dihydroxy-3,4-dihydroquinazolines and evaluation as potential dopamine agonists. *J. Med. Chem.* **1982**, *25*, 703-708.
154. Roth, B. L., PDSP. In National Institute of Mental Health's Psychoactive Drug Screening Program: 2009.
155. Jacobsen, J. P. R.; Nielsen, E. Ø.; Hummel, R.; Redrobe, J. P.; Mirza, N.; Weikop, P. Insensitivity of NMRI mice to selective serotonin reuptake inhibitors in the tail suspension test can be reversed by co-treatment with 5-hydroxytryptophan. *Psychopharmacology* **2008**, *199*, 137-150.
156. van der Hayden, J. A. M.; Molewijk, E.; Olivier, B. Strain differences in response to drugs in the tail suspension test for antidepressant activity. *Psychopharmacology* **1987**, *92*, 127-130.
157. Nomura, S.; Okada, H.; Naruse, R.; Yamaoka, K. The tail suspension test for screening antidepressant drugs: comparison of movement in ICR and NMRI mice. *Jpn. J. Psychiatry Neurol.* **1991**, *45*, 113-114.
158. Hapfelmeier, G.; Tredt, C.; Haseneder, R.; Zieglgaensberger, W.; Eisensamer, B.; Rupprecht, R.; Rammes, G. Co-expression of the 5-HT_{3B} serotonin receptor subunit alters the biophysics of the 5-HT₃ receptor. *Biophys. J.* **2003**, *84*, 1720-1733.

159. Peters, J.-U.; Lübbers, T.; Alanine, A.; Kolczewski, S.; Blasco, F.; Steward, L. J. Cyclic guanidines as dual 5-HT_{5A}/5-HT₇ receptor ligands: structure-activity relationship elucidation. *Bioorg. Med. Chem. Lett.* **2008**, *18*, 256-261.
160. Peters, J.-U.; Lübbers, T.; Alanine, A.; Kolczewski, S.; Blasco, F.; Steward, L. J. Cyclic guanidines as dual 5-HT_{5A}/5-HT₇ receptor ligands: optimising brain penetration. *Bioorg. Med. Chem. Lett.* **2008**, *18*, 262-266.
161. Mnie-Filali, O.; Lambás-Señas, L.; Zimmer, L.; Haddjeri, N. 5-HT₇ receptor antagonists as a new class of antidepressants. *Drug News Perspect.* **2007**, *20*, 613-618.
162. Arias, B.; Collier, D. A.; Gastó, C.; Pintor, L.; Gutiérrez, B.; Vallès, V.; Fañanás, L. Genetic variation in the 5-HT_{5A} receptor gene in patients with bipolar disorder and major depression. *Neurosci. Lett.* **2001**, *303*, 111-114.
163. Birkett, J. T.; Arranz, M. J.; Munro, J.; Osborurn, S.; Kerwin, R. W.; Collier, D. A. Association analysis of the 5-HT_{5A} gene in depression, psychosis and antipsychotic response. *NeuroReport* **2000**, *11*, 2017-2020.
164. Young, R.; Glennon, R. A. MDMA (*N*-methyl-3,4-methylenedioxyamphetamine) and its stereoisomers: similarities and differences in behavioral effects in an automated activity apparatus in mice. *Pharmacol. Biochem. Behav.* **2008**, *88*, 318-331.
165. Belzung, C.; Le Guisquet, A. M.; Barreau, S.; Calatayud, F. An investigation of the mechanisms responsible for acute fluoxetine induced anxiogenic-like effects in mice. *Behav. Pharmacol.* **2001**, *12*, 151-162.
166. Greenwood, B. N.; Strong, P. V.; Brooks, L.; Fleshner, M. Anxiety-like behaviors produced by acute fluoxetine administration in male Fischer 344 rats are prevented by prior exercise. *Psychopharmacology* **2008**, *199*, 209-222.
167. Maksay, G.; Bikádi, Z.; Simonyi, M. Binding interactions of antagonists with 5-hydroxytryptamine_{3A} receptor models. *J. Recept. Signal Transduct.* **2003**, *23*, 255-270.
168. Thompson, A. J.; Price, K. L.; Reeves, D. C.; Chan, S. L.; Chau, P.-L.; Lummis, S. C. R. Locating an antagonist in the 5-HT₃ receptor binding site using modeling and radioligand binding. *J. Biol. Chem.* **2005**, *280*, 20476-20482.
169. Cordi, A. A.; Desos, P.; Randle, J. C. R.; Lepagnol, J. Structure-activity relationships in a series of 3-sulfonylamino-2-(1H)-quinolones, as new AMPA/Kainate and glycine antagonists. *Bioorg. Med. Chem.* **1995**, *3*, 129-141.

170. Kasuga, J.; Nakagome, I.; Aoyama, A.; Sako, Y.; Ishizawa, M.; Ogura, M.; Makishima, M.; Hirono, S.; Hashimoto, Y.; Miyachi, H. Design, synthesis, and evaluation of potent, structurally novel peroxisome proliferator-activated receptor (PPAR) δ -selective agonists. *Bioorg. Med. Chem.* **2007**, *15*, 5177-5190.
171. Valgeirsson, J.; Nielsen, J.; Peters, D.; Mathiesen, C.; Kristensen, A. S.; Madsen, U. Bioisosteric modifications of 2-aryluroidobenzoic acids: selective noncompetitive antagonists for the homomeric kainate receptor subtype GluR5. *J. Med. Chem.* **2004**, *47*, 6948-6957.
172. Houlihan, W. J., *Indoles*. Wiley-Interscience: New York, 1972; Vol. 25.
173. Caron, S.; Vazquez, E.; Stevens, R. W.; Nakao, K.; Koike, H.; Murata, Y. Efficient synthesis of [6-chloro-2-(4-chlorobenzoyl)-1*H*-indol-3-yl]-acetic acid, a novel COX-2 inhibitor. *J. Org. Chem.* **2003**, *68*, 4104-4107.
174. Monte, A. P.; Marona-Lewicka, D.; Cozzi, N. V.; Nichols, D. E. Synthesis and pharmacological evaluation of benzofuran, indan, and tetralin analogs of 3,4-(methylenedioxy)amphetamine. *J. Med. Chem.* **1993**, *36*, 3700-3706.
175. Hwang, K.-J.; Lee, T.-S. Synthesis of kynurenic analogues as potential NMDA receptor glycine site antagonists. *Korean J. Med. Chem.* **1999**, *9*, 75-78.
176. Davis, A. L.; Chambers, W. H.; Kelley, D. H.; Fell, D. A.; Haynes, J. R.; Hulme, K. L.; Gage, L. D.; McCord, T. J. Synthesis and antibacterial activities of some chloro analogs of 3-amino-3,4-dihydro-1-hydroxycarbostyryl. *J. Med. Chem.* **1975**, *18*, 752-755.
177. Kalir, A.; Mualem, R. One-step synthesis of 2- and 4-nitrobenzyl cyanides. *Synthesis* **1987**, *5*, 514-515.
178. Heesing, A.; Schmaldt, W. Zum substituenteneinfluß der guanidino- und der guanidiniumgruppe, teil I: der effekt auf die ¹⁹F-NMR-spektren von fluorbenzolen und auf die aromatische substitution. *Chem. Ber.* **1978**, *111*, 320-334.
179. Keyser, G. E.; Leonard, N. J. Linear benzoguanine. Synthesis by two independent methods. *J. Org. Chem.* **1976**, *41*, 3529-3532.
180. Kasuga, J.; Nakagome, I.; Aoyama, A.; Sako, K.; Ishizawa, M.; Ogura, M.; Makishima, M.; Hirono, S.; Hashimoto, Y.; Miyachi, H. Design, synthesis, and evaluation of potent, structurally novel peroxisome proliferator-activated receptor (PPAR) δ -selective agonists. *Bioorg. Med. Chem.* **2007**, *15*, 5177-5190.

181. Zhou, L.; Zhang, T.-X.; Li, B.-R.; Cao, X.-P.; Kuck, D. C_{3v} -Symmetrical tribenzotriquinacenes extended by six C_1 -functional groups and the first triquinacene-based tris(dithiametacyclophanes). *J. Org. Chem.* **2007**, *72*, 6382-6389.
182. Ahmad, A.; Dunbar, L. J.; Green, I. G.; Harvey, I. W.; Shepherd, T.; Smith, D. M.; Wong, R. K. C. Polyaza heterocycles. Part 2. Nucleophilic substitution of halogens in halogenoquinoxalino[2,3-*c*]cinnolines. *J. Chem. Soc. Perkin Trans. I* **1994**, *19*, 2751-2758.
183. Spalding, D. P.; Moersch, G. W.; Mosher, H. S.; Whitmore, F. C. Heterocyclic basic compounds. IX. 3,6-Dichloro-9-(1-methyl-4-diethylaminobutyl)-aminoacridine. *J. Am. Chem. Soc.* **1946**, *68*, 1596-1598.
184. Stadler, H. Metaboliten der 1,5-dihydroimidazo[2,1-*b*]chinazolin-2(3*H*)-one. Synthese und reaktionen einiger 1,5-dihydro-3-hydroxyimidzo[2,1-*b*]chinazolin-2(3*H*)-one. *Helv. Chim. Acta* **1986**, *69*, 1887-1897.
185. Winer, B. J. *Statistical Principles in experimental design*. McGraw-Hill: New York, 1962.
186. Larkin, M. A.; Blackshields, G.; Brown, N. P.; Chenna, R.; McGettigan, P. A.; McWilliam, H.; Valentin, F.; Wallace, I. M.; Wilm, A.; Lopez, R.; Thompson, J. D.; Gibson, T. J.; Higgins, D. G. Clustal W and clustal X version 2.0. *Bioinformatics* **2007**, *23*, 2947-2948.

Appendix A

HPLC Data for Standards in Log P Analysis

Compound		Acetonitrile			
		40%	50%	60%	70%
Uracil	RT	3.973	4.032	4.136	4.034
Acetanilide	RT	5.360	4.745	4.664	4.541
	RRT	1.387	0.713	0.528	0.507
	$\log k'$	-0.457	-0.753	-0.894	-0.900
Benzophenone	RT	8.551	5.478	4.928	4.593
	RRT	4.578	1.446	0.792	0.559
	$\log k'$	0.062	-0.445	-0.718	-0.858
Naphthalene	RT	9.119	6.256	5.054	5.016
	RRT	5.146	2.224	0.918	0.982
	$\log k'$	0.112	-0.258	-0.654	-0.613
Diphenylamine	RT	10.467	6.502	4.750	4.954
	RRT	6.494	2.470	0.614	0.920
	$\log k'$	0.213	-0.213	-0.828	-0.642
Imidazole	RT	4.859	4.924	5.577	5.226
	RRT	0.886	0.892	1.441	1.192
	$\log k'$	-0.652	-0.655	-0.458	-0.529

HPLC Data for Halogen Series in Log P Analysis

Compound		Acetonitrile		
		55%	65%	75%
Uracil	RT	3.314	3.391	3.466
27	RT	10.093	9.833	10.596
	RRT	6.779	6.441	7.130
	$\log k'$	0.311	0.279	0.313
2	RT	9.286	9.423	10.168
	RRT	5.972	6.032	6.703
	$\log k'$	0.256	0.250	0.286

42	RT	9.498	9.529	10.083
	RRT	6.184	6.138	6.618
	$\log k'$	0.271	0.258	0.281
43	RT	11.039	10.468	10.801
	RRT	7.725	7.077	7.336
	$\log k'$	0.368	0.319	0.326
44	RT	11.792	10.989	10.980
	RRT	8.478	7.598	7.514
	$\log k'$	0.408	0.350	0.336
35	RT	13.646	11.518	10.630
	RRT	10.332	8.127	7.164
	$\log k'$	0.494	0.380	0.315
Uracil	RT	3.045	3.239	3.380
17	RT	8.439	8.417	9.299
	RRT	5.394	5.178	5.919
	$\log k'$	0.248	0.204	0.243

HPLC Data for Quinazoline Series in Log P Analysis

Compound		Acetonitrile				
		55%	60%	65%	70%	75%
Uracil	RT	3.314	3.209	3.391	3.435	3.466
46	RT	11.297	10.893	11.059	11.207	11.276
	RRT	7.983	7.684	7.667	7.772	7.810
	$\log k'$	0.382	0.379	0.354	0.355	0.353
	47	RT	11.253	10.801	11.424	11.471
RRT		7.939	7.593	8.033	8.036	8.016
$\log k'$		0.379	0.374	0.374	0.369	0.364
48	RT	11.431	10.867	11.463	11.441	11.588
	RRT	8.117	7.658	8.071	8.007	8.122
	$\log k'$	0.389	0.378	0.377	0.368	0.370

Vita

Katie Elizabeth Alix was born to Michael and Linda Ownby August 15, 1984 in Landstuhl, Germany. She received her Bachelor of Science in Biochemistry and completed the equivalent work for a Bachelor of Art in Chemistry from Virginia Tech in May 2006. During her undergraduate career she authored a paper in the Journal of Biological Chemistry in 2005 entitled, "A *Methanocaldococcus jannaschii* archaeal signature gene encodes for a 5-formaminoimidazole-4-carboxamid-1- β -d-ribofuranosyl 5'-monophosphate synthetase: a new enzyme in purine biosynthesis." After receiving her bachelor degrees she subsequently enrolled in Virginia Commonwealth University's School of Pharmacy Medicinal Chemistry graduate program.